PhD Thesis Title

Single-Cell Multi-OMICs and Functional Immune Profiling Reveal Increased Innateness and Interferon-Driven Pathways in Behçet's Disease Skin and Blood

by

Saba Khoshbakht

A Dissertation Submitted to the

Graduate School of Health Sciences in Partial

Fulfillment of the Requirements for the Degree

of

Doctor of Philosophy

in

Cellular and Molecular Medicine

KOÇ ÜNİVERSİTESİ

January, 2025

PhD Thesis Title

Single-Cell Multi-OMICs and Functional Immune Profiling Reveal Increased Innateness and Interferon-Driven Pathways in Behçet's Disease Skin and Blood

Koc University

Graduate School of Health Sciences

This is to certify that I have examined this copy of a doctoral dissertation by

Saba Khoshbakht

and have found that it is complete and satisfactory in all respects,
and that any and all revisions required by the final
examining committee have been made.

Committee Members:

Assoc. Prof. Seçil Vural (Advisor)

Prof. Füsun Can [Co-Advisor]

Assoc. Prof. Vuslat Yılmaz

Prof. Dr. Güher Saruhan Direskeneli

Assoc. Prof. Atay Vural

Assoc. Prof. Tuğba Kevser Uzunçakmak

Date: 15/01/2025

ABSTRACT

Single-Cell Multi-OMICs and Functional Immune Profiling Reveal Increased Innateness and Interferon-Driven Pathways in Behçet's Disease Skin and Blood

Saba Khoshbakht

Doctor of Philosophy in Cellular and Molecular Medicine 15/01/2025

Behçet's Disease (BD) is a chronic, multi-system inflammatory disorder with both autoimmune and autoinflammatory features, arising in genetically predisposed individuals exposed to environmental triggers. While prior studies have largely focused on immune dysfunctions in peripheral blood, including increased Th17, Th1, and cytotoxic CD8+ T cells. Innate immune cells, including natural killer (NK) cells and γδ T cells have also been implicated in BD pathophysiology. Despite these advances, a significant gap remains in understanding the immune landscape of BD, particularly in affected skin tissues, one of the cardinal sites of disease pathogenesis. To date, no comprehensive study has integrated single-cell, molecular, and functional analyses to characterize immune dysregulation in both the blood and skin of BD patients.

To address this gap, we performed single-cell RNA sequencing (scRNAseq), TCR sequencing, flow cytometry, and functional analyses on BD skin tissue and PBMCs, comparing them with healthy controls.

Our scRNAseq and flow cytometry analyses revealed significant enrichment of plasmacytoid dendritic cells (pDCs), mucosal-associated invariant T (MAIT) cells, NK cells, ILC3s, and memory B cells in BD skin lesions. These populations were associated with robust type I immune responses and heightened expression of cytotoxic molecules, including granzyme B, granzyme K, and perforin. Effector memory CD4+ and CD8+ T cells exhibited a cytotoxic and inflammatory profile, characterized by increased production of IFN-γ, GZMK, and CCL5, while pathway analysis indicated significant activation of the JAK-STAT signaling pathway. Additionally, myeloid cells demonstrated upregulation of inflammasome-related genes linked to enhanced toll-like receptor signaling, as revealed by scRNAseq.

Functional studies showed increased IFN-γ and TNF-α expression in Th, Tc, and MAIT cells in BD skin, contrasting with their decreased expression in blood Th cells.

Overall, our findings reveal that innate immune cells and innate T lymphocytes, in conjunction with an activated Th1/Tc1 pathway, play a central role in BD pathogenesis. This study highlights the intricate immune dysregulation underlying BD, offering insights into potential therapeutic targets for this complex disease.

Key words: Behçet's Disease (BD), Skin Tissue Immune Landscape, Single-cell RNA Sequencing (scRNAseq), Flow cytometry, Plasmacytoid Dendritic Cells (pDCs), JAK-STAT Pathway Activation, Skin Lesion Pathophysiology, Type I immune response

OZETCE

Tek Hücreli Multi-OMIK ve Fonksiyonel Bağışıklık Profilleme, Behçet Hastalığı Deri ve Kanında Artmış Doğal Bağışıklığı ve İnterferonla İlişkili Yolları Ortaya Koymaktadır

Saba Khoshbakht

Hücresel ve Moleküler Tıp, Doktora

15/01/2025

Behçet Hastalığı (BH), genetik yatkınlığı olan bireylerde çevresel tetikleyicilere maruz kalma sonucu ortaya çıkan, otoimmün ve otoenflamatuar özelliklere sahip kronik, multisistemik bir enflamatuar hastalıktır. Önceki çalışmalar, Th17, Th1 ve sitotoksik CD8+ T hücrelerinin artışı gibi periferik kanda gözlenen bağışıklık disfonksiyonlarına odaklanmıştır. Ayrıca, doğal öldürücü (NK) hücreler ve γδ T hücreleri gibi doğuştan gelen bağışıklık hücrelerinin de BH patofizyolojisinde rol oynadığı bildirilmiştir. Ancak, BH'nin özellikle deri dokusu gibi hastalığın temel patogenez bölgelerindeki bağışıklık manzarasını anlamaya yönelik önemli bir eksiklik bulunmaktadır. Şimdiye kadar, BD hastalarının kan ve deri dokularındaki bağışıklık disfonksiyonlarını tek hücre, moleküler ve fonksiyonel analizlerle kapsamlı bir şekilde inceleyen bir çalışma yapılmamıştır.

Bu eksikliği gidermek amacıyla, Behçet hastalarının deri dokusu ve periferik kan mononükleer hücrelerinde (PBMC) tek hücre RNA dizilimi (scRNAseq), TCR dizilimi, akım sitometrisi ve fonksiyonel analizler gerçekleştirilmiş ve sağlıklı kontrollerle (HC) karşılaştırılmıştır.

Tek hücre RNA dizilimi ve akım sitometrisi analizlerimiz, Behçet deri lezyonlarında plazmasitoid dendritik hücreler (pDC), mukozaya özgü invariyan T (MAIT) hücreleri, NK hücreleri, ILC3'ler ve hafıza B hücrelerinin anlamlı şekilde zenginleştiğini ortaya koymuştur. Bu hücre popülasyonları, güçlü tip I bağışıklık yanıtları ve granzyme B, granzyme K ve perforin gibi sitotoksik moleküllerin artan ekspresyonuyla ilişkilendirilmiştir. Efektör hafıza CD4+ ve CD8+ T hücreleri, artmış IFN-γ, GZMK ve CCL5 üretimi ile sitotoksik ve enflamatuar bir profil sergilemiş, yolak analizleri ise JAK-STAT sinyal yolunun anlamlı aktivasyonunu göstermiştir. Ayrıca, scRNAseq analizleri, miyeloid hücrelerde inflamatuvar sinyalle ilişkilendirilen inflamozomla ilişkili genlerin yukarı regülasyonunu ve gelişmiş toll-like reseptör sinyalini ortaya koymuştur.

Fonksiyonel çalışmalar, Behçet deri dokusunda Th, Tc ve MAIT hücrelerinde artan IFN-γ ve TNF-α ekspresyonunu, buna karşın kan Th hücrelerinde azalan ekspresyonu göstermiştir. Sonuç olarak, bulgularımız, doğuştan gelen bağışıklık hücreleri ve doğuştan gelen T lenfositlerinin, aktif bir Th1/Tc1 yolak ile birlikte, BH patogenezinde merkezi bir rol oynadığını ortaya koymaktadır. Bu çalışma, BH'nin altında yatan karmaşık bağışıklık disfonksiyonlarını vurgulamakta ve bu kompleks hastalık için potansiyel terapötik hedeflere yönelik önemli bilgiler sunmaktadır.

ACKNOWLEDGMENT

First and foremost, I would like to express my deepest gratitude to my advisor, Assoc. Prof. Seçil Vural, for her invaluable guidance, encouragement, and unwavering support throughout my Ph.D. journey. Her mentorship has been instrumental in shaping my research and professional growth.

I am also deeply grateful to my co-advisor, Prof. Füsun Can, for her insightful advice and continuous encouragement. Her expertise and feedback have significantly contributed to the progress and success of this project.

I extend my heartfelt thanks to Assoc. Prof. Atay Vural for his generous support and assistance during the course of this research. His input and mentorship have been a great source of inspiration and motivation.

My sincere appreciation goes to Dr. Özgür Albayrak, whose knowledge and expertise have been invaluable throughout this project. His guidance has been instrumental in overcoming many challenges.

I would like to thank Dr. Ergun Tiryaki for his crucial participation in bioinformatics analysis, which played a significant role in this study.

I also wish to acknowledge the contributions of the following doctors who provided the samples: Dr. Pınar Gizem Sun, Dr. Ayşe Boyvat, Dr. Ayşe Öktem, Dr. Deniz Devrim Kuşçu, Dr. Elif Er Gülbezer, and Dr. Orhan Ağcaoğlu. Your support has been vital to the success of this research.

On a personal note, I am profoundly thankful to my parents and my brother for their unconditional love, support, and encouragement. Their belief in me has been a constant source of strength and perseverance.

Lastly, I would like to acknowledge my friends and Vural Lab members, whose support and camaraderie have made this journey more enjoyable and memorable.

To all of you, I am deeply grateful for your contributions to this milestone in my life.

Funding

This work was supported by the European Academy of Dermatology and Venereology (EADV, Grant No. PPRC-2021-31) and the Scientific and Technological Research Council of Turkey (TUBITAK, Grant No. 221S877). Additionally, the services and facilities of the Koç University Research Center for Translational Medicine (KUTTAM) were instrumental in completing this project.

Ethics statement

The studies involving humans were approved by Koç University Committee on Human Research (protocol number 2022.058.IRB2.007). The studies were conducted in accordance with the local legislation and institutional requirements.

TABLE OF CONTENTS

LIST OF TABLES

LIST OF FIGURES

ABBREVIATIONS

AS	Ankylosing Spondylitis
BD	Behcet's Disease
CD	Crohn's Disease
CTLs	Cytotoxic T lymphocytes
DAMP	Damage-Associated Molecular Patterns
DC	Dendritic Cells
EN	Erythema Nodosum-like lesion
ERAP	Endoplasmic Reticulum Aminopeptidase Enzyme
FACS	Fluorescence-Activated Cell Sorting
FMF	Familial Mediterranean Fever
GEM	Gel Bead-in-Emulsion
GrK	Granzyme K
GrB	Granzyme B
GU	Genital Ulcer
GWAS	Genome-Wide Association Studies
HC	Healthy Control
HS	Hidradenitis Suppurativa
IBD	Inflammatory Bowel Disease
MAIT	Mucosal-associated invariant T cell
MFI	Mean Fluorescence Intensity
MHC	Major Histocompatibility Complex
MS	Multiple Sclerosis
NK cells	Natural Killer cells
PAMP	Pathogen-Associated Molecular Patterns
PBMC	Peripheral Blood Mononuclear Cells
pDC	plasmacytoid DC
PPE	Papulopustular Eruptions
PPT	Positive Pathergy Test
ScRNAseq	Single-Cell RNA Sequencing
SLE	Systemic Lupus Erythematosus
SNP	Single Nucleotide Polymorphism
SPT	Skin Pathergy Test
TCR	T Cell Receptors
THLs	T Helper Lymphocytes
TRM	Resident Memory T Cells

CHAPTER 1

INTRODUCTION

CHAPTER 1

INTRODUCTION

1.1 Behcet's Disease

Behcet's disease (BD) is a multi-system, chronic inflammatory condition, initially documented in 1937 by Dr. Hulusi Behçet a Turkish dermatologist (1). It predominantly impacts individuals in their 30s and 40s, with a similar incidence rate across genders, although severe complications are more prevalent in men (2). As individuals grow older, the disease tends to become less active after severe recurrent episodes in younger individuals and represents a notable economic burden on society. While BD is classified as a rare disease in Western countries, affecting 1-10 people per 100,000, it is more prevalent in regions like Turkey, with a prevalence of 0.4-4 cases per 1000 individuals, as well as Japan and the Middle East (3, 4).

At present, BD is diagnosed based on clinical symptoms, as no specific laboratory test exists for its confirmation. According to the guidelines established by The International Study Group in 1990, a BD diagnosis requires the presence of oral ulcers and two of the following: eye inflammation, genital ulcers, other skin lesions, and a positive skin pathergy test (SPT) (4). While mucocutaneous symptoms are commonly the initial signs (5), patients can also experience vasculitis and systemic manifestations, leading to significant health challenges (3, 6). Vascular complications, including both arterial and venous involvement, are a hallmark of Behçet's disease. Patients may endure arterial aneurysms, intracardiac thromboses, and recurrent deep vein thromboses (6). Colchicine is typically prescribed for mucocutaneous symptoms, while immunosuppressive or immunomodulatory therapies are used for treatment-resistant cases or systemic symptoms (3, 6). Nevertheless, some individuals may not respond well to current therapies for controlling repeated episodes.

BD presents as a complex disorder characterized by a combination of autoinflammatory and autoimmune features, occurring in individuals carrying genetic susceptibility when encountering environmental triggers (7, 8). Genetic factors are critical in BD's development, evident through substantial familial clustering, with sibling risk ratios ranging from 11.4 to 52.5 in different regions of Turkey (9, 10). A recent Korean large-scale study, which analyzed

over 21 million people from 12 million families, also reported a significantly increased susceptibility to BD in first-degree relatives, particularly twins, with susceptibility escalating by 165 times (11).

A critical genetic factor linked to susceptibility to BD is the HLA class I allele HLA-B*51. Other studies have also identified gene variants in non-HLA genes, such as interleukin-10 (IL-10), the endoplasmic reticulum aminopeptidase enzyme (ERAP1), and IL-23 receptor/IL-12 receptor beta-2 (IL23R/IL-12RB2), as contributing to the development of BD (4). For individuals those genetically predisposed, environmental factors like microbial agents or endogenous self-antigens such as heat shock proteins are believed to trigger autoimmune responses, resulting in inflammatory status and disease characteristics of BD (3, 12). Deviations in immune responses instigate a cascade of cytokine activation, leading to changes in cytokine levels that attract inflammatory cells to tissues, causing tissue damage (12).

1.2 Genetic susceptibility

1.2.1 HLA-B*51 Association

Extensive research has concentrated on genetic factors and their involvement in BD, with the HLA-B*51 allele recognized as the predominant contributing aspects for the condition. Additionally, the distribution of this gene in populations worldwide aligns with the prevalence of BD (13, 14).

In Silk Road countries, approximately 20–25% of the overall public and 50–80% of individuals with BD possess the HLA-B51 allele. While, in the USA and northern Europe, the prevalence of the HLA-B51 allele is lower, ranging from 2–8% in the population to around 15% in BD patients (15, 16). Turkey exhibits a notable prevalence of the HLA-B51 allele among BD patients, with rates between 50% and 70%, while approximately 25% of the general population in Turkey carries this allele (17-22). The presence of HLA-B51 significantly elevates the likelihood for the development of the BD by nearly 6–10 times, with carriers having a risk ratio of 5.90 (20, 21, 23). Investigations have been conducted on the clinical subtypes of BD and their association with HLA-B*51. Variations in findings have been observed, likely attributable to the diverse ethnic compositions of the study cohorts. Nevertheless, there is a propensity

towards an increased prevalence of vasculitis, ocular manifestations, neurological complications, and more severe disease in HLA-B51 carriers (18, 24-30). Kirino et al. (31) have identified a recent evolution in BD, characterized by a reduction in the complete-type BD cases and the frequency of HLA-B51 positivity.

The HLA-B51 gene is believed to impact the peptidome linked to Behçet's disease, which might uncover certain microbial or self-antigens that could initiate an autoimmune reaction (12). Yet, the exact mechanisms through which HLA-B51 contribute to the pathogenesis of BD remain unclear.

To date, over 19,000 HLA class I alleles have been documented, though just four have been strongly associated with specific diseases, collectively categorized as major histocompatibility complex (MHC) class I-opathy or MHC-I-related disorders. For instance, HLA-B*51 is linked to BD, HLA-B27 with the spondyloarthritis group, HLA-C06:02 with psoriasis, and HLA-A29:02 with birdshot chorioretinopathy. These associations highlight the crucial role of the HLA system in immune responses and its influence on predisposition to the disease (32-35).

The repertoire of peptides displayed by HLA molecules is influenced by various factors, such as the specific HLA molecule, the structure of the peptide-binding region, the pathways involved in peptide processing, and the machinery for antigen processing, as depicted in Figure 1.1 (36). These peptides may originate from self-antigens, foreign sources, or viral proteins. Consequently, HLA molecules are essential for immune surveillance, activation, and regulation, as they present peptides to T cells, enabling their recognition and activation or supporting immune tolerance (34).

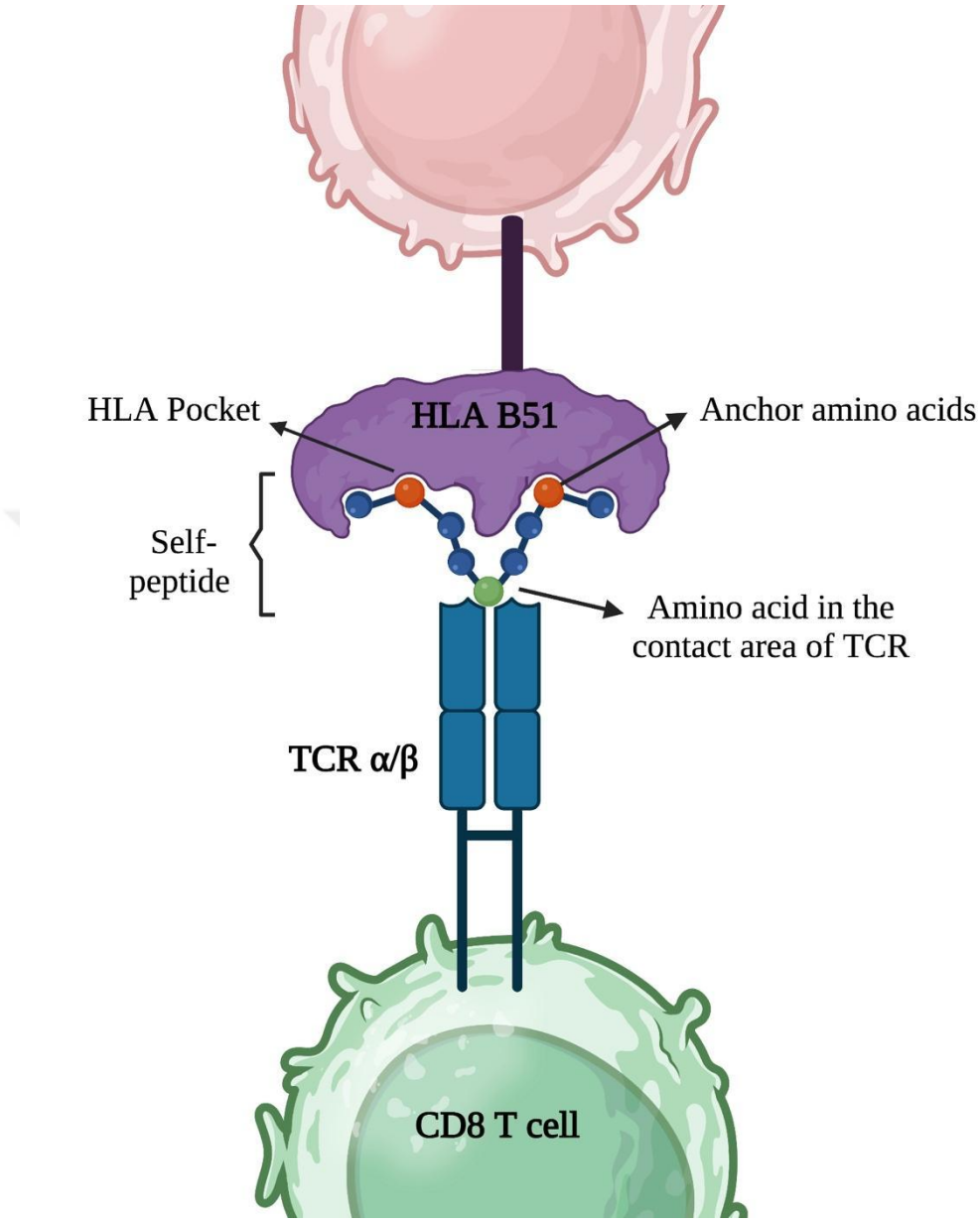

Figure 1.1. The process of antigen presentation by HLA class I to CD8+ T cells.

HLA class I molecules are characterized by anchor residues that are highly rigid and stable, which are essential for the presentation of peptides. Typically, these peptides are 8 to 10 amino acids long, and their specific amino acid sequence pattern shaped by the unique structure of HLA anchor residues. While T cell receptors (TCRs) demonstrate poly-specific reactivity towards antigens displayed on HLA molecules, they can

specifically identify matching HLA-peptide combinations based on particular amino acid sequences. The interaction between HLA anchor residues and TCR contact points collectively influences these sequences. It is noteworthy that positions within the peptide sequence beyond the anchors allow for flexibility and variation (37). HLA allele genetic polymorphisms have a vital role in creating a wide range of repertoire of peptides, resulting in the production of unique peptidomes (38).

1.2.2 HLA-B*51 and ERAP1 Epistasis

Genome-wide association studies (GWAS) have underscored ERAP1 as a pivotal genetic component in BD, alongside HLA-I (39, 40). In BD, there is a specific epistatic relationship between HLA-B51 and ERAP1, rendering certain ERAP1 variants a risk factor solely when the HLA-B51 allele is present. These polymorphisms of ERAP1 can influence enzyme activity and antigen presentation, thereby modifying the HLA-I peptidome and binding affinity (12, 13, 25). The ERAP2 and ERAP1 enzymes play a role in trimming peptide fragments to optimize HLA class I presentation, thereby affecting antigenicity (33, 41). ERAP1/2 polymorphisms are closely tied to HLA-I-related conditions such as AS, birdshot chorioretinopathy, psoriasis, and BD (41). There are ten main variations of ERAP1, known as Hap1-10. Hap10 is particularly related with a higher risk of BD because of its diminished activity resulting in longer peptides (42-44). In a study by Cavers et al. (44) it was illustrated that the ERAP1-Hap10 allotype in conjunction with HLA-B*51 causes a transition of CTLs from a naive state to an activated state. This transition is likely to trigger the migration of CD8+ T cells to inflamed regions.

The ERAP1-Hap10 variant, which is related to a heightened vulnerability to BD, demonstrates a strong correlation with HLA-B51. Individuals homozygous for Hap10 and carrying HLA-B51 exhibit a 10.96-fold increased risk of BD, whereas those without HLA-B51 do not experience any alteration in risk (43). The diminished enzymatic activity of Hap10 results in prolonged peptide trimming, particularly affecting proteins bound to HLA-B51 (44). Guasp et al. (45) performed a comparative assessment of the alterations of Hap10 in the Ala-2 and Pro-2 sub-peptidomes of HLA-

B51, leading to a higher ratio of Ala-2/Pro-2 and the generation of low-affinity HLA-B51 peptides. This modification impacts the functionality of and natural killer (NK) cells (33, 45). This change affects the activity of CTLs and NK cells, as low-affinity peptides can stimulate T cell responses, while poor peptide-MHC-I recognition by KIRs heightens NK cell cytotoxicity (45, 46).

In studies on the impact of ERAP1 in BD immune reaction, mice with BD induced by herpes simplex virus (HSV), featuring partial ERAP1 expression (ERAP1 heterozygotes, +/−), it was observed that reduced ERAP1 expression augmented the IL-17 and IFN-γ production by CD4+ T cells in BD mice (47). Furthermore, an independent study reported that ERAP1−/− mice had reduced peripheral regulatory T cells, vital for preventing autoreactive immune activity against self-antigens (48). Consequently, diminished ERAP1 activity disrupts the equilibrium between Th1/Th17 and Treg cells in BD. These results highlight the complex relationship between ERAP1 and HLA-B*51 and their important influence on the antigen presentation process, providing insight into the genetic determinants that contribute to the development of BD.

1.2.3 The Repertoire of HLA-B*51 and Peptide-binding

In a research conducted by Gebreselassie et al. (49), the investigation into the significance of the peptidome in relation to BD was undertaken. The investigation specifically examined the peptides linked to six distinct HLA-I alleles: HLA-A03, HLA-A31, HLA-B18, HLA-B51, HLA-Cw01, and HLA-Cw07. The results demonstrated that HLA-B18 displays the highest affinity for binding peptides among the alleles studied, whereas HLA-B51 exhibits binding to a larger pool of peptides with minimal affinity. High-affinity self-peptides bound to HLA aid in promoting tolerance, whereas low-affinity peptides generally don't trigger an immune response. On the other hand, peptides with medium affinity could present a challenge as they are less effective in fostering tolerance while eliciting an immune response. Thus, the reduced binding affinity of peptides by HLA-B5101 might increase susceptibility to specific autoimmune responses (49).

Further investigation into the low- binding affinity of HLA-B51 and its possible role in BD revealed that just HLA-B5101, not HLA-B5201, is associated with BD, suggesting a crucial role of peptide presentation. The two variants have only two residue differences at positions 63 (Asp63Glu) and 67 (Phe67Ser) within the B pocket of the peptide-binding groove, leading to distinct peptidomes (50, 51). Structural analysis of peptide-binding by HLA-B alleles, HLA-B51 and HLA-B52, utilizing peptides YAYDGKDYI, LPRSTVINI, and IPYQDLPHL, showed that peptides bound to HLA-B51 exhibited higher fluctuation, resulting in less selective and looser binding in comparison with HLA-B*52 (51).

Examination of the positions of polymorphic amino acids within HLA-B concluded that positions 67, 97, 116, and 152 have an individual and distinct impact on the BD development risk (52). The antigen-binding groove of the MHC-I structure in the HLA-B protein contains these important residues, directly interacting with six of the nine peptide residues. Among these, positions 67 and 116 serve as anchor points, significantly affecting peptide specificity within the antigen-binding groove by engaging with P2 and P9 peptide positions, respectively (53). The interaction between HLA-B molecules and the receptors KIR3DL1 and KIR3DS1, which are crucial for modulating NK cell and CD8+ CTL activation, is mediated by these positions (54). Notably, residue 67 is one of the two points where HLA-B51 varies from the closely related HLA-B52; however, this particular variation does not appear to affect the risk of developing BD.

1.2.4 Other HLA Class I Alleles

Studies have revealed significant links between BD and particular HLA class I alleles beyond HLA-B51. Ombrello et al. (52) showed that HLA-B15 and HLA-B27 independently increase BD risk, while HLA-B49 shows a protective effect. Furthermore, analysis using stepwise logistic regression on both the full dataset and the HLA-B51-negative subset revealed that HLA-A03 provides a substantial protection against BD, with HLA-B15, HLA-B27, and HLA-A26 as risk factors. Al-Okaily et al. (55) observed higher rates of HLA-A31 and HLA-A26, as well as a reduction of HLA-

B15, in Saudi Arabia BD patients. A Japanese research identified a modest association between HLA-B3901 and HLA-A2602 with BD among patients lacking the HLA-B51 allele (22). Kang et al. (56) found higher frequencies of HLA-A26:01, HLA-A02:07, and HLA-A30:04, and lower incidences of HLA-A33:03, in BD patients. Another study involving BD patients from Germany and Turkey unveiled a notable association of HLA-Bw4-80I and HLA-A26 within the subgroup of patients without the HLA-B51 allele (57). In the UK population, HLA-A26, HLA-B08, and A25 are proposed as risk alleles, while HLA-B58 and HLA-A*33 is revealed to confer a protective effect (58).

Even though substantial research has focused on the implications of HLA-B51 in pathophysiology of BD, it is imperative to note that a significant number of Behçet's patients do not exhibit this allele. Therefore, antigen presentation plays a crucial role across individuals with diverse HLA class I alleles. Significantly, HLA-A26 has been identified as a risk factor in numerous studies across varied ethnic groups. Thorough examination of the polymorphic amino acid residues in HLA-A has unveiled substantial and independent connection between 97 and 161 of HLA-A residues and BD (52). These residues are situated in the MHC-I antigen-binding groove, corresponding to risk-associated positions recognized in HLA-B*51.

1.2.5 KIR3D Receptor Polymorphisms

The presence of KIR haplotypes has been linked to HLA class-I-related disorders like birdshot chorioretinopathy, psoriasis, and ankylosing spondylitis. Killer-cell immunoglobulin-like receptors (KIR), located on chromosome 19q13.4, are a diverse group of molecules allowing NK cells to engage with HLA class I molecules. Activating KIR genotypes have been linked to decreased risk of infections but enhanced susceptibility to autoimmune diseases. On the other hand, inhibitory KIR genotypes are associated with lower risk of inflammatory diseases. The interplay of KIR on NK cells and HLA class I molecules demonstrates genetic epistasis, as both receptor and ligand presence are crucial for functionality (59).

The data concerning the correlation between KIR3D receptors and BD present some discrepancies. In a comprehensive study encompassing 1710 healthy controls and 1799

BD patients from Turkey, alongside HLA-B51 information, no notable link was detected between the inhibitory KIR3DL1 or activating KIR3DS1 alleles and the susceptibility to BD. Interestingly, within the subgroup of individuals with ocular manifestations of the disease, a higher prevalence of KIR3DS1 alleles was observed, regardless of HLA-B51 status (60). A flow cytometry based study also reported that KIR3DL1+ NK cells and T cells, were not statistically different in the PBMC of BD patients with respect to healthy individuals (61).

While a study examining the KIR3DL1/S1 alleles revealed that having KIR3DL1/S1 alleles with diminished expression along with KIR3DS1, significantly increased the likelihood of manifesting BD. Conversely, having IR3DL1/S1 variants exhibiting high expression together with null-expressing KIR3DL1 variants, decreased the probability of disease occurrence (58).

1.2.6 Gene Loci Related to IL23/Th17 Pathways

The IL23R-IL12RB2 locus plays a pivotal role in the IL-12/IL-23 receptor, which supports Th17 cell differentiation and mediates IL-12 signaling. Prior genome-wide association studies in patients with BD revealed two key single nucleotide polymorphisms (SNPs) within this gene: rs1495965 and rs924080 (62). Moreover, another research supporting the involvement of IL-23R in BD demonstrated that missense variants of this gene, resulting in decreased responses to IL-23, confer protection against BD. Interestingly, these variants also have protective effect against various other diseases, like Crohn's disease (CD), ankylosing spondylitis (AS), psoriasis, and inflammatory bowel disease (IBD) (14, 62).

1.2.7 Gene Loci Related to Innate Immunity

Innate immunity-related BD susceptibility loci mentioned in previous studies include, but are not limited to, MEFV, MICA, FUT2, TLR, TNFAIP3, STAT4, IL10 and CD40.

Mutations in the MEFV gene are believed to lead to Familial Mediterranean Fever (FMF), a genetic autoinflammatory disease predominantly found in the Mediterranean region, possibly suggesting a selective advantage. Previous studies have indicated that genetic variants associated with FMF may contribute to susceptibility to BD (63, 64). In their study, Kirino et al. (65) utilized deep sequencing of GWAS data to explore the involvement of MEFV gene variants in BD, finding that the p.Met694Val (M694V) mutation, a common FMF variant linked to sever inflammation, was significantly associated with BD in Turkish patients even when present in a heterozygous form (odds ratio: 2.65–2.73), but not among Japanese patients. The M694V mutation has also been recognized as a susceptibility factor for IBD, severe hidradenitis suppurativa (HS), and AS in the Turkish demographic (66). The impact of MEFV gene variants on disease manifestation was further bolstered by a study that identified MEFV mutations in 70.6% of neuro-BD cases with more pronounced white matter involvement, underscoring the mutation's role in inflammatory diseases (67). The available research indicates that MEFV variants linked to FMF are gain-of-function variants, leading to heightened sensitivity to bacterial components. For example, mice with the M694V mutation exhibit increased caspase-1 activity, causing excessive interleukin-1β production following lipopolysaccharide stimulation (68).

The MHC class I polypeptide-related sequence A (MICA) gene, situated between the TNF and MHC-B genes on chromosome 6, is associated with BD. Variations within the MICA gene have been detected in some BD patients. MICA interacts with CD314 (NKG2D), which activates the NK receptor expressed on various immune cells like ILCs, cytotoxic T cells, NKT cells, and NK cells. This interaction can trigger an immune response, that may lead to tissue damage. A study by Zhang et al., through meta-analysis (69) established MICA-A6 allele as a contributing factor for BD, while the MICA-A4, A5, A5.1, and A9 alleles may have protective effects against BD development (35, 69).

The fucosyltransferase 2 (FUT2) gene, known for its role in intestinal mucosal immunity, has been linked to BD (70, 71). Xavier et al. (70) identified the link between the FUT2 gene and BD in GWAS, with findings strengthened by a meta-analysis incorporating their data alongside a Turkish GWAS involving Iranian patients. Their research also indicated that FUT2 is an independent genetic risk factor for BD separate from the HLA-B gene, and they did not find any evidence of epistasis (70). The FUT2 gene encodes a protein essential for synthesizing and releasing the H antigen—precursor to the ABO blood antigens—into body fluids and intestinal mucosa. Due to genetic diversity, about 80% of people possess a functional FUT2 allele, displaying a "secretor" phenotype, while the remaining 20% are "non-secretors" (72). The non-secretor phenotype, linked to BD, has also been associated with CD, rheumatic fever, and type 1 diabetes, while being linked to reduced susceptibility to infections from pathogens like Norwalk virus, *Campylobacter jejuni*, and *Helicobacter pylori* (70). According to the Human Microbiome Project, the FUT2 phenotype affects the diversity and levels of *Bifidobacterium* within the microbiome, with non-secretors showing decreased *Bifidobacterium longum* (73). While more research is needed to fully comprehend the FUT2 gene's influence on gastrointestinal microbial flora, some research inducate that FUT2 serves as a link between environmental and genetic factors (70, 71).

The TLR gene family offers additional insights into immune responses to bacterial infections in BD (71). Of this gene family, TLR4 shows the strongest association with BD. Variations in the TLR4 gene have been connected to an increased chance of developing inflammatory conditions, such as ulcerative colitis, rheumatoid arthritis (RA), and CD (74). Studies involving Japanese patients have demonstrated the association between TLR4 and BD (75). Moreover, research on Korean patients showed that the TAGCGGTAA haplotype was significantly more prevalent among HLA-B*51+ BD patients compared to healthy individuals (74). Kirino et al. (65) noted that two TLR4 variations, specifically p.Asp299Gly (D299G) and p.Thr399Ile (T399I), provided protection against BD, despite these variants are also linked to an heightened risk of CD due to reduced immune responsiveness. Moreover, studies conducted on the Han Chinese population have identified a link between the TLR2 gene and BD. In

particular, two specific TLR2 genotypes— rs3804099 and rs2289318—were observed to be more widespread in patients with ocular BD than in healthy subjects (76).

The tumor necrosis factor alpha-inducible protein 3 (TNFAIP3) gene, responsible for encoding the A20 enzyme, has been identified in relation to BD and a similar autoinflammatory syndrome called haploinsufficiency of A20 (HA20) (77-79). TNFAIP3 plays a crucial role in regulating inflammatory responses triggered by TNF, TLR, or NOD2-induced NF-κB signaling (80, 81). Variations in TNFAIP3 have also been linked to autoimmune disorders like RA (82), systemic lupus erythematosus (SLE) (83), psoriasis (84), and multiple sclerosis (MS) (85). In Han Chinese BD patients, specific SNPs in TNFAIP3, such as rs7753873, rs10499194, and rs9494885, have been identified as increasing BD risk (78). HA20, characterized by A20 haploinsufficiency due to nonfunctional TNFAIP3 variants, presents with symptoms resembling BD, including oral and genital ulcers, gastrointestinal issues, and arthritis (77). HA20 is more common in women (male-to-female ratio of 1:2), typically develops in childhood around the age of 5.5, and often involves recurrent high fever during flare-ups. Despite being rare, HA20 is globally distributed and shows a lower association with the HLA-B*51 antigen compared to BD (86).

The signal transducer and activator of transcription-4 (STAT4) is linked to an increased susceptibility to various autoimmune conditions, like RA, primary Sjögren's syndrome, and SLE (13, 87). In a GWAS conducted on Turkish individuals, STAT4 was found to have a connection with BD (39). Another SNP, rs897200 risk allele A, identified in GWAS on Han Chinese BD patients, was associated with more severe BD symptoms, such as elevated production of interleukin 17 (IL-17), increased STAT4 expression, and more pronounced clinical manifestations (88).

Other genetic loci connected to BD susceptibility have been uncovered in GWAS on BD patients. Among these genes is the IL-10 gene, a cytokine that is typically diminished in the blood of individuals with BD. In research conducted in Iran and Turkey, the IL-10 SNP rs1518111 was connected with BD, with the risk allele A (identified in Turkish GWAs) leading to a 35% decrease in IL-10 expression in monocytes (16, 36, 55, 89). Furthermore, the CD40 gene displayed two associated SNPs, rs1883832 and rs4810485. These SNPs showed a susceptibility effect in TT

genotypes and a safeguarding effect in GT genotypes for rs4810485 (37, 55). Predisposition to BD is influenced by a range of genetic regions and environmental interactions, highlighting the need for further research for developing prospective treatments and precise diagnostic approaches.

1.3 Antigens in Behcet's Disease

The theory linking HLA class I to disease indicates that enhanced antigenicity of peptides presented by HLA-B*51 may prompt CD8+ T cells to recognize self-proteins, thereby initiating the disease process. This hypothesis is supported by demonstration of enhanced CTLs in the aqueous humor of the eye, along with oligoclonal and clonal expansions of these cells in the BD patients' peripheral blood (90, 91). One study reported that 67% of individuals with clinically active BD exhibited oligoclonal expansions of both CD8+ and CD4+ T cells, with a CD8+ T cell clone containing the Vb5.1 chain identified in five out of nine patients (91). Additionally, another study found that 57% of patients' PBMCs contained one or more CD8+ or CD4+ T cell clones. Long-term follow-up revealed that all active BD patients possessed a distinct clone of T cells linked to the disease (90).

Peptides generated from a protein within cells that resemble a peptide found in a harmful bacterium can activate CD8+ T cells, potentially contributing to the development of BD. Although the specific self-peptides involved in BD onset have not been identified yet, studies have primarily examined environmental antigens linked to BD autoimmunity, such as viral antigens (e.g., Epstein-Barr virus, hepatitis, HSV1, and cytomegalovirus) and bacterial peptides (e.g. Helicobacter pylori, Mycobacterium tuberculosis, and Streptococcus sanguinis) (92, 93). The 50% similarity between human 60-kDa heat shock protein (HSP-60) and HSP-65 in Mycobacterium tuberculosis and Streptococcus sanguinis implies a possible mechanism for initiation of BD (92, 94, 95). The shared features between human and bacterial HSP could lead to self-reactive T-cell activation and autoimmune responses (95, 96). BD patients often have antibodies against HSP-65 that cross-react with oral epithelium antigens. Specific Mycobacterium HSP-65 epitopes (amino acids 111-125, 154-172, 219-233, and 311-326) can stimulate T and B cell responses (94, 97-100). In BD patients, T cells activated with a peptide mix from the 65-kDa HSP revealed four main immunogenic regions (111-125, 154-172, 311-

325, and 219-233) (101). These Mycobacterium tuberculosis HSP regions induced γδT cell activation and expansion in 76% of patients, without an increase in αβ CD8+ T cells (102).

Recent research conducted in Turkey identified autoantibodies against neurofilament-M, an intracellular protein, in the sera of BD patients. The peptide structure of this protein showed similarity with three immunogenic regions (amino acids 111-126, 213-232, and 304-363) of M. tuberculosis HSP and (161-176, 304-363, and 340-359) of S. sanguinis HSP. Moreover, BD patient blood displayed immune responses to the self-antigen neurofilament medium, which shares amino acid sequences (111-126, 213-232, 304-363) with Mycobacterium HSP-65 (94, 97-100). Sera containing autoantibodies against neurofilament-M reacted to bacterial HSP (99). Other studies have indicated the presence of autoreactive CD8+ T cells in BD patients when stimulated with the S. sanguinis HSP and MICA peptide (95, 100, 103).

Research indicates that BD patients often present disrupted oral flora and compromised oral health, with the severity of the disease being linked to the plaque index. Antibiotics can be beneficial in managing disease recurrence (3, 97, 104). In studies focusing on S. *sanguinis* produced these results:

(1) BD patients show an enhanced prevalence of S. *sanguinis* in their oral flora than healthy individuals.

(2) BD patients demonstrate increased sensitivity to antigens from S. *sanguinis*.

(3) Gnotobiotic animal models infected with S. *sanguinis* exhibited symptoms resembling BD.

(4) γδT cells from BD patients respond to antigens from this bacterium.

HSV1 is a virus that has been widely investigated in relation to BD. Remarkably, HSV1 DNA has been detected both in BD lesions of the oral and genital areas and in blood samples of BD patients, who show increased levels of HSV1 antibodies than healthy people. Intriguingly, animal models exposed to HSV1 developed symptoms resembling BD (47, 97, 105).

1.4 Different Immune Cells in Behcet's Disease

Both the adaptive and innate immune systems play significant roles in the onset of BD (Figure 1.2). Adaptive immunity activation in BD may be triggered by innate immunity through PAMPs from tissues in contact with the external environment, or DAMPs produced by stressed tissues. In the adaptive immune response, there are increased Th17, Th1, and cytotoxic CD8+ T cells, along with a decrease in regulatory T cells (Tregs) (12, 106, 107). Besides, cell types such as γδ-T cells, neutrophils, and NK cells contribute to the BD pathophysiology (108). This part will explore the different immune cells implicated in BD development.

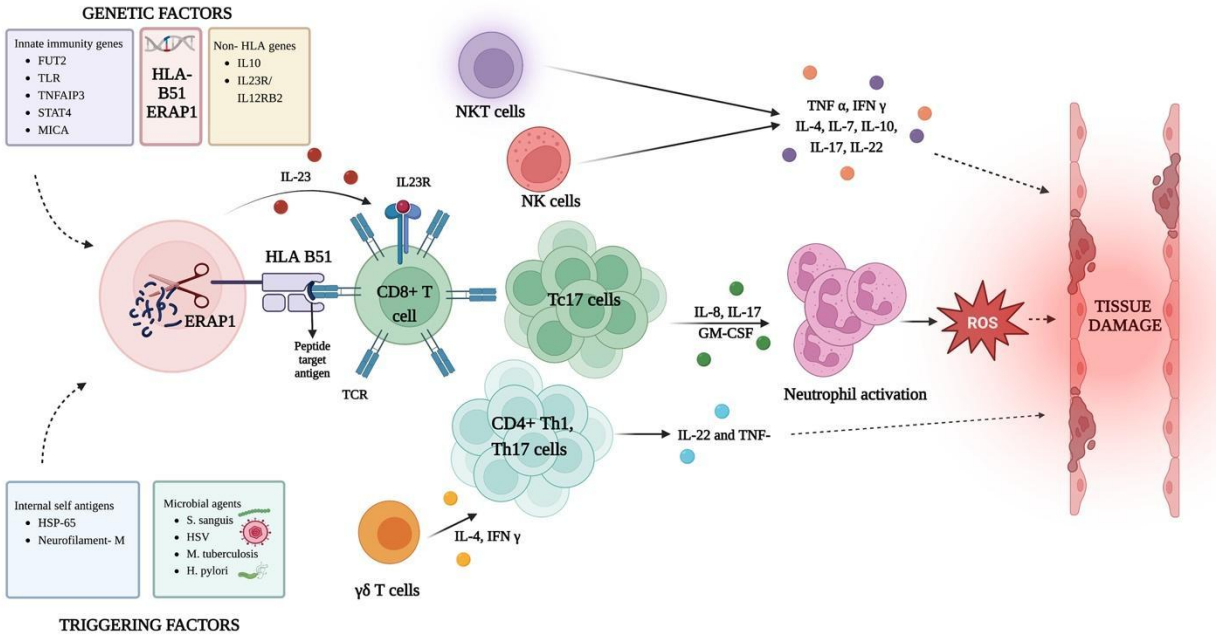

Figure 1.2. Graphic overview of pathogenesis in BD. This diagram illustrates how genetic factors and specific triggering antigens can initiate an immune response when self-peptides, resembling environmental antigens, are presented to CD8+ T cells. This process is more enhanced by the production of IL-23. As a result of immune dysregulation, various immune cells, including Th17, Tc17, NK, and NKT cells, secrete a range of cytokines. Key cytokines such as IL-17, IFNY, TNFα, and IL-8 are central to activating neutrophils, leading to reactive oxygen species production and neutrophil extracellular trap formation. Ultimately contributing to tissue damage.

1.4.1 Cytotoxic T lymphocytes (CTLs)

HLA-B51 contributes significantly to the genetic risk of developing BD, particularly involved in the display of peptides to CTLs, which are crucial in the disease's development. Evidence supporting this includes enhanced CTLs found in the aqueous humor (109) and clonal expansions of these cells in the BD patients' peripheral blood (90, 91). These cells produce cytokines such as IL-17, GM-CSF, IL-8, which enhance activation of neutrophils and facilitate the interplay between the adaptive and innate immune systems in BD pathogenesis (35). In patients with active BD who carry the HLA-B51 allele, CD8+ T cell levels in blood are higher than in healthy controls and inactive BD patients (110). Another research group investigated the levels of NKT cells and CTLs in the aqueous humor and PBMC of 17 patients with BD uveitis, 7 patients with Vogt–Koyanagi–Harada syndrome, 13 patients with idiopathic intermediate uveitis, and 18 patients with idiopathic recurrent acute anterior uveitis. Generally, in uveitis patients, the percentage of CD4+ T cells and the CD4+/CD8+ cell ratio were higher in the aqueous humor than in PBMC. However, in BD patients, CTLs were elevated in the aqueous humor, leading to a reversed ratio (109). Research also indicates that IL-17-secreting T cells in BD skin lesions are mainly CD8+, not CD4+ cells (106). Additionally, Okubo et al. used weighted gene co-expression network analysis from transcription data of peripheral blood immune cells to show that in HLA-B51+ BD patients, IL-17-associated genes are enhanced in CD8+ memory cells, which could reflect the expanded Tc17 number or function in this disease (111).

Inflammatory cytokines and cytotoxic substances from immunosenescent cells may cause chronic inflammation. Investigations are currently being conducted into their role in SLE, RA, and type 1 diabetes. In this context, 39 BD patients (19 active and 20 inactive) were compared to 15 disease-control patients with recurrent aphthous ulcers and 15 healthy controls for senescent CTLs, helper T cells, and B cells. Only senescent CTLs in the active BD group increased statistically compared to the disease control ($p=0.001$) and the healthy control ($p=0.005$), with mean percentages of 39.0% (95% CI 32.4-45.5%) for active BD, 31.6% for inactive BD, 21.7% for disease control, and 24.4% for healthy control (112). These data imply that immunosenescent CD8+ T cells may contribute to active BD

pathophysiology and may be a therapeutic target. However, more research is needed to validate these findings and clarify the role of immunosenescence in BD.

1.4.2 T Helper 1 Cells

T helper 1 (Th1) cells are crucial in the development of BD, with studies showing that patients with active BD exhibit increased Th1 cell counts and higher levels of associated cytokines like IFN-γ, compared to those with inactive BD and healthy individuals. In conditions involving non-infectious ocular inflammation, like BD, sarcoidosis, and Vogt–Koyanagi–Harada (VKH) syndrome, Th1 cell infiltration is also notably elevated (113). Additionally, Ye et al. (114) underscored the role of decreased B and T lymphocyte attenuator (BTLA) in BD, as this decrease intensifies Th1 and Th17 cell activity, exacerbating BD-related ocular inflammation. Investigating this pathway could provide potential therapeutic avenues for BD uveitis. Interestingly, VKH syndrome, the second leading cause of uveitis, does not seem affected by BTLA reduction. Additionally, Th1-associated cytokine mRNA expression is notably increased in the mucocutaneous lesions of BD patients (113-115).

1.4.3 T Helper 17 Cells

Th17 cells are of great interest due to their involvement in numerous inflammatory and autoimmune diseases, including IBD, RA, MS, and psoriasis (116). In mouse models, the development of Th17 cells from naive T cells is mainly regulated by IL-6 and transforming growth factor-β (TGF-β). Additionally, cytokines like IL-1 and TNF-α further promote Th17 cell differentiation in their presence. Interestingly, TGF-β, which usually suppresses most T cell responses and enhances regulatory T cell (Treg) formation, paradoxically enhances Th17 cell development (117). Research by Xu et al. (118), demonstrated that Treg cells can convert into inflammatory Th17 cells when exposed to IL-6, losing their suppressive function and potentially intensifying Th17-driven inflammation. This intricate interaction highlights the vital role of Th17 cells in the etiology of immune-mediated diseases.

Various research has presented different viewpoints on the impact of TGF-β in Th17 cell differentiation. Some studies suggest that TGF-β is essential for Th17 cell differentiation, particularly when utilizing naive T cells from cord blood. The TGF-β concentration is crucial, as lower levels promote Th17 differentiation, while higher levels favor Treg differentiation. On the other hand, conflicting studies propose that although TGF-β is necessary for Th17 cell differentiation in mice, it inhibits Th17 cell generation in humans. This discrepancy complicates the translation of knowledge from murine models to human clinical contexts (116, 118-122). Additional research is required to elucidate the complex effects of TGF-β on Th17 cell differentiation and its implications in various diseases.

Th1 cells were originally thought to be the primary mediators of BD; however, extensive research has shown a heightened number of Th17 cells in BD patients, indicating their involvement in BD etiology (123-125). BD patients display elevated levels of both Th17 and Th1 cells, alongside a significant rise in Th17-related cytokines, such as IL-22 and TNF-α. Moreover, the transcription factor retinoic acid-related orphan receptor γ (RORγt), crucial for Th17 cell differentiation, is elevated in BD patients (115, 123, 126). In conclusion, Th17 cells play a pivotal role within the immune response framework of BD, enhancing our understanding of the disease's cause and showing promise for advancing future treatment options.

1.4.4 Natural Killer T Cells

NKT cells release cytokines such as IL-10, IFN-γ, IL-4, TNF, and IL-17 when they are activated. Various cytokines are produced based on criteria such as the subtype of NKT cells, the strength of the signaling, and the type of antigen-presenting cells (APCs). Deficiencies in NKT cells are important indicators for several diseases and are undergoing research for potential therapeutic and preventative interventions (127-130).

In individuals with BD involving ocular symptoms, there is a rise in the NKT cell numbers, particularly the CD56+CD8+ NKT subset in the aqueous humor (109). Nevertheless, findings on NKT cell levels in the BD patients peripheral blood vary, with some investigations reporting an enhancement, while others show a decline (131). In BD patients with neurological symptoms, higher levels of IFN-γ-expressing NKT cells are observed in

the cerebrospinal fluid (CSF) during active disease phases, with these levels dropping as patients enter remission. This phase also correlates with a decrease in NKT cell activity in the blood (132).

1.4.5 Gamma-Delta (γδ) T Cells

γδ-T cells, which differ from typical αβ T cells, usually do not express CD8 or CD4 markers and do not depend on MHC class I or II molecules for recognizing antigens (133). These cells expand significantly in the blood during infections. In mouse models, γδ T cells have been identified as the main producers of IL-17, a key pro-inflammatory cytokine essential in diseases like BD, especially during the early stages.

There are two main subgroups of γδ T cells that produce IL-17. The first group is natural Tγδ17 cells, which are found in the bloodstream and become active when exposed to infections. These cells release IL-17 and other cytokines as part of their immune response. The second group is induced γδ T17 cells, which rapidly multiply upon infection without needing clonal expansion. Despite this different approach, they are essential in fighting off pathogens. This ability of γδ T cells to release IL-17 in two distinct ways demonstrates their flexibility in regulating the immune system. Additionally, γδ T cells possess a distinctive capability to act as professional APCs. Several studies have shown their effectiveness in stimulating other immune cells, such as CD4+ and CD8+ T cells, in lymph nodes (134-137).

The proportions of γδ T cells are considerably different in active BD patients in contrast to HCs and those with inactive BD (110). These unique T cells release high levels of cytokines, which amplify neutrophil activity and stimulate Th1 and Th17 cell responses (138). Within the framework of BD, the noteworthy elevation of the Vγ9Vδ2 T cell phenotype in patients is particularly intriguing. These cells contribute to inflammation by producing cytokines like IL-17 and cytotoxic molecules such as granzyme A, both of which are implicated in BD's pathogenesis (139, 140).

The connection between BD and γδ T cells was first identified in the early 1990s, with studies documenting elevated levels of these cells in the BD patients' PBMCs (141, 142).

Upon activation, these cells release IFN-γ and TNFα (143). Notably, γδ T cells play a crucial role in modulating the adaptive immune reaction by producing cytokines like IFN-γ and IL-4, which can affect the balance of immune response towards Th1, Th2, and Th17 CD4+ T cell profiles. In a recent research, Abbasova (144) evaluated IL-17, IL-22, IFN-γ, and CD107a in γδ T cells from PBMC after stimulating them with PMA-ionomycin and reposted increase in only IFN-γ production in BD compared to healthy γδ T cells.

Additionally, γδ T cells are known to interact efficiently with neutrophils and monocytes following exposure to bacterial antigens during acute infections. Their functional adaptability allows them to play a crucial role in conditions like BD, which affects multiple body systems. There is conflicting evidence regarding these cells' role in the disease. An boost in γδ T cell numbers has been detected in various studies (141-143, 145), whereas other studies have not observed a substantial rise in this cell subset in the PBMCs of BD patients (135, 146, 147).

1.4.6 Regulatory T (Treg) Cells

Tregs are a subset of T cells known for expressing the forkhead box protein P3 (FoxP3), and they have a crucial function in preserving immune equilibrium and averting autoimmune reactions (148-151). It is clear that any dysfunction or decrease in the number of these Tregs can contribute to autoimmune conditions, as demonstrated by diseases such as SLE, MS, myasthenia gravis, and RA (148).

Research on Tregs in BD has yielded contradictory results. A reduction in Treg cell numbers has been suggested by some studies in BD patients, potentially linked to higher IL-21 levels, which correlates with disease activity (107). In contrast, another study examining BD patients with neurological involvement found an elevation in Treg levels in cerebrospinal fluid compared to those with non-inflammatory neurological conditions. However, these Tregs seemed to lose their ability to control T helper responses, implying a potential decrease in their functionality. Additionally, in inflammatory settings with IL-2 and IL-1β presence, these cells were observed transitioning into Th17 cells (152). The ambiguous role of Treg cells in BD, where their numbers may vary under different

circumstances while their effectiveness diminishes, underscores the intricate immune mechanisms involved in this condition.

1.4.7 Natural Killer Cells

Natural killer cells (NK cells) are a crucial element of the innate immune system. They communicate with HLA class I molecules, that act as ligands for their KIR receptors. In various autoimmune conditions like MS, SLE, RA, and Sjögren's syndrome, NK cell numbers and functionality are often diminished. NK cells are classified into two primary types:

1) $CD56^{bright}CD16$ NK cells, mainly located in lymph nodes, are specialized in cytokine secretion.
2) $CD56^{dim}CD16+$ NK cells, mainly found in the blood and areas of inflammation, primarily perform cytotoxic actions using proteins such as granzyme and perforin, although they release fewer cytokines than the former group (153, 154).

In BD, a decrease in the number of NK cells in the blood is similarly noted, potentially due to their relocation to sites of inflammation. Remarkably, within the NK cell subset, there is a rise in $CD56^{bright}$NK cells, recognized for their production of cytokines, particularly IFN-γ (155, 156).

NK cells can be classified into five groups depending on the cytokines they produce: NK-reg, NK-1, NK-2, NK-17, and NK-22. Each category is linked to the secretion of certain cytokines like IL-10, Th1, Th2, IL-17, and IL-22, respectively. Research in people with BD shows an increased percentage of NK-1 cells and reduced percentages of NK-2, NK-17, and NK-reg cells. Research has revealed a significant change in the NK-1/NK-2 ratio during the active versus remission periods of BD, with NK-1 driving a Th1 response in active disease and NK-2 promoting a Th2 response during remission (108, 157, 158).

1.4.8 Neutrophils

Individuals with BD often show enhanced neutrophil activity and increased neutrophil count, which has been confirmed by multiple studies. Furthermore, active patients with BD have raised levels of G-CSF, which contributes to increased neutrophil apoptosis (159). Furthermore, multiple studies have found a heightened neutrophil-to-lymphocyte ratio in patients with BD, emphasizing its possible usage as a marker for BD and the severity of the disease (160, 161). Le Joncour et al. (162) displayed increased levels of neutrophil extracellular traps (NETs) and related markers such as myeloperoxidase and cell-free DNA in individuals with BD, suggesting their involvement in the disease's etiology. NETs were detected in papulopustular BD lesions (106). Neutrophils concentrate prominently in all sorts of BD lesions, including those that impact on the mucocutaneous areas, skin, and eyes. Hyperactive neutrophils in patients with BD cause tissue damage mediated by reactive oxygen species (163).

1.4.9 Dendritic cells (DCs)

Dendritic cells (DCs) are integral to the immune system, playing a critical role as antigen-presenting cells that mediate the connection between innate and adaptive immunity. These cells are broadly classified into conventional DCs (further divided into cDC1 and cDC2 subsets), plasmacytoid DCs (pDCs), inflammatory DCs, and Langerhans cells (164). Each subset has unique surface markers, developmental origins, and functional roles. Among them, pDCs are a distinct population that specializes in recognizing viral and bacterial pathogens as well as endogenous DNA through Toll-like receptors (TLR7 and TLR9) (165). Although pDCs are not typically present in the skin under physiological conditions, they migrate from the bloodstream to sites of skin injury, where they produce substantial amounts of type I interferons, particularly IFN-α. This response contributes to inflammation and tissue damage, and the involvement of pDCs has been documented in various autoimmune conditions, such as psoriasis, SLE, and lichen planus, as well as in cutaneous malignancies. High expression of the CD123 marker is a key feature for identifying these cells (166).

In BD, pDCs appear to contribute to immune dysregulation. Elevated IFN-α production by pDCs has been observed in BD patients. Unstimulated PBMCs from BD patients exhibit a significantly higher percentage of IFN-α+ pDCs in comparison to healthy controls (HCs) and patients with ankylosing spondylitis (AS). This disparity disappears upon stimulation, but the mean fluorescence intensity (MFI) of IFN-α+ pDCs remains significantly higher in BD patients (167). Notably, serum IFN-α levels are consistently elevated in BD, whereas IFN-β levels are lower than those seen in HCs or AS patients, further emphasizing a skewed type I interferon response (168).

Aberrations in DC function are further implicated in the Th1/Th17 polarization characteristic of BD. In BD lesions, CD11c+ DCs express IL-23A, which supports the activation of Tc17 cells. These Tc17 cells are predominantly localized in perivascular regions of the dermis and subcutaneous tissue, rather than the epidermis, as seen in psoriasis. This distinct localization pattern underscores the specific role of DCs in driving the inflammatory environment in BD (106). Additionally, epigenetic modifications in dendritic cells contribute to immune dysregulation in BD. Reduced expression of interferon regulatory factor 8 (IRF8), an important transcription factor in DC differentiation and function, has been reported in monocyte-derived dendritic cells (moDCs) from patients with active ocular BD. Treatment with 5-Aza-2'-deoxycytidine (DAC) restores IRF8 expression and normalizes DC function, providing insights into potential therapeutic targets (169). Moreover, the interplay between CXCL16 expression and IFN-α production has been explored in BD. Although the percentage and MFI of pDCs expressing CXCL16 do not differ significantly among BD patients and controls, serum levels of CXCL16 and IFN-α are elevated in BD. A positive correlation has been identified between pDCs expressing CD123+CXCL16+ and IFN-α levels in BD, suggesting a potential link between these molecules in disease pathogenesis (170).

1.4.10 B cells

In BD, alterations in the composition and function of B lymphocyte subsets have been documented. Notably, a study comparing BD patients with healthy controls (HC) revealed an augmented presence of activated and memory B cell subsets in BD patients, although no significant change was observed in the total B cell count (171). In a separate study conducted by Suzuki et al, B lymphocyte functionality was assessed in 23 Behçet's disease patients across various disease stages. Patients with active disease displayed heightened numbers of spontaneously secreting immunoglobulin-secreting cells compared to those with inactive disease. Additionally, B cells from active BD patients exhibited reduced responsiveness to the T cell-independent B cell mitogen, Staphylococcus aureus Cowan 1, whereas nearly all BD patients showed unresponsiveness to the T cell-dependent polyclonal activator, pokeweed mitogen. These findings underscore the potential involvement of B cell abnormalities, some correlating with disease activity, in the pathogenesis of BD (172). Additionally, B cells were found in active mucosal ulcers (173), and it was demonstrated that the removal of B cells was useful in reducing the severity of the ocular condition (174). Furthermore, investigations by Hetta et al depicted a notable reduction in both total and regulatory B cell counts in BD patients in comparison with HC counterparts. Regulatory B cells (Bregs), particularly, displayed upregulation in cases associated with genital ulcers or vascular manifestations. Importantly, Bregs, rather than total B lymphocytes, exhibited correlations with Behçet’s Syndrome Activity Score (BSAS) and erythrocyte sedimentation rate (ESR), indicating potential involvement in disease activity. Conversely, neither total B lymphocytes nor Bregs showed significant associations with C-reactive protein (CRP) levels, sexual function, or depression scores. Noteworthy, among administered medications, low-dose aspirin intake correlated with notably elevated proportions of B-regs (175).

Traditionally, B cells were presumed absent in the skin, with research on the skin immune system primarily focusing on other leukocyte populations. However, recent revelations indicate the presence of B cells in healthy human and mammalian skin, suggesting putative roles in host defense, microbial community regulation, and wound healing. In various autoimmune conditions with cutaneous manifestations, the involvement of B cells and antibodies was traditionally considered systemic, with autoantibodies originating in

lymphoid tissues and disseminating into the skin to induce pathology. New evidence, however, underscores the role of B cells as key players within the immune infiltrates in autoimmune and inflammatory skin conditions. Elevated B cell counts have been observed in lesional skin relative to control samples across various inflammatory conditions, including psoriasis, pemphigus, lupus profundus, systemic sclerosis, Sjögren's syndrome, discoid lupus erythematosus, atopic dermatitis, IgG4-related skin diseases, and allergic contact dermatitis. This augmentation in skin-infiltrating B cells suggests their potential role in cutaneous inflammation, a notion supported by the effectiveness of systemic B cell depletion using rituximab in several of these diseases (176).

1.5 Single-cell RNA sequencing

Single-cell RNA sequencing (scRNA-seq) is a robust methodology utilized in the realm of immunology research. This technique enables the examination of gene expression at the individual cell level, facilitating a deeper understanding of immune cell heterogeneity and functionality. Traditional cell-based assays predominantly focus on measuring the average response of a cell population, assuming this average response is representative of each individual cell. However, this approach may overlook crucial information about small yet potentially significant subpopulations. The presence of genetic and environmental variability among different cell types, results in distinct behaviors and implications in pathological conditions, rendering conventional analyses inadequate (177). Consequently, the development of novel technologies for isolating individual cells from complex samples and investigating their genomes and proteomes has the potential to shed light on genome variability and gene expression mechanisms. It is widely acknowledged that single-cell analyses have far-reaching implications across various disciplines, including biomedical research and life sciences (178).

Early on, researchers employed low-throughput single-cell analysis techniques, like single-cell PCR, fluorescence in situ hybridization (FISH), and immunofluorescence to detect specific molecular markers in individual cells (179, 180). Although these methods could measure a limited number of parameters per cell, the introduction of high-throughput genomic technologies, such as DNA and RNA sequencing, has transformed the field. Nevertheless, genomic studies typically rely on analyzing collective averages derived from pooling

thousands to millions of cells, thereby hindering comprehensive genome-wide assessments of cell-to-cell variability. Consequently, the emergence of single-cell sequencing was deemed essential in research, earning it the distinction of being named the "method of the year" by Nature Methods in 2013.

ScRNA-seq is a potent methodology employed for evaluating transcriptomics at the individual cell level. While high-throughput RNA sequencing has become a crucial tool for profiling gene expression at the mRNA level (181), scRNA sequencing has demonstrated its advantages (such as the capability of identification of rare cell populations and mutations in individual cells, and antigen-specific T-cell or B-cell receptors) and gained popularity within the life sciences domain (182). Nonetheless, the inherent challenge of scRNA sequencing lies in the limited RNA content present in individual cells. Recent advancements in scRNA sequencing technology have significantly enhanced its capabilities, enabling a broader spectrum of researchers to leverage this sophisticated tool in diverse fields of study, including embryonic development, cancer biology, and immunology (183-185). Although the utilization of scRNA sequencing in dermatology research remains relatively limited, its potential as a promising method for uncovering insights beyond the reach of conventional approaches is undeniable.

Even though extensive research has explored the immune dysfunctions in peripheral blood of BD patients, high-throughput analyses of skin tissue, a common site of BD pathology, remain limited. In this study, we address this gap by performing single-cell RNA-seq analysis and flow cytometry on BD skin tissue and PBMCs. By integrating single-cell data from PBMCs and skin samples, we further elucidated the specific immune cell subtypes infiltrating BD skin lesions. Furthermore, we demonstrate differential gene expressions, activated pathways, and T cell clonality in immune cells present in BD skin lesions.

1.6 Objectives

Objective 1: To have a comprehensive understanding of the immune cell types in Behcet's disease skin lesions using flow cytometry and scRNA-seq.

Objective 2: To detect the key molecular pathways involved in Behcet's disease pathogenesis by using scRNA-seq.

Objective 3: To determine the presence and frequency of common and rare T cell clones in different BD patients and to determine the sequence of paired TCR α/β chains by scRNA-seq.

Single-cell RNA sequencing, immune profiling, and clonality analysis have not been performed in BD before. By analyzing patient-derived lesional skin tissue, our project will make it possible to delineate the contribution of local inflammatory pathways and adaptive immune systems to Behcet's disease pathogenesis.

CHAPTER 2

MATERIAL AND METHODS

CHAPTER 2

MATERIAL AND METHODS

2.1. Sample collection

Peripheral blood and skin tissue samples were obtained from active BD patients, who were not using any immunosuppressive drugs, were diagnosed according to the criteria specified by the International Study Group for Behcet's Disease, and agreed to participate in this study. Samples were collected from 3 centers:

1) Koç University Hospital, Dermatology and Plastic Surgery
2) Istanbul Başakşehir Çam and Sakura Hospital, Behçet's disease outpatient clinic (Rheumatology & Dermatology)
3) Ankara University, Department of Dermatology and Venereology

Skin samples of BD patients: After sterilization and local anesthesia, a 4 mm biopsy sample was taken from the lesional zone using a punch technique. The tissues were preserved in MACS® Tissue Storage Solution (130-100-008, Miltenyi Biotec, Germany) while being transported to the laboratory. Skin samples were used directly for tissue dissociation and cell suspension preparation before freezing.

Skin samples for healthy control group: Skin samples for healthy control (HC) were collected via surgical excision using a scalpel from individuals undergoing cosmetic procedures at Koç University Hospital. These samples were cut into 150-170 mg pieces for tissue dissociation.

2.2. Sample processing

Isolation of PBMCs: Peripheral blood samples (15 ml) were obtained from 41 active Behçet's disease patients using BD Vacutainer tubes containing K2EDTA. Each blood sample was mixed with PBS in a 1:1 ratio and carefully layered over an equal volume of density gradient medium (Lymphoprep, 1.077 g/ml; Axis-Shield, Norway). The mixture then underwent centrifugation at 500 × g for 30 minutes at ambient temperature, with the brakes turned off.

Afterwards, the PBMC layer was carefully isolated, washed with an equivalent volume of PBS containing 1% BSA, and centrifuged again at the same speed for 5 minutes. The resulting cell pellet was washed, resuspended, and preserved at -80 °C in a cryoprotective solution composed of 10% DMSO and 90% FBS. After 72 hours of initial freezing, for long-term preservation, the cryovials were stored in liquid nitrogen.

Processing of Skin Samples: Skin tissue samples were washed with PBS, and visible subcutaneous fat was removed. The tissues were then dissociated using both enzymatic and mechanical methods, following the protocol of the Whole Skin Dissociation Kit (130-101-540, Miltenyi Biotec, Germany). Specifically, 435 µL of Buffer L was combined with 12.5 µL of Enzyme P in a gentleMACS C tube (130-093-237, Miltenyi Biotec, Germany). To this mixture, 50 µL of Enzyme D and 2.5 µL of Enzyme A were added. The tissue samples were combined with the enzyme mixture and incubated at 37 °C. To refine the protocol, incubation times of 1, 3, and 16 hours were tested using healthy skin samples. Considering that Enzyme P enhances cell yield but might degrade certain immunological epitopes, comparisons of samples processed with and without this enzyme were also performed.

Following enzymatic treatment, 500 µL of cold DMEM (Gibco, USA) was added to each tube, and the samples were subjected to mechanical dissociation using the gentleMACS Octo Dissociator (Miltenyi Biotec, Germany), following the “h_skin_01” program. The resulting cell suspensions were briefly centrifuged and passed through a 70 µm cell straine (83.3945.070, Sarstedt, Germany) using 4 ml of DMEM for washing. The filtered cells were then centrifuged at 350 × g for 10 minutes, and the pellet was resuspended in 1 ml of PBS. Live cell counts were determined using the trypan blue exclusion method.

Based on the cell viability count, between one-quarter to half of the total cells (approximately 10^5 cells) were immediately stained and analyzed by flow cytometry, while the remaining cells were cryopreserved in 1–2 aliquots for later analyses, including single-cell RNA sequencing. Aliquots containing approximately 10^5 to 3×10^5 skin cells were stored in 1 ml of a solution comprising fetal bovine serum and 10% DMSO.

2.3. Flow Cytometry Immune phenotyping

The final antibody panel (Panel 1) for HC and BD skin samples and paired PBMC BD samples is shown in Table 1. In the next steps, PBMC samples from BD patients and healthy individuals were used for analysis of different cell types using 2 more panels demonstrated in Table 2 (Panle2) and 3 (Panel 3).

Both skin and PBMC samples underwent multicolor staining for surface and intracellular markers. Approximately 10^5 cells per sample were prepared for flow cytometry. Cell suspensions in PBS were centrifuged at 500 × g for 5 minutes, after which the supernatant was discarded, and the cells were resuspended in 100 µL of PBS. To assess cell viability, 1 µL of Zombie NIR fixable viability dye was applied, and the mixture maintained on ice in the dark for 10 minutes. Following this step, 2 mL of FACS buffer (PBS with 1% BSA) was added, and the tubes were then centrifuged with the same conditions. The supernatant was carefully discarded, and cocktail of surface antibodies were added to the resuspended cells, followed by a 20-minute incubation in the dark and subsequent washing with FACS buffer.

Then, fixation and permeabilization was performed with 20 minutes incubation of cells in 500 µL of Fixation Buffer (BioLegend, USA; 420801), centrifugation, and washing with 1× Intracellular Staining Permeabilization Wash Buffer (BioLegend, USA; 421002). Subsequently, the fixed cells were treated with intracellular antibody cocktails for 20 minutes at an ambient temperature. After this step, another washing step with permeabilization buffer, and the final pellet was resuspended in FACS buffer.

Flow cytometry data acquisition was performed using an Attune NxT flow cytometer (Invitrogen) or a FACS Aria III cell sorter (BD Biosciences, USA). Data analysis was performed using FlowJo software, version 10.10.0 (BD Biosciences, USA), and statistical evaluations of the results were conducted by GraphPad Prism, version 10 (GraphPad Software, USA).

Table 1. Antibody Panel 1

Target antigen	Fluorochrome	Clone	Catalog	Brand
CD20	BV421	2H7	302330	Biolegend
CD45	BrV605	HI30	304042	Biolegend
CD69	BV711	FN50	310944	Biolegend
Granzyme K	FITC	GM26E7	370508	Biolegend
CD3	PE-Cy5	HIT3a	300310	Biolegend
CD158e1(KIR3DL1,NKB1)	PE	DX9	312708	Biolegend
CD158b(KIR2DL2/L3,NKAT2)	PE	DX27	312606	Biolegend
CD158f(KIR2DL5)	PE	UP-R1	341304	Biolegend
KIR2DL1/KIR2DS5	PE	143211	FAB1844P	R&D
KIR3DL2/CD158k	PE	539304	FAB2878P	R&D
CD4	PE-Dazzle 594	OKT4	317448	Biolegend
Granzyme B	PE-Cy7	QA16A02	372214	Biolegend
CD56	APC	5.1H11	362504	Biolegend
CD8	Alexa Fluor 700	SK1	344724	Biolegend
CD14	APC-Cy7	HCD14	325620	Biolegend
CD19	APC-Cy7	HIB19	302218	Biolegend
Zombie NIR			423106	Biolegend

Table 2. Antibody Panel 2

Target antigen	Fluorochrome	Clone	Catalog	Brand
CD3	PE-Cy5	HIT3a	300310	Biolegend
CD4	PE Dazzle 594	OKT4	317448	Biolegend
CD8	AF 700	SK1	344724	Biolegend
CD56	APC	5.1H11	362504	Biolegend
TCR γδ	BV 510	B1	331220	Biolegend
TCR Vα7.2	BV 785	3C10	351721	Biolegend
CD159c (NKG2C)	PE	S19005E	375003	Biolegend
Granzyme K	FITC	GM26E7	370508	Biolegend
Granzyme B	PE-Cy7	QA16A02	372213	Biolegend
CD161	BV 421	HP-3G10	339913	Biolegend
CD14	APC Cy7	63D3	367108	Biolegend
Zombie NIR			423106	Biolegend
CCR7 (CD197)	BV605	G043H7	353223	Biolegend
CD45RO	BV650	UCHL1	304231	Biolegend

Table 3. Antibody Panel 3

Target antigen	Fluorochrome	Clone	Catalog	Brand
CD11c	PE	S-HCL-3	333149	BD
CD14	BV605	M5E2	301834	Biolegend
CD16	BV421	3G8	302038	Biolegend
HLA DR	AF488	L243	307620	Biolegend
Granzyme B	PE-Cy5	QA16A02	372225	Biolegend
CD123	PE-Cy7	S18016F	396712	Biolegend
CD19	APC	HIB19	302212	Biolegend
CD3	AF700	UCHT1	300424	Biolegend
CD56	APC-Cy7	HCD56	318332	Biolegend
CD27	BV650	L128	563228	BD Horizon
Zombie Aqua				Biolegend

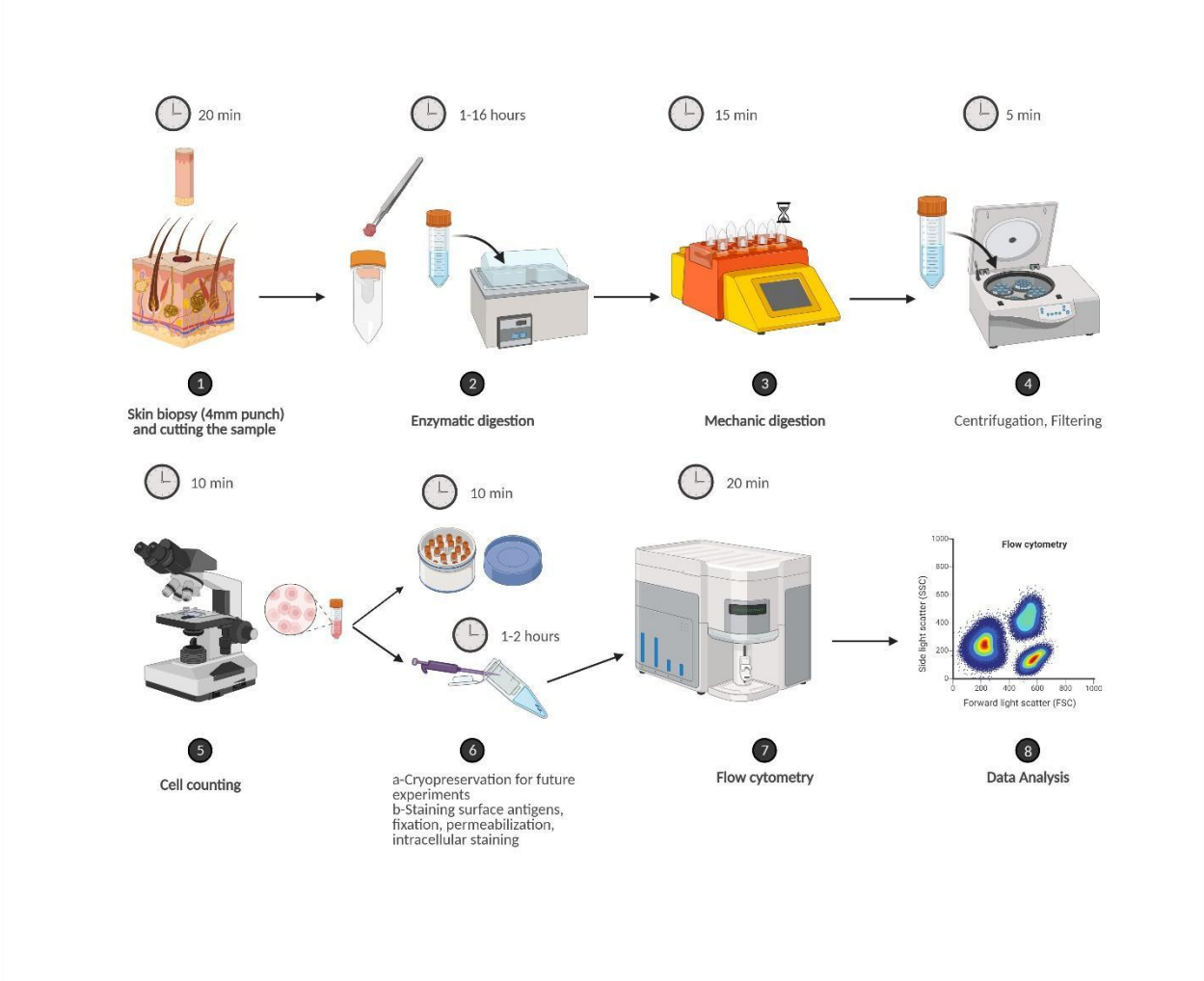

Figure 2.1. A schematic depiction of the experimental workflow. Starting with skin biopsy collection followed by two-step enzymatic and mechanical tissue dissociation via the Whole Skin Dissociation Kit. A portion of these cells were stained for flow cytometry analysis, and the rest of the cells were stored using cryopreservation for later scRNA-seq analysis.

2.4. Flow Cytometry Functional Analysis

The functional studies for skin and PBMC samples were performed as follows, and the antibody panels for PBMC and skin samples are mentioned in Table 4 and Table 5 and 6, respectively. The samples were thawed and seeded on a 96 U bottom well plate. Then anti-human CD107a antibody and Cell Activation Cocktail (without Brefeldin A) (423301, Biolegend, USA) in 100 µl of RPMI was administered to stimulate the cells. The plate was

kept at 37°C with 5% CO_2 for 1 hour. Afterward, 0.1 µl Brefeldin A was mixed in each well, and the plate was incubated for an additional 3 hours under the same conditions. Following stimulation, the plate was centrifuged at 500 g for 5 minutes at normal room temperature, and the supernatant was discarded. The cells were processed using standard protocols for surface immunophenotyping and intracellular staining in 96-well U-bottom plates. Finally, the samples were analyzed using flow cytometry.

Table 4. Antibody panel for functional analysis of PBMC samples.

Target Antigen	**Fluorochrome**
CD3	FITC
CD8	APC
CD107a	BV605
TCR γδ	PED 594
CD56	PECy5
IL17a	AF700
CD161	BV421
IFN γ	PE
TCR Vα7.2	BV785
CD4	BV510
TNFα	PECy7
CD14, CD19, Zombie	APC Cy7

Table 5. Antibody panel 1 for functional analysis of Skin samples.

Target Antigen	**Fluorochrome**
CD3	FITC
CD4	APC
CD45	BV605
TCR γδ	PED 594
CD56	PECy5
IL17a	AF700
CD161	BV421
IFN Y	PE
TCR Vα7.2	BV785
CD8	BV510
TNFα	PECy7
CD14, CD19, Zombie	APC Cy7

Table 6. Antibody panel 2 for functional analysis of Skin samples.

Target Antigen	**Fluorochrome**
CD3	FITC
CD56	APC
CD107a	BV605
CD4	PED 594
GM-CSF	PerCP/Cy 5.5
CD8	AF700
CD161	BV421
IFN Y	PE
TCR Vα7.2	BV785
TCR γδ	BV510
CD45	PECy7
CD14, CD19, Zombie	APC Cy7

2.5. Single-cell RNA Sequencing (scRNA-seq)

Sample Preparation: To optimize experimental costs and minimize batch-to-batch variability, a pooling strategy was employed, combining 2–4 samples for analysis. Cryopreserved cell suspensions were first thawed, and stained with Zombie NIR viability dye in PBS, followed by staining with anti-human CD45 PE-Cy5 in FACS buffer. Subsequently, CD45+ live cells were isolated from both skin and blood samples in parallel using Cytoflex SRT (Beckman Coulter) and FACS Aria III (BD Biosciences, USA) cell sorters. During the sorting process, key parameters were carefully maintained to ensure optimal cell viability and purity. A 100 µm nozzle was used, with a pressure setting of 20 psi. The sample chamber was kept at 4 °C, and a low sorting speed was employed. Specifically, the target sorting speed was limited to fewer than 1500 events per second, with the speed adjusted between levels 1 and 3 as needed to maintain this event rate and ensure high-quality results.

The Chromium Single Cell 5' Reagent Kit user guide recommends an optimal cell concentration ranging from 700 to 1200 cells per microliter for Gel Bead-in-Emulsion (GEM) generation. However, the cell sorting process frequently yields concentrations lower than that. This situation necessitates the concentration of the cell suspension after cell sorting. For that purpose, we undertook an extra step of centrifuging cells for 5 minutes at 850 g. After careful aspiration of the supernatant, the cells were resuspended in 40-50 µl of PBS, and count the cells again. Once the optimum cell concentration according to the Chromium Controller system and Chromium Next GEM Single Cell 5' Reagent Kits V2 (Dual Index, 10X Genomics, USA) guide was achieved, the protocol was started.

Library preparation and sequencing: Chromium Controller and the Chromium Next GEM Single Cell 5' Reagent Kits V2 (Dual Index, 10X Genomics, USA) were used for library preparation. The overall protocol steps and timing is demonstrated in Figure 2.2.

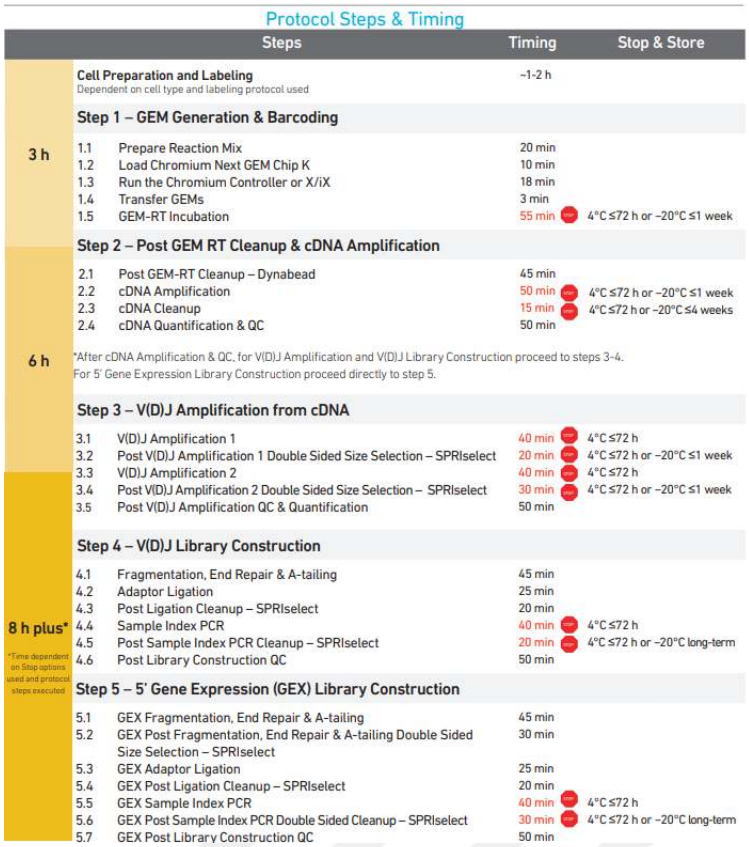

Protocol Steps & Timing

	Steps		Timing	Stop & Store
3 h	**Cell Preparation and Labeling** Dependent on cell type and labeling protocol used		~1-2 h	
	Step 1 – GEM Generation & Barcoding			
	1.1	Prepare Reaction Mix	20 min	
	1.2	Load Chromium Next GEM Chip K	10 min	
	1.3	Run the Chromium Controller or X/iX	18 min	
	1.4	Transfer GEMs	3 min	
	1.5	GEM-RT Incubation	55 min	4°C ≤72 h or –20°C ≤1 week
6 h	**Step 2 – Post GEM RT Cleanup & cDNA Amplification**			
	2.1	Post GEM-RT Cleanup – Dynabead	45 min	
	2.2	cDNA Amplification	50 min	4°C ≤72 h or –20°C ≤1 week
	2.3	cDNA Cleanup	15 min	4°C ≤72 h or –20°C ≤4 weeks
	2.4	cDNA Quantification & QC	50 min	
	*After cDNA Amplification & QC, for V(D)J Amplification and V(D)J Library Construction proceed to steps 3-4. For 5' Gene Expression Library Construction proceed directly to step 5.			
	Step 3 – V(D)J Amplification from cDNA			
	3.1	V(D)J Amplification 1	40 min	4°C ≤72 h
	3.2	Post V(D)J Amplification 1 Double Sided Size Selection – SPRIselect	20 min	4°C ≤72 h or –20°C ≤1 week
	3.3	V(D)J Amplification 2	40 min	4°C ≤72 h
	3.4	Post V(D)J Amplification 2 Double Sided Size Selection – SPRIselect	30 min	4°C ≤72 h or –20°C ≤1 week
	3.5	Post V(D)J Amplification QC & Quantification	50 min	
8 h plus* *Time dependent on Stop options used and protocol steps executed	**Step 4 – V(D)J Library Construction**			
	4.1	Fragmentation, End Repair & A-tailing	45 min	
	4.2	Adaptor Ligation	25 min	
	4.3	Post Ligation Cleanup – SPRIselect	20 min	
	4.4	Sample Index PCR	40 min	4°C ≤72 h
	4.5	Post Sample Index PCR Cleanup – SPRIselect	20 min	4°C ≤72 h or –20°C long-term
	4.6	Post Library Construction QC	50 min	
	Step 5 – 5' Gene Expression (GEX) Library Construction			
	5.1	GEX Fragmentation, End Repair & A-tailing	45 min	
	5.2	GEX Post Fragmentation, End Repair & A-tailing Double Sided Size Selection – SPRIselect	30 min	
	5.3	GEX Adaptor Ligation	25 min	
	5.4	GEX Post Ligation Cleanup – SPRIselect	20 min	
	5.5	GEX Sample Index PCR	40 min	4°C ≤72 h
	5.6	GEX Post Sample Index PCR Double Sided Cleanup – SPRIselect	30 min	4°C ≤72 h or –20°C long-term
	5.7	GEX Post Library Construction QC	50 min	

Figure 2.2. Chromium Next GEM Single Cell 5' Reagent Kits V2 (Dual Index) protocol steps and timing.

Step 1 involves the generation and barcoding of GEMs using the Chromium Next GEM Chip K (depicted in Figure 2A). In this process, a master mix comprising cells, RT Reagent B, Poly-dT RT Primer, Reducing Agent B, and RT enzyme C was loaded into row 1, barcoded Single Cell VDJ 5' Gel Beads into row 2, and partitioning oil into row 3. Subsequently, the gasket was sealed, and the chip was placed in the Chromium Controller (illustrated in Figure 2B) for Gel Beads-in-emulsion (GEMs) formation. To ensure single-cell resolution, cells were introduced at a limiting dilution, resulting in the majority of generated GEMs (approximately 90–99%) being devoid of cells, while the remainder primarily contained a single cell. After generating GEMs, the Gel Beads dissolved, releasing oligonucleotides into the lysed cells. The oligonucleotides were combined with the cell lysate and a master mix containing reverse transcription (RT) reagents and poly(dT) RT primers. Incubation of the GEMs facilitated the

synthesis of full-length cDNA tagged with 10x Barcodes, derived from the polyadenylated mRNA of the cells.

Figure 2.3. Workflow for GEM Generation Using the Chromium Next GEM Chip. Chromium Next GEM Chip K was utilized to generate GEMs. A master mix containing cells, Reverse Transcription (RT) Reagent B, poly-dT RT primer, Reducing Agent B, and RT enzyme C was loaded into Row 1 of the chip. Barcoded Single Cell V(D)J 5' Gel Beads were loaded into Row 2, while partitioning oil was added to Row 3. After loading, a gasket was attached to the chip, which was then placed in the Chromium Controller for GEM generation.

Step 2 involves the cleanup and amplification of cDNA post-GEM-RT. After the GEM-RT reaction mixtures are retrieved, GEMs are broken and pooled. Silane magnetic beads are employed for the purification of 10x Barcoded first-strand cDNA from the resulting post-GEM-RT reaction mixture, eliminating residual biochemical reagents and primers. Subsequently, 10x Barcoded, full-length cDNA undergoes PCR amplification using primers targeting the common 5' and 3' ends introduced during GEM-RT. This amplification yields a sufficient quantity of material, enabling the construction of multiple libraries from the same

cells, such as both T cell libraries (as outlined in steps 3 and 4) and 5' Gene Expression libraries (as detailed in step 5). Quality control (QC) and quantification procedures were conducted using the Agilent 2100 Bioanalyzer (Agilent Technologies, USA).

In Step 3, cDNA amplification is carried out to amplify full-length V(D)J segments (10x Barcoded) from poly-adenylated mRNA. This involves PCR amplification using primers specific to the TCR constant regions. The amplification process includes two steps, and following each PCR, double-sided size selection is performed using SPRIselect (Beckman Coulter, USA). Quality control (QC) and quantification were performed using the Agilent 2100 Bioanalyzer.

Moving on to Step 4, V(D)J library construction involves enzymatic fragmentation and size selection to generate variable-length fragments spanning the V(D)J segments of the amplified TCR transcripts. This is done prior to library construction. Through End Repair, A-tailing, Adaptor Ligation, and Sample Index PCR, P5, P7, i5, and i7 sample indexes, along with an Illumina R2 sequence (read 2 primer sequence), are added. The final libraries feature P5 and P7 priming sites necessary for Illumina sequencing. Quantification, QC, and determination of average fragment size were conducted using the Agilent 2100 Bioanalyzer.

In Step 5, the construction of the 5' Gene Expression (GEX) Library is initiated by utilizing amplified full-length cDNA obtained from poly-adenylated mRNA. To optimize the cDNA amplicon size before 5' gene expression library construction, enzymatic fragmentation and size selection are employed. The addition of P5, P7, i5, and i7 sample indexes, along with the Illumina R2 sequence (read 2 primer sequence), is accomplished through End Repair, A-tailing, Adaptor Ligation, and Sample Index PCR. The final libraries are equipped with the P5 and P7 priming sites essential for Illumina sequencers. Quantification, quality control (QC), and determination of the average fragment size were carried out using the Agilent 2100 Bioanalyzer.

Finally, paired-end sequencing was conducted using the Illumina NovaSeq 6000 platform. For 5’ gene expression analysis and TCR sequencing, the recommended reading depth of a minimum of 20,000 and 5,000 per cell were used, respectively.

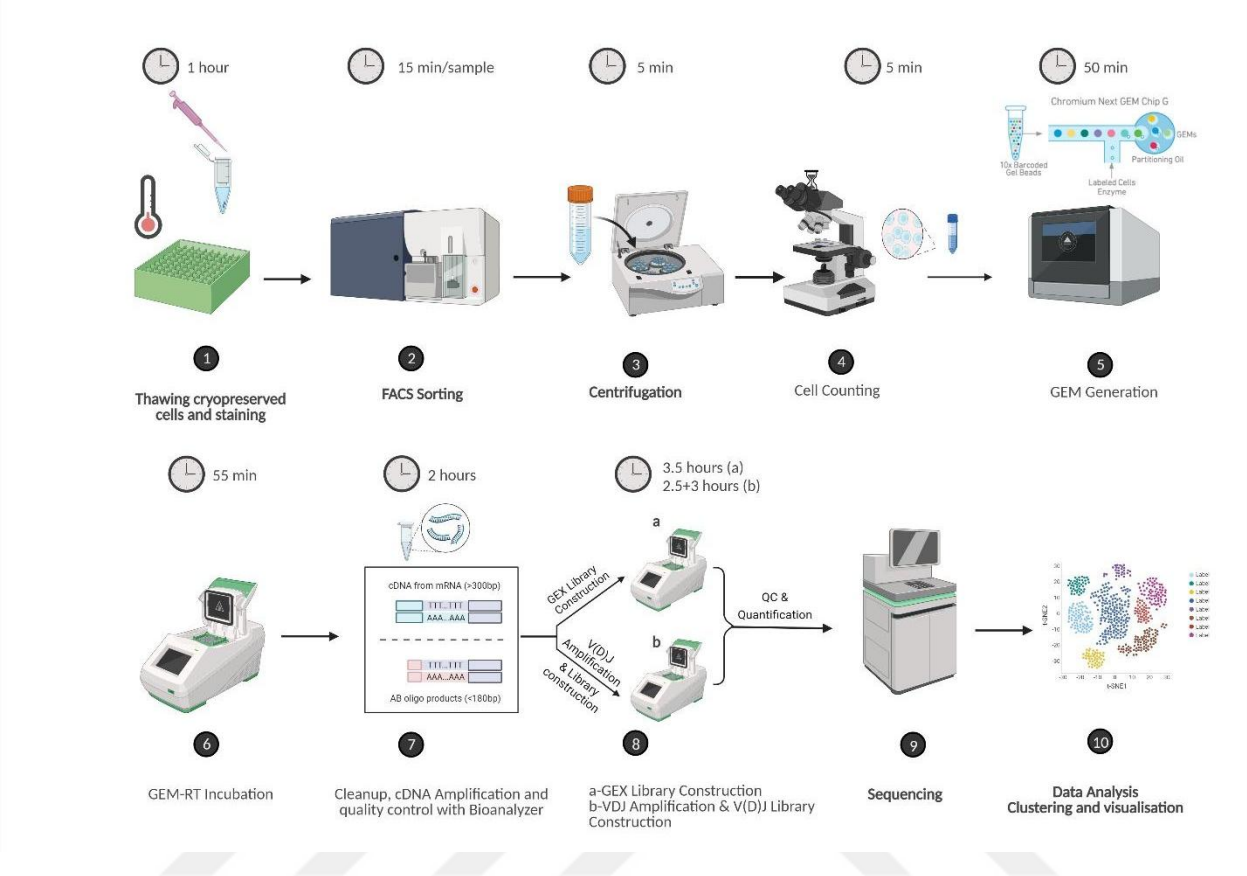

Figure 2.4. Overview of the Steps for Single-Cell Analysis. The workflow includes the thawing of cryopreserved cells, followed by sorting CD45+ live cells using FACS. Cell counting is performed using the trypan blue exclusion method. Subsequently, Gel Beads-in-Emulsion (GEM) are generated, followed by library preparation, sequencing, and data analysis.

2.6. Bioinformatics Analysis

The overall workflow of bioinformatics analysis used for scRNA-seq is demonstrated in Figure 2.5.

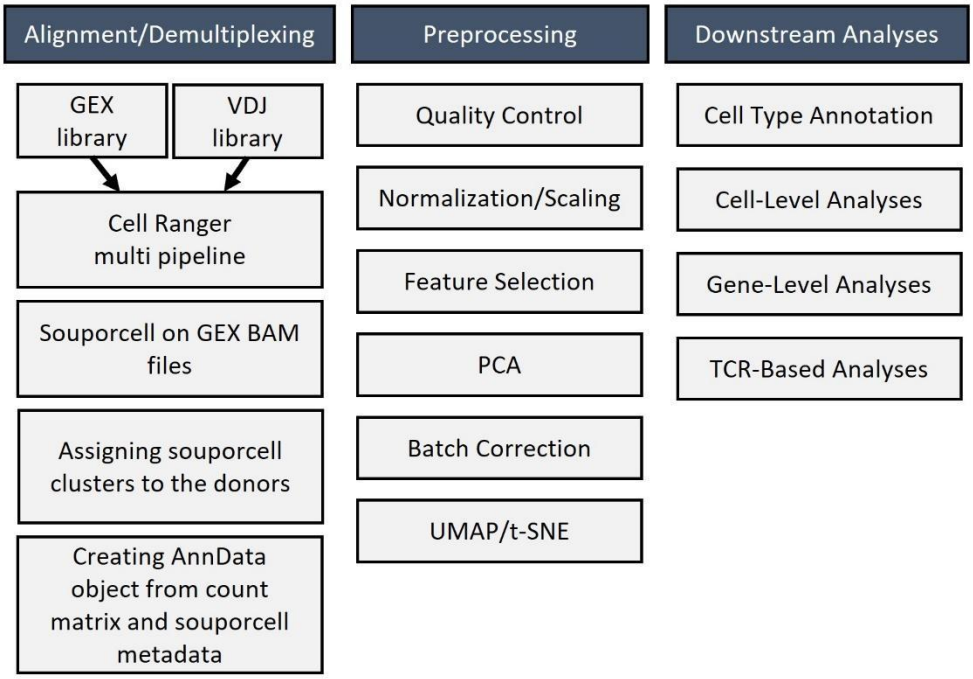

Figure 2.5. Bioinformatic analysis workflow.

2.6.1. Alignment and demultiplexing

The raw FASTQ files were aligned to the GRCh38 reference genome using the Cell Ranger multi pipeline (v7.1.0) from the official 10X Genomics platform. To demultiplex the pooled samples, the souporcell tool was utilized (186). This tool processes BAM files generated by Cell Ranger and uses SNPs observed in scRNA-seq reads to differentiate data emerging from individual donors. This labeling-free computational approach, freely available and efficient, Performed on a high-performance computing cluster utilizing the Singularity image provided by the Souporcell developers. The processing was performed with the "souporcell_pipeline.py" script, utilizing the same reference transcriptome as the initial alignment.

After demultiplexing with souporcell, cluster identification relied on two main criteria: 1) Matching genotypes observed in PBMC and skin samples from the same donor across separate reactions, and 2) determining the sex of the donor. Identification of matching PBMC and skin samples was achieved through the "shared_samples.py" module in the souporcell toolkit. The sex of each cluster was inferred by examining the expression of specific Y chromosome-associated genes (187).

2.6.2. Preprocessing and cell annotation

Following alignment and demultiplexing, the resulting count matrices were conducted using the Scanpy toolkit . Cells expressing fewer than 200 genes or genes detected in fewer than three cells, were filtered out. Additionally, cells with more than 4000 expressed genes were eliminated from further analysis to eliminate potential artifacts. To identify doublets, those flagged as cross-genotype doublets by souporcell were removed, and expression-based doublets were detected using the Scrublet tool.

Normalization of the data was performed by scaling counts to 10,000 per cell, followed by a log(x+1) transformation. Highly variable genes were then selected utilizing the “sc.pp.highly_variable_genes” function in Scanpy. A principal component analysis (PCA) was conducted on the scaled expression matrix derived from these highly variable genes. To address technical variations such as donor-specific differences and sequencing depth—while retaining biologically relevant signals like cell-type distinctions and disease-related effects—BBKNN's ridge regression approach was employed (188, 189).

Following preprocessing, datasets from different pools were integrated using the Harmony algorithm (190). The harmony-corrected principal components were then used to construct a neighborhood graph and generate UMAP embedding for downstream analysis.

2.6.3. Downstream Analysis

Differential Gene Expression (DGE) Analysis: DGE analysis was conducted using the Wilcoxon rank-sum test with Benjamini-Hochberg correction for multiple testing, as implemented in Scanpy (191). This ensured robust identification of differentially expressed genes across conditions or clusters.

Pathway and Functional Analysis: To identify enriched biological pathways and functional processes, functional enrichment analysis was performed using the decoupleR package (192) (Python implementation, version 1.6.0). This enabled the detection of significant pathways and insights into the biological mechanisms underlying the observed transcriptional changes.

Cell Type Abundance Analysis: Differences in cell type abundance between conditions were assessed using the single-cell Compositional Data Analysis (scCODA) method (193). This approach allowed for rigorous statistical evaluation of compositional changes in cell populations.

Clonality Analysis: Clonality analysis was conducted using the Scirpy package (194). Filtered contig annotations generated by CellRanger are provided to clonality analysis pipeline.

2.7. Statistical Analysis

A repeated measures one-way ANOVA was employed to evaluate differences across various incubation times. To examine the impact of enzyme P and compare paired skin and PBMC samples from BD patients, a paired t-test was conducted. For comparisons between healthy controls (HC) and BD samples, an unpaired t-test was utilized. All statistical analyses were carried out using GraphPad Prism (version 8, GraphPad Software, USA), and a significance threshold of $P < 0.05$ was applied.

CHAPTER 3
RESULTS

CHAPTER 3
RESULTS

3. 1 Optimization of Skin Sample Processing

The healthy skin samples were initially dissociated through a three-hour incubation with enzymes A and D, excluding enzyme P, followed by immediate analysis post-staining using flow cytometry. Our gating strategy and the utilization of fluorescence-minus-one (FMO) controls for dimly expressed markers are depicted in Figures 3.1 and 3.2, respectively. Employing the antibody panel outlined in this investigation enabled the prompt identification of various T cell subsets, encompassing CD4+ T THLs, CD8+ CTLs, and CD69+ resident memory T cells (TRMs), alongside NK cells. Furthermore, the assessment revealed the presence of intracellular granzyme K and granzyme B expression.

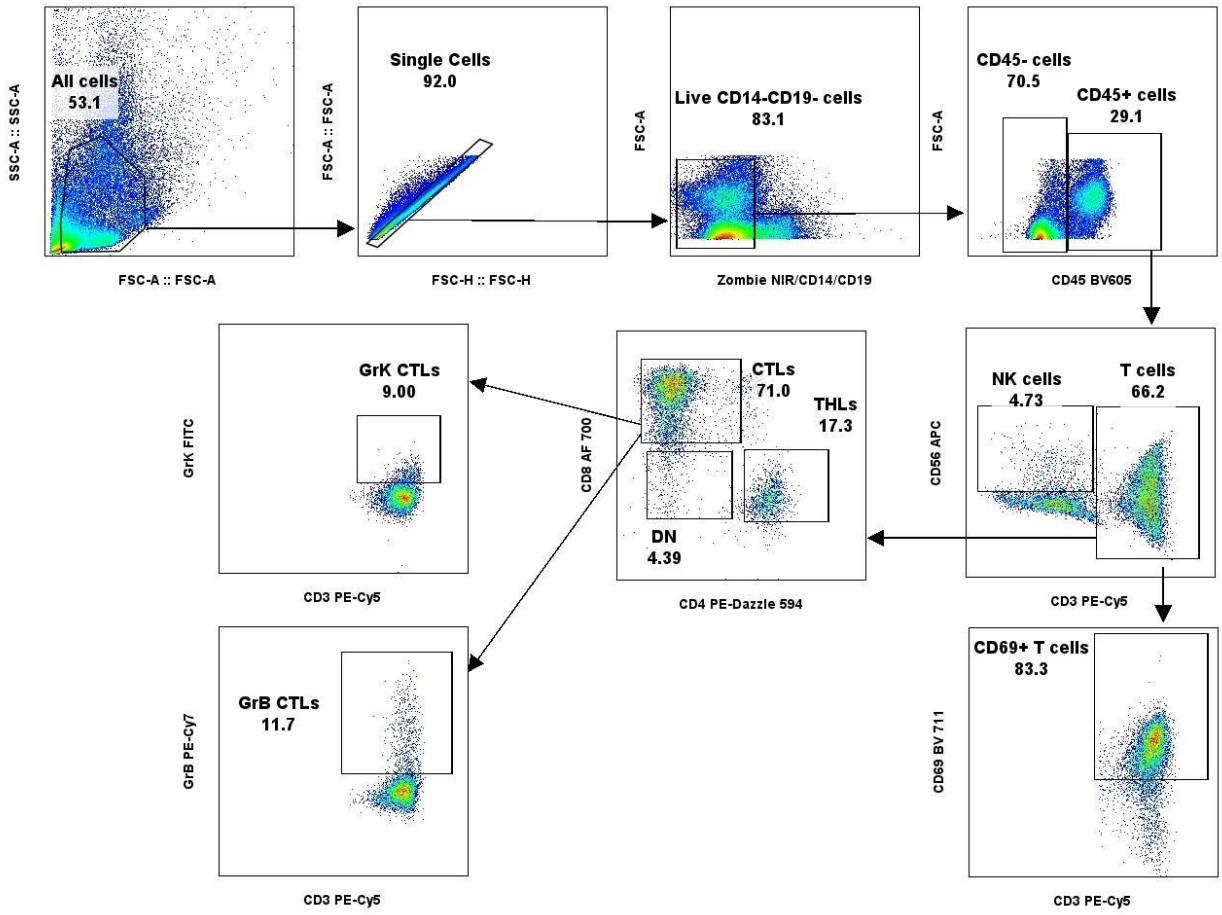

Figure 3.1. Representative gating strategy of the flow cytometry analysis. The panel used here was designed to study T cells and NK cells, therefore Zombie NIR, CD14 and CD19 were present together in the APC-Cy7 dump channel. All cells are initially gated via forward scatter (FSC) versus side scatter (SSC). Next, doublets were excluded using FSC-A versus FSC-H parameters. The Zombi NIR-positive dead cells, CD19+ B cells, and CD14+ monocytes that are in the dump channel were excluded. Then, CD45+ leukocytes were gated. After that, CD3+ T cells, and CD56+ NK cells were gated. From T cell population, distinct subtypes including CD69+ T cells (TRMs), CD8+ CTLs and CD4+ THLs were gated. Finally, from the CTLs population, Granzyme K+ and Granzyme B+ cells were gated.

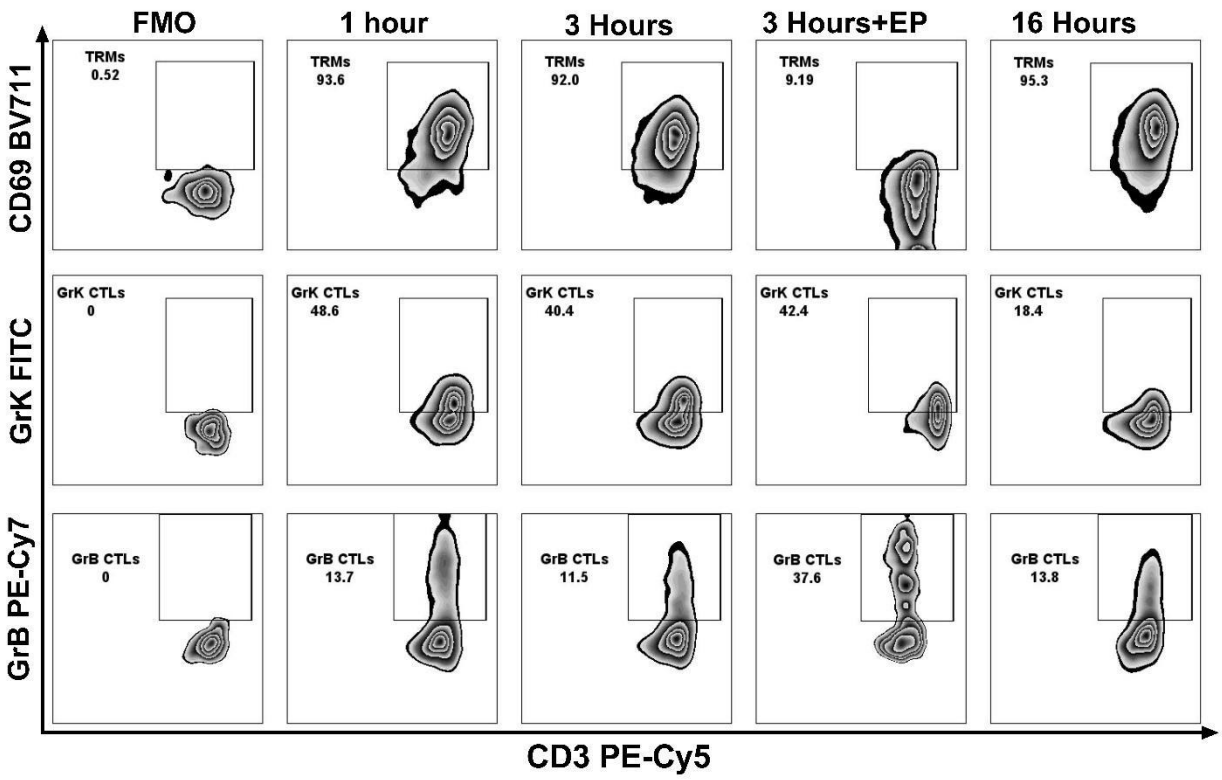

Figure 3.2. Fluorescence minus one (FMO) control for CD69, granzyme K, and granzyme B antibodies.

3.1.1. The Influence of Enzymatic Incubation Duration and Enzyme P

Prolonged incubation led to a notable rise in the retrieval of viable cells, as indicated by trypan blue exclusion (Figure 3.4A). A 1-hour incubation produced live cell counts ranging from 5.5×10^4 to 1.22×10^5, which were inadequate for downstream applications. Extending the incubation to 3 hours improved yields to between 7.5×10^4 and 1.5×10^5, while a 16-hour incubation further enhanced viability, yielding 1.15×10^5 to 2.5×10^5 live cells. Additionally, a higher percentage of CD45+ leukocytes was observed after 16 hours compared to 3 hours.

The proportions of T cells, NK cells, THLs, CTLs, double-negative cells, and TRMs remained stable across all incubation conditions (Figure 3.4A). However, a notable reduction in granzyme B+ CD8+ T cells was evident after 16 hours compared to 1 hour

(median values: 24.8, range 14.5–30.3 vs. 13.8, range 11.6–24.0; p=0.027). In contrast, the proportion of granzyme K-expressing CD8+ T cells showed no significant change.

Regarding mean fluorescence intensity (MFI), markers such as CD8, CD3, CD69, CD56, and granzyme K display consistent levels across incubation times. However, CD4 expression demonstrated a marked decrease with extended incubation (1h vs. 16h: median MFI 33,169, range 13,566–45,794 vs. 6,387, range 4,494–12,979; p=0.0077; 3h vs. 16h: 21,511, range 9,628–28,753 vs. 6,387, range 4,494–12,979; p=0.0071). Similarly, granzyme B MFI decreased significantly with prolonged enzymatic treatment (1h vs. 16h, p=0.042).

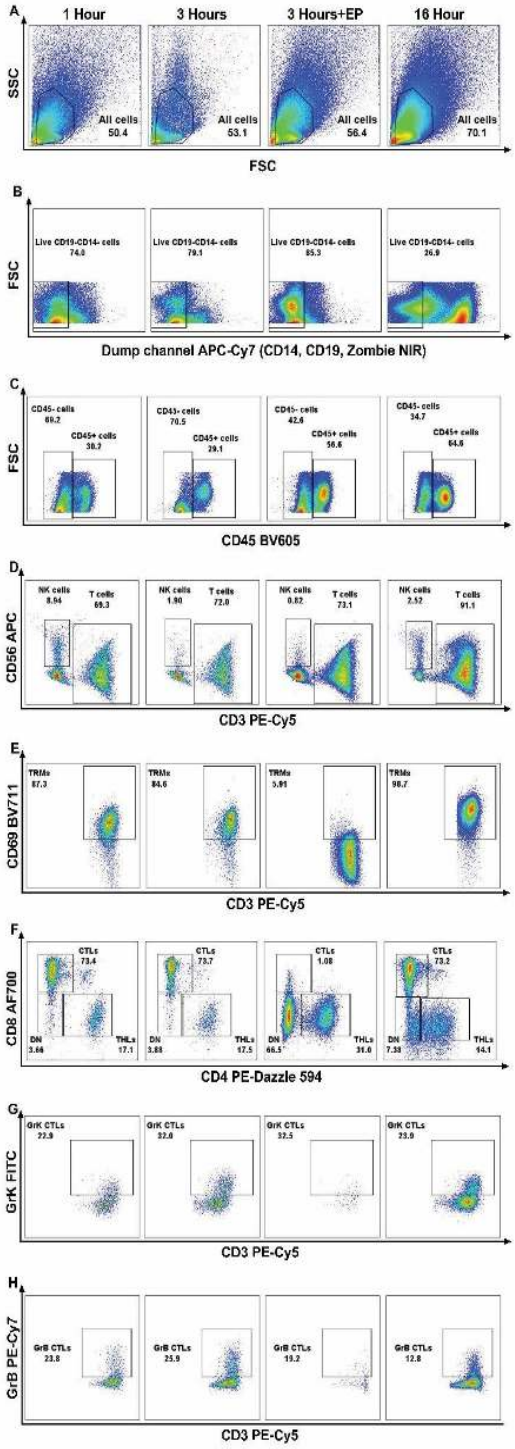

Figure 3.3. Flow cytometry plots illustrating the impact of enzymatic treatment on various cell populations under different conditions: 1-hour, 3-hour, and 16-hour incubation durations, as well as 3-hour treatment with enzyme P. Results show a significant reduction in TRM (E) and CTL (F) populations after enzyme P treatment, possibly resulting from the enzymatic breakdown of CD69 and CD8 antigens

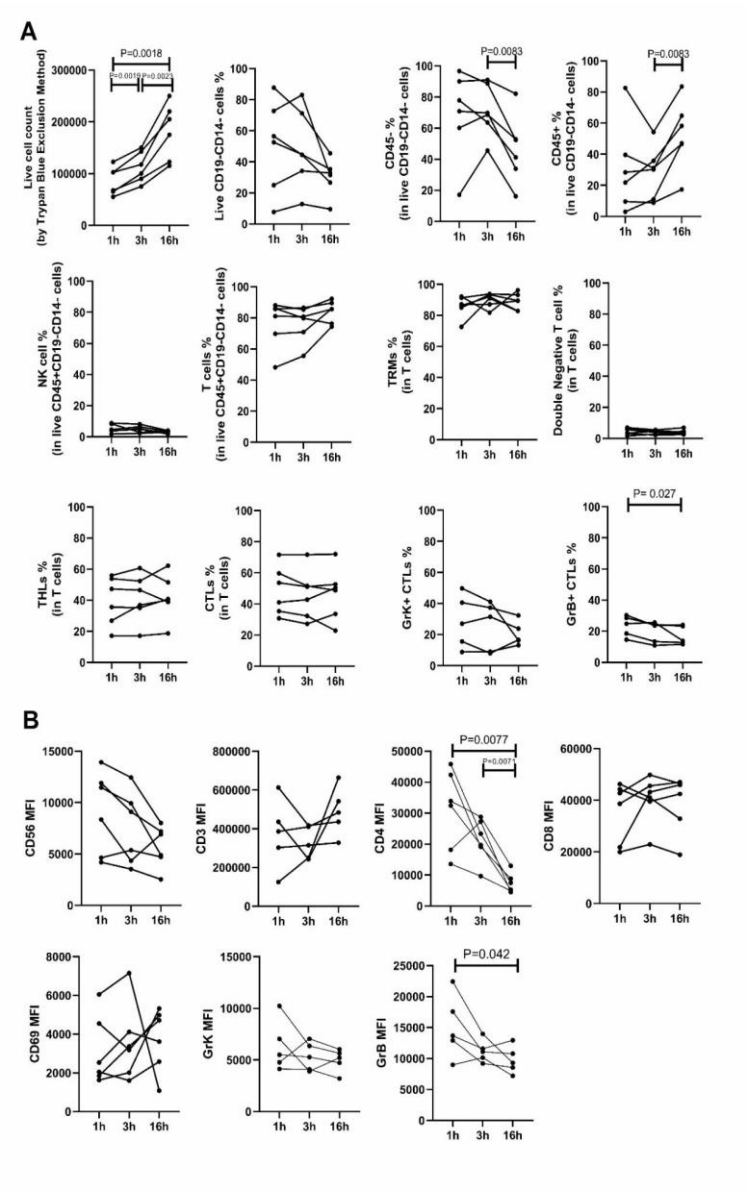

Figure 3.4. Effects of different enzymatic incubation durations (1 hour, 3 hours, 16 hours) on cell percentages (A) and MFI (B). A) Trypan blue exclusion analysis showed that cell yield improved with longer incubation times, reflecting an increase in viable cell counts. The proportion of viable CD14-CD19- leukocytes did not vary significantly in different incubation periods. However, CD45- cell percentages declined, resulting in a notable increase in CD45+ cells after 16 hours compared to 3 hours. Lymphocyte subtype percentages were largely consistent, a reduction in Granzyme B+ CTLs after 16 hours of incubation compared to 1 hour. B) MFI values for CD8, CD3, CD69, CD56, and GrK remained consistent across all incubation times. However, both CD4 and GrB MFI levels significantly decreased after 16 hours of enzymatic treatment.

In our study, we also examined the enzyme P's effects in the 3-hour incubation group (Figure 3.5). Without enzyme P, the live cell count was in the range of 7.5×10^4 to 1.5×10^5, while the inclusion of enzyme P resulted in a notable increase to 8.5×10^4 to 1.85×10^5. Enzyme P did not significantly affect the percentages of T cells, THLs, GrB+ CTLs, or GrK+ CTLs. However, a significant decline in the percentage of CTLs ($p=0.005$) and TRM cells ($p=0.044$) was seen when enzyme P was present. Additionally, NK cell percentages decreased significantly (5.03, 1.90-6.48 vs 1.25, 0.82-4.33; $p=0.026$) after enzyme P treatment. Consistent with expectations, there was a notable reduction in the MFI of CD8 ($p=0.0009$), CD56 ($p=0.039$), and CD69 ($p=0.038$) in the enzyme P-treated group in comparison to the untreated group.

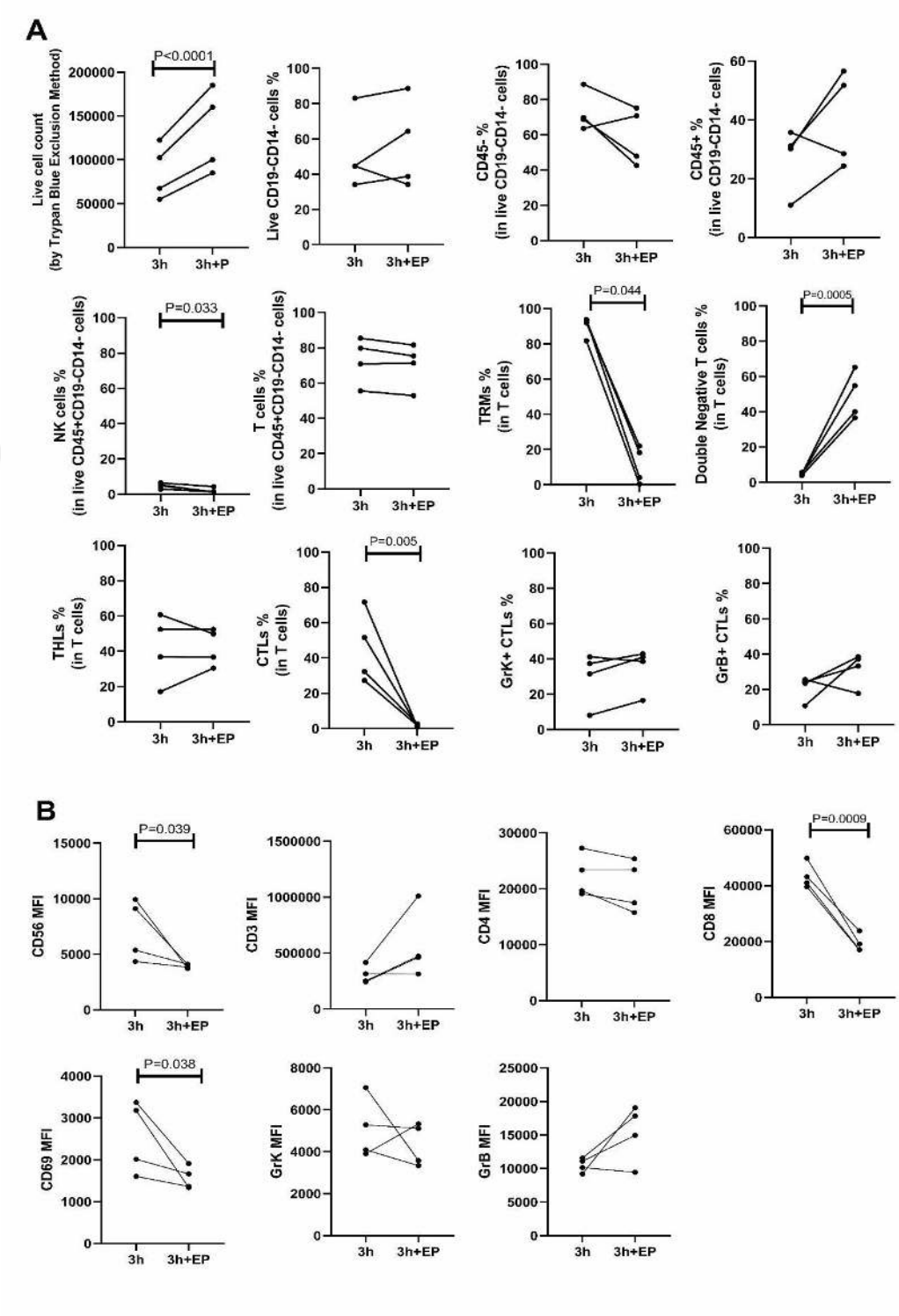

Figure 3.5. The effects of enzyme P on cell percentages (A) and MFI values (B) are presented. A) The inclusion of enzyme P resulted in an increase in overall cell yield, although the percentage of TRMs, NK cells, and CTLs showed a significant reduction. B) Enzyme P treatment led to a marked decrease in the MFI of CD8, CD56, and CD69.

Based on the outcomes of these investigations, an enzymatic incubation for 3 hours without enzyme P was selected for the lesional skin analysis to facilitate concurrent flow cytometry and scRNAseq analyses.

3.1.2. The Effect of Cryopreservation on Dissociated Skin Cells

Sample multiplexing is a valuable strategy for mitigating technical batch effects and reducing cost in scRNAseq. Nevertheless, the implementation of multiplexing with freshly isolated cells presents challenges, particularly in achieving coordinated sample collection from multiple sources. Freezing of isolated cell suspensions for long-term storage emerges as a viable approach to overcoming this logistical challenge. In our investigation, the dissociated skin cells were preserved in liquid nitrogen for later cell sorting and scRNAseq analysis. This method enabled a comparative assessment of the viability of CD45+ cells in freshly isolated and thawed samples. Our results demonstrate that the proportion of live CD45+ cells exceeded 85% in both freshly isolated and thawed skin cells, without statistically significant disparity observed between the two cohorts (Figure 3.6).

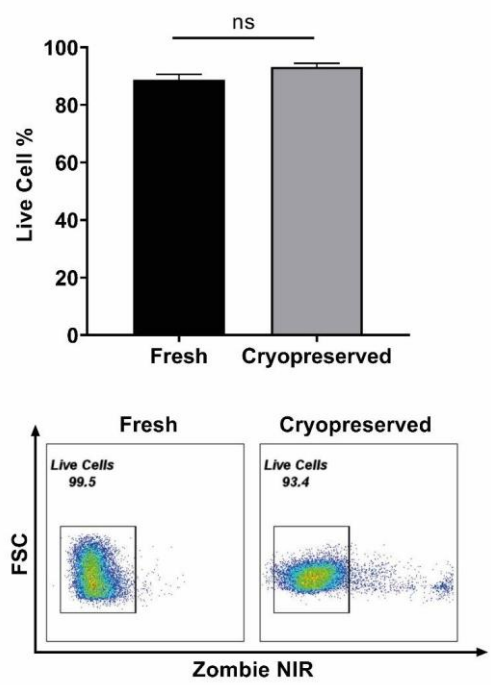

Figure 3.6. Freezing and thawing did not have a statistically significant effect on the percentage of live CD45+CD14-CD19- leukocytes, as compared to using freshly isolated cells. Statistical analysis was done with Wilcoxon matched pairs signed rank test.

3. 2 Results of Single-cell RNA Sequencing and TCR Sequencing Analysis

3.2.1. Novel Label-Free Sample Multiplexing Design and Demultiplexing Process

Current methods for multiplexing samples in scRNAseq analysis typically involve the use of sample barcoding kits. We aimed to analyze matched cutaneous and blood samples were collected from various individuals across several batches using scRNAseq. To accomplish this, we devised a new approach for sample multiplexing utilizing a recently introduced label-free demultiplexing algorithm known as 'souporcell'. This approach relies on unique SNP patterns to distinguish between genetically distinct individuals (186). Our method improves upon the original strategy by enabling the simultaneous analysis of two or more samples without requiring extra tissue barcoding procedures (195).

Initially, two samples can be combined using a simple setup, closely resembling the method described in the original study (186). Here, PBMCs and skin cells from the same individual are allocated in two distinct tubes, with an unrelated sample added to each tube (these unrelated samples are not paired). The four samples are then analyzed through scRNAseq in two separate reactions. Souporcell is used to demultiplex the samples, allowing for the identification of paired samples from the same individual based on their shared SNP profiles. Since the paired samples' identities are known, it is possible to annotate these clusters accordingly. Once the identity of one sample in each pair is confirmed, the others are easily identified. Using this strategy, nine pairs of PBMC and skin samples can be processed in just nine reactions rather than 18, effectively reducing the number of required reactions by half.

Our second step combines two types of genetic information: the shared SNP profile of paired samples and the sex of the donor (Figure 3.14). As in the first approach, PBMC and skin samples from each individual are separated into two reactions, with two unrelated samples added per tube, making three samples per tube. Importantly, the unrelated samples must come from individuals of different sexes. After conducting scRNAseq, demultiplexing using Souporcell enables the identification of matched pairs with identical SNP profiles. The sex of the remaining two samples is then determined using Y chromosome gene expression as an indicator of male sex. This information allows for the accurate identification of the remaining samples. By using this setup, nine pairs of skin and PBMC samples can be analyzed in six reactions instead of 18. Table 7 shows the samples used in each reaction.

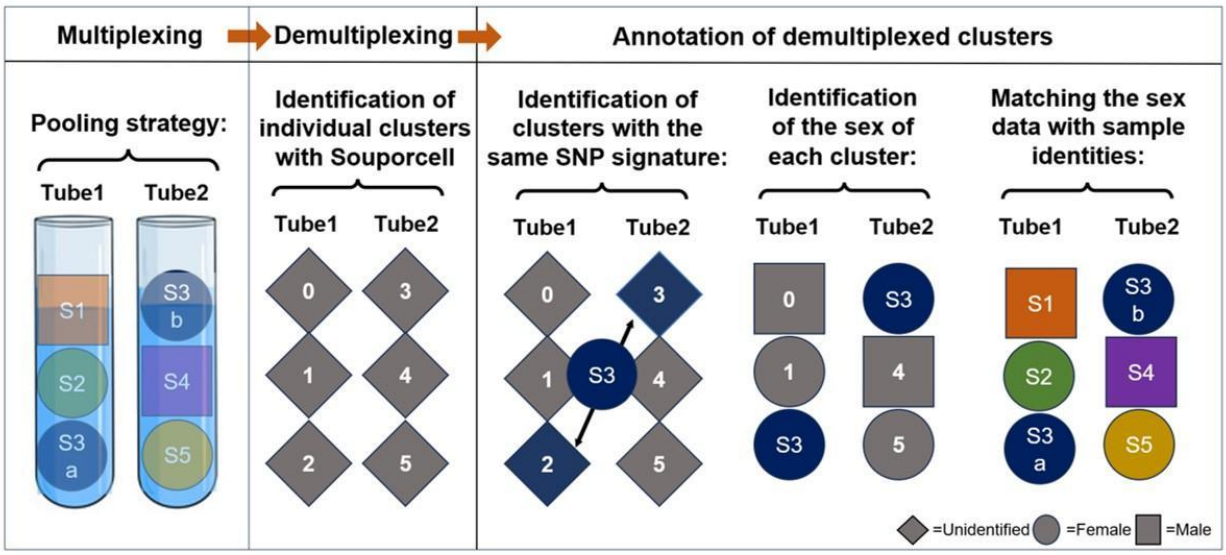

Figure 3.7. Label-Free demultiplexing Strategy for Sample Identification in Single-Cell RNA Sequencing. Diagram illustrating the label-free triplet pooling method. Initially, paired PBMCs (S3a) and dissociated skin samples (S3b) from the same individual are separated into two distinct tubes. To each tube, two additional genetically unrelated samples—one male (square) and one female (circle)—are added, resulting in a total of three samples per tube. After performing single-cell RNA sequencing (scRNA-seq) and demultiplexing with Souporcell, clusters sharing identical single nucleotide polymorphism (SNP) profiles across both reactions are identified and assigned to their corresponding samples. Next, the expression of Y chromosome genes is analyzed to determine the sex of the remaining two samples in each tube. Using this information, the identities of all remaining clusters are accurately resolved. "S" denotes sample, and different colors represent distinct individuals.

Table 7. Overview of Single-Cell RNA Sequencing Reactions. The table summarizes the experimental setup for scRNA-seq, including the multiplexing status, donor samples involved in each reaction, and their corresponding souporcell clusters. F= Female, M= Male

Reaction ID	Multiplexed	Tissue	Donors	Souporcell Cluster
Sample 1	No	Skin	HC18(F)	0=HC18
Sample 2	No	Skin	BD9(F)	0=BD9
Sample 3	Yes (2 donors)	Skin	HC13(F) + BD17(F)	0=HC13 1=BD17
Sample 4	Yes (4 donors)	PBMC	BD5(M) + BD9(F) + BD17(F) + S49(F)	0=BD5 1=BD9 2=S49 3=BD17
Sample 5	Yes (3 donors)	PBMC	BD12(F) + BD13(F) + BD14(M)	0=BD13 1=BD14 2=BD12
Sample 6	Yes (3 donors)	Skin	HC8(F) + BD5(M) + BD13(F)	0=BD5 1=HC8 2=BD13
Sample 7	Yes (3 donors)	PBMC	BD4(M) + BD7(F) + BD22(M)	0=BD22 1=BD4 2=BD7
Sample 8	Yes (3 donors)	Skin	BD4(M) + BD20(F) + HC21(F)	0=HC21 1=BD20 2=BD4
Sample 9	Yes (3 donors)	PBMC	BD3(M) + BD21(F) + BD25(F)	0=BD21 1=BD25

				2=BD3
Sample 10	Yes (3 donors)	Skin	BD3(M) + BD7(F) + BD21(F)	0=BD7 1=BD3 2=BD21
Sample 11	Yes (4 donors)	Skin + PBMC	BD14(M) + BD18(F) + BD25(F) + BD27(F)	0=BD18 1=BD27 2=BD25 3=BD14
Sample 12	Yes (4 donors)	Skin + PBMC	BD22(M) + BD27(F) + HC26(F) + BD20(F)	0=BD27 1=BD22 2=HC26 3=BD20

3.2.2. Quality Control of scRNASeq Data

We analyzed a total of 17,587 skin cells and 27,242 PBMCs from BD patients (n=12), and 8,412 skin cells from healthy controls (n=5). For PBMCs from HCs, we utilized publicly available data from a previously published study by Domínguez Conde et al. (196) and analyzed 17,174 cells from this group. Quality control metrics, shown in Figure 3.16, evaluated library size, the number of detected genes per cell, and mitochondrial gene percentages, identifying cells to retain or filter out. Scatter plots depict these metrics for all samples collectively and for individual samples, ensuring that low-quality or doublet cells were excluded from further analysis. Figure 3.17 summarizes cell counts and quality distributions across samples, with bar plots illustrating cell counts and mean detected genes per cell, along with filtering status. Density plots further show the distributions of detected genes and total counts per cell, providing a comprehensive overview of data quality. Additionally, Table 8 presents the mean and median values for the number of

detected genes and total counts per cell, supporting the evaluation of sequencing quality. After applying batch correction, as shown in Figure 3.15, the samples were evenly distributed, confirming that batch effects did not influence the analysis outcomes. Together, these metrics demonstrate the robustness of the dataset and ensure the reliability of downstream analyses.

Figure 3.8. Visualization of sample distribution following batch correction. The plot shows the even distribution of samples from different groups, confirming the successful elimination of batch effects and ensuring unbiased analysis results.

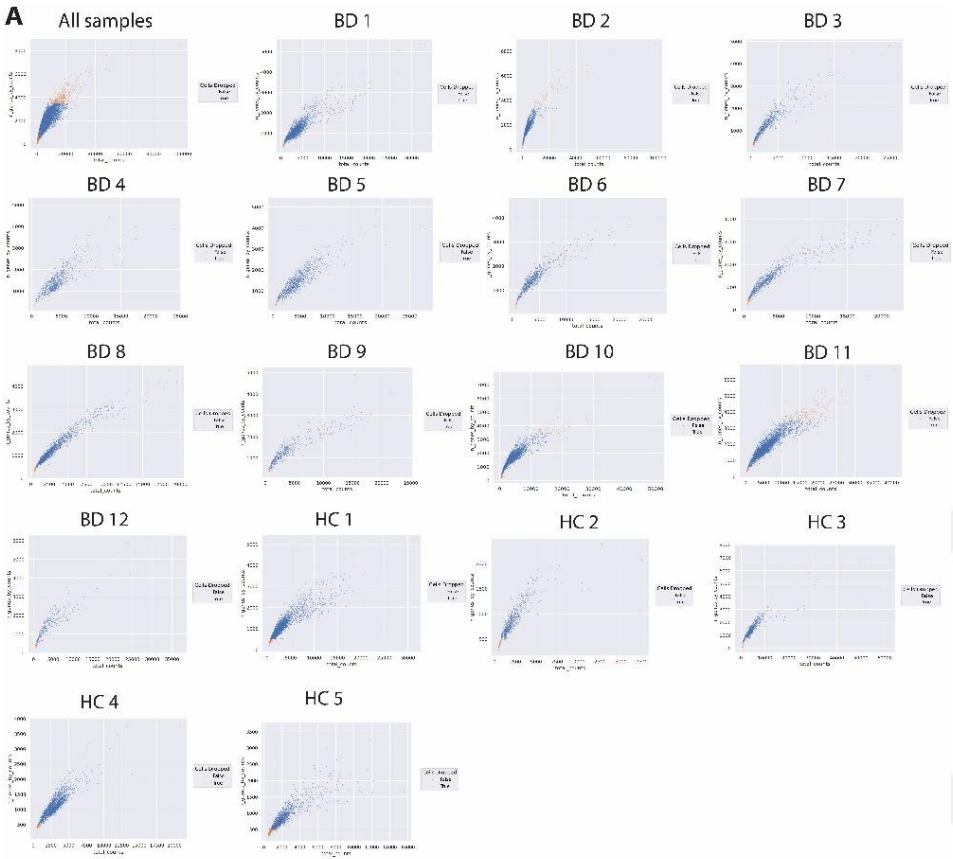
A
All samples
BD 1
BD 2
BD 3
BD 4
BD 5
BD 6
BD 7
BD 8
BD 9
BD 10
BD 11
BD 12
HC 1
HC 2
HC 3
HC 4
HC 5

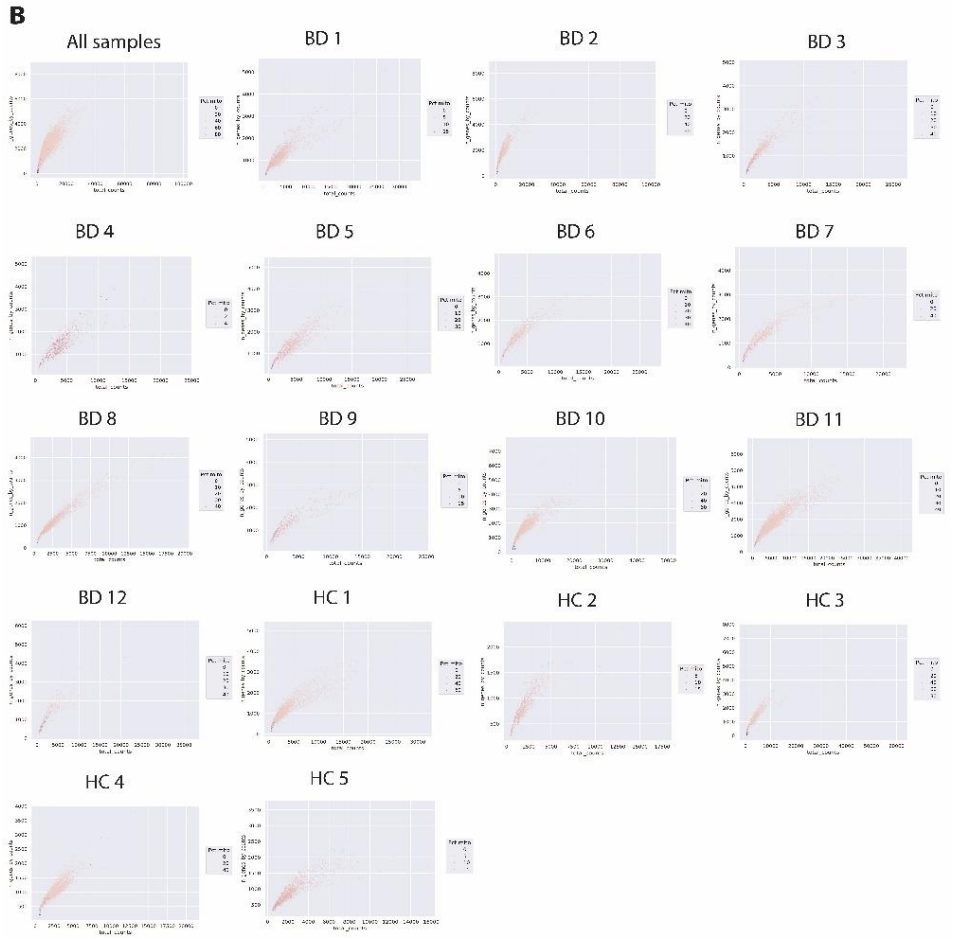
B
All samples
BD 1
BD 2
BD 3
BD 4
BD 5
BD 6
BD 7
BD 8
BD 9
BD 10
BD 11
BD 12
HC 1
HC 2
HC 3
HC 4
HC 5

Figure 3.9. Quality control metrics for the scRNAseq data. (A) Scatter plots illustrating the total library size (total counts) versus the number of detected genes per cell. Dot colors indicate whether a cell is retained or excluded. Cells were filtered out based on criteria such as being identified as doublets (detected by Souporcell or Scrublet) or failing standard quality control thresholds, including the number of detected genes, total library size, and percentage of mitochondrial gene expression. The upper left plot represents data from all samples, while the remaining plots correspond to individual samples (BD1-12 and HC1-5, from left to right). (B) Scatter plots showing the total library size versus the number of detected genes per cell, with dot colors reflecting the percentage of mitochondrial gene expression.

Table 8. The mean and median values for the number of detected genes and the total counts per cell.

Sample	Number of Genes per cell (mean)	Number of Genes per cell (median)	Total counts per cell (mean)	Total counts per cell (median)
BD1	1237.744831	1131	4120.70166	3441
BD2	1896.001876	1745	5272.220215	3971
BD3	1309.604116	1241	3343.737305	2711
BD4	1497.464935	1390	4496.964844	3972
BD5	1463.356455	1384.5	4670.245605	4197
BD6	1503.392898	1422	4370.128418	3642
BD7	1397.815385	1308.5	4031.67041	3216
BD8	1242.095561	1083	3094.102295	2387
BD9	1443.541436	1303	4730.83252	3329
BD10	1589.849971	1546.5	4056.471436	3309.5
BD11	1997.863953	1865	6614.453125	5740
BD12	1534.097345	1432	4454.271484	3292
HC1	1115.627997	994	3392.648926	2626
HC2	856.2671756	799	2194.703613	1885.5
HC3	1428.763906	1357	4612.018555	4033
HC4	1107.182273	1079.5	2940.197266	2863.5
HC5	906.8408834	814	2461.49707	1939.5

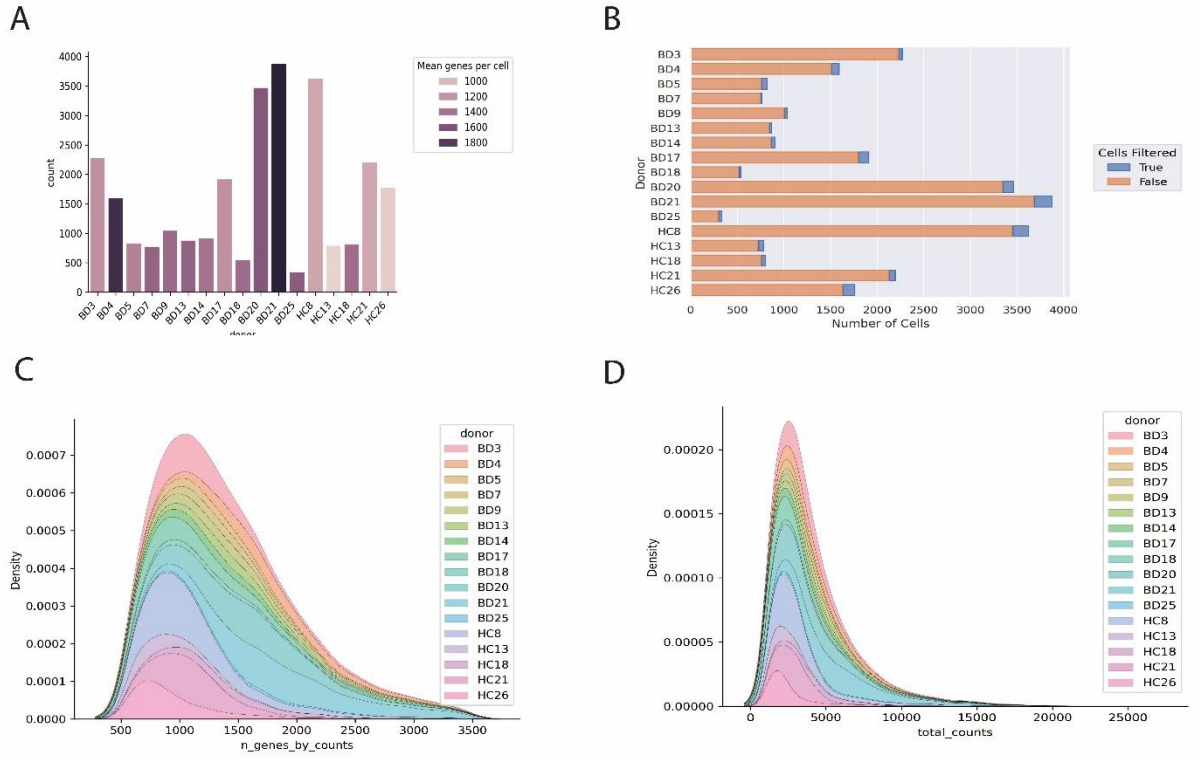

Figure 3.10. Overview of Cell Counts and Quality Metrics. (A) Bar plot displaying the cell counts for each sample, with color coding representing the mean number of detected genes per cell. (B) Bar plot similar to (A), but with color coding indicating whether cells were retained or filtered out during preprocessing. (C) Density plots illustrating the distribution of the number of detected genes per cell. (D) Density plots showing the distribution of total counts per cell.

Clustering and annotation of cell types were performed with the automated CellTypist method (196). Figure 3.18 shows a UMAPs presenting major cell types and their subsets, in skin cells from HC (Figure 3.18 A and B, respectively), and BD (Figure 3.18 C and D, respectively). In addition, Figure 3.19 shows UMAPs presenting major cell types and their subsets, in PBMCs from HC (Figure 3.19 A and B, respectively), and BD (Figure 3.19 C and D, respectively).

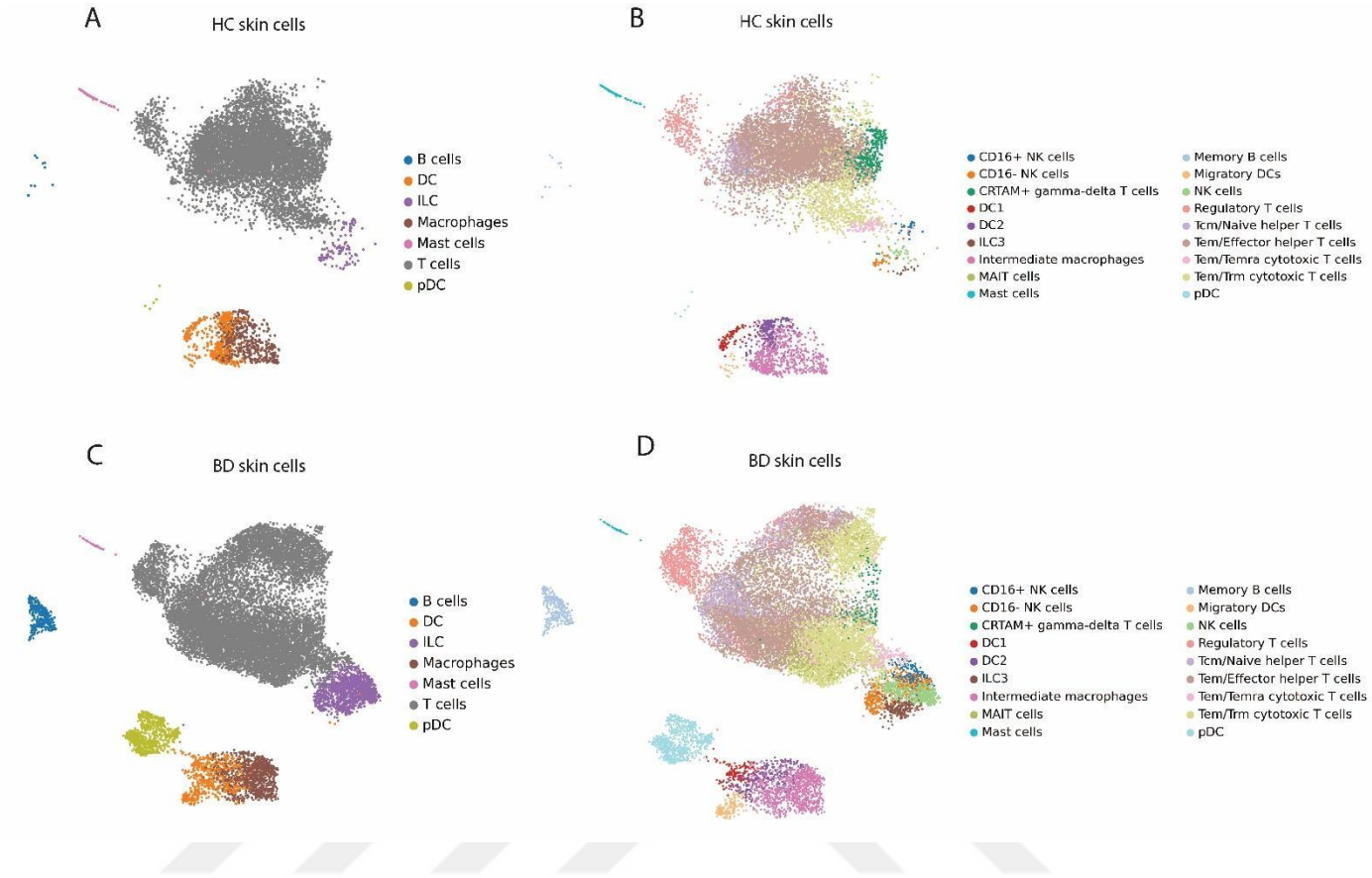

Figure 3.11. UMAP plots displaying the clustering and annotation of major cell types and their subsets in skin cells. (A) Major cell types identified in skin cells from healthy controls (HC). (B) Subsets of cell types in skin cells from HC. (C) Major cell types identified in skin cells from Behçet's disease (BD) patients. (D) Subsets of cell types in skin cells from BD patients. Cell type annotation was performed using the automated CellTypist tool.

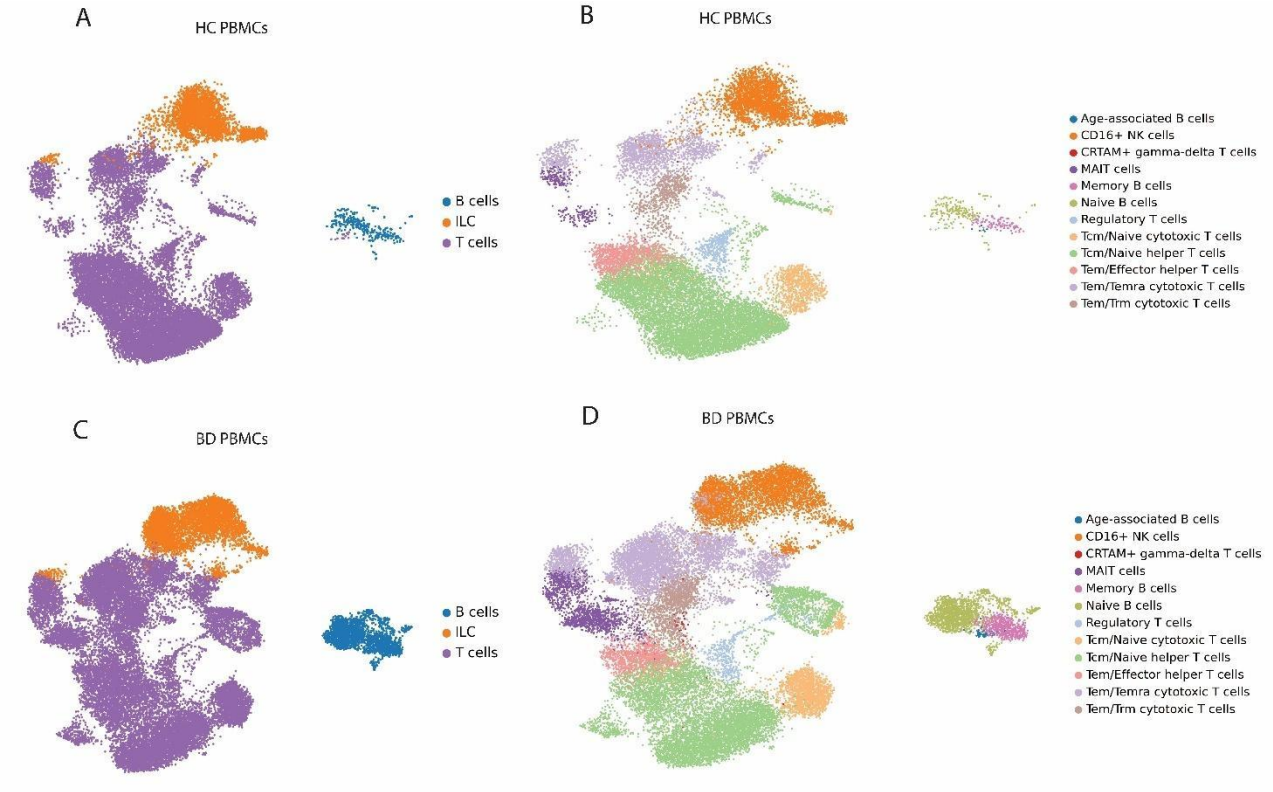

Figure 3.12. UMAP plots displaying the clustering and annotation of major cell types and their subsets in PBMCs. (A) Major cell types identified in PBMCs from healthy controls (HC). (B) Subsets of cell types in PBMCs from HC. (C) Major cell types identified in PBMCs from Behçet's disease (BD) patients. (D) Subsets of cell types in PBMCs from BD patients. Cell type annotation was performed using the automated CellTypist tool.

3.2.3. Differential Abundance Analysis of Immune Cells in Skin and Blood

Differential abundance of immune cells between BD and HC skin cells were statistically analyzed with the scCoda algorhytm. We found that memory B cells, NK cells, CD16- NK cells, ILC3 cells, MAIT cells, and pDCs are increased in BD lesions compared to HC skin (Figure 3.20 A). Also, differential abundance test between BD PBMCs and the HC PBMCs showed an increased number of naive B cells and MAIT cells in BD PBMC (Figure 3.20 B).

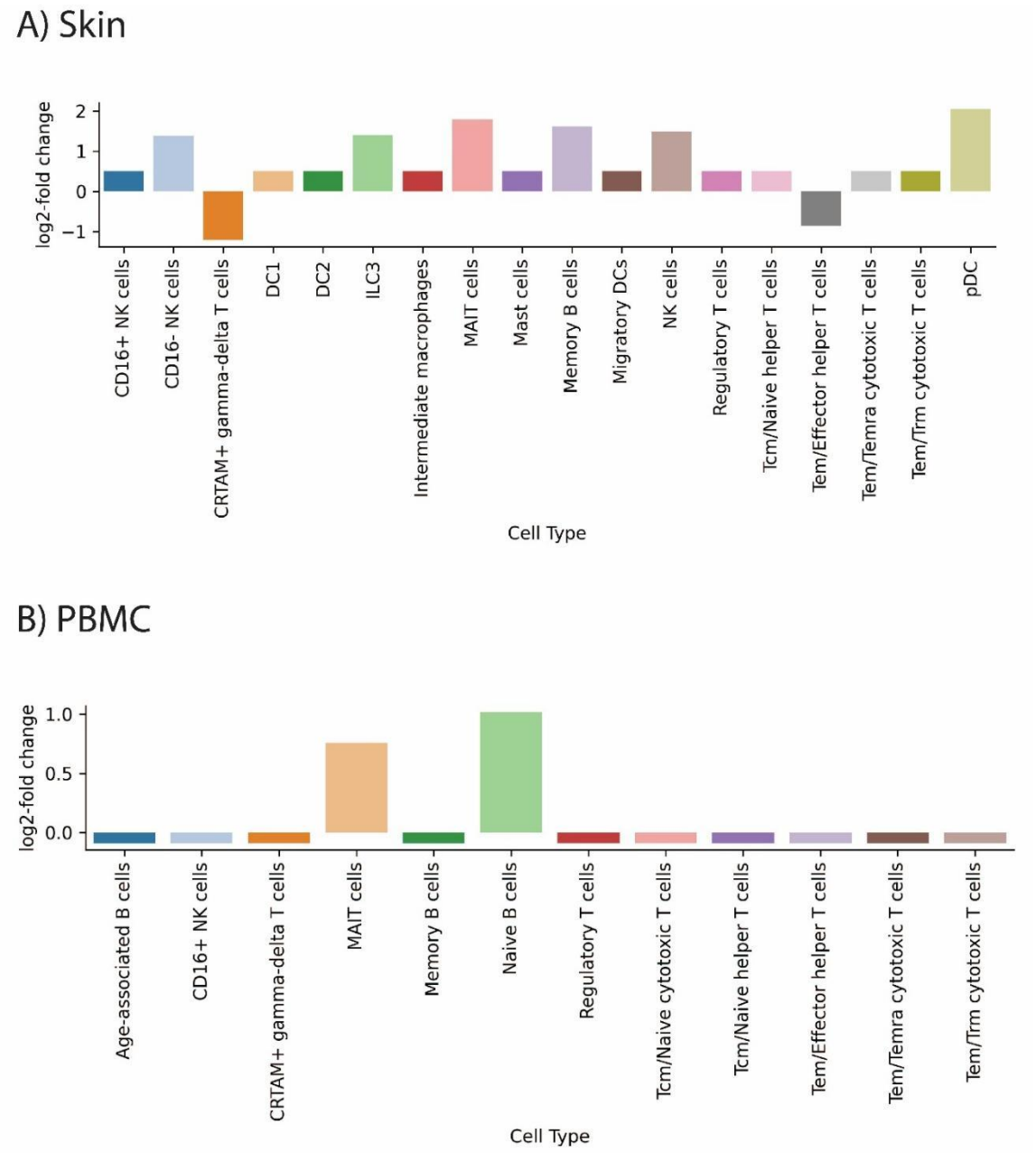

Figure 3.13. Differential abundance analysis of cell populations in Behçet's disease (BD) and healthy controls (HC). (A) Increased abundance of memory B cells, NK cells, MAIT cells, and pDCs in BD skin cells compared to HC skin cells. (B) Increased abundance of naive B cells and MAIT cells in BD PBMCs compared to HC PBMCs, with HC data pooled from publicly available datasets.

3.2.4. Analysis of Upregulated Genes in BD Lesions

The pseudobulk analysis of BD and HC skin cells was conducted using the Wilcoxon rank-sum test with Benjamini-Hochberg correction for multiple testing, and some selected differentially expressed genes, over-expressed in BD lesions are demonstrated in Table 9. Furthermore, a volcano plot (Figure 3.21) visually represents these differentially expressed genes. Functional enrichment analysis was conducted to determine the biological pathways enriched in skin lesions of BD. The results indicated significant activation of the JAK-STAT pathway (Figure 3.22).

Table 9. Selected differentially expressed genes over-expressed in Behçet's disease (BD) skin lesions compared to healthy controls (HC).

	log2FoldChange	pvalue	padj
GZMB	3.67	7.78E-11	1.45E-08
C1QB	3.67	1.59E-03	9.81E-03
MEFV	3.66	1.79E-04	1.86E-03
CXCL10	3.35	3.61E-03	1.83E-02
CXCL9	3.10	7.35E-03	3.14E-02
IFI35	2.73	5.49E-06	1.26E-04
PRF1	2.53	1.00E-07	5.56E-06
CR1	2.44	6.21E-03	2.78E-02
IFI30	2.43	1.12E-04	1.32E-03
IL12B	2.23	2.87E-01	
IL12RB2	2.12	4.78E-06	1.15E-04
IL1B	1.97	8.41E-03	3.48E-02
GZMA	1.92	2.13E-04	2.12E-03
STAT1	1.90	5.35E-04	4.34E-03
NLRP3	1.89	4.13E-03	2.04E-02
TLR7	2.27	0.0035	0.01817

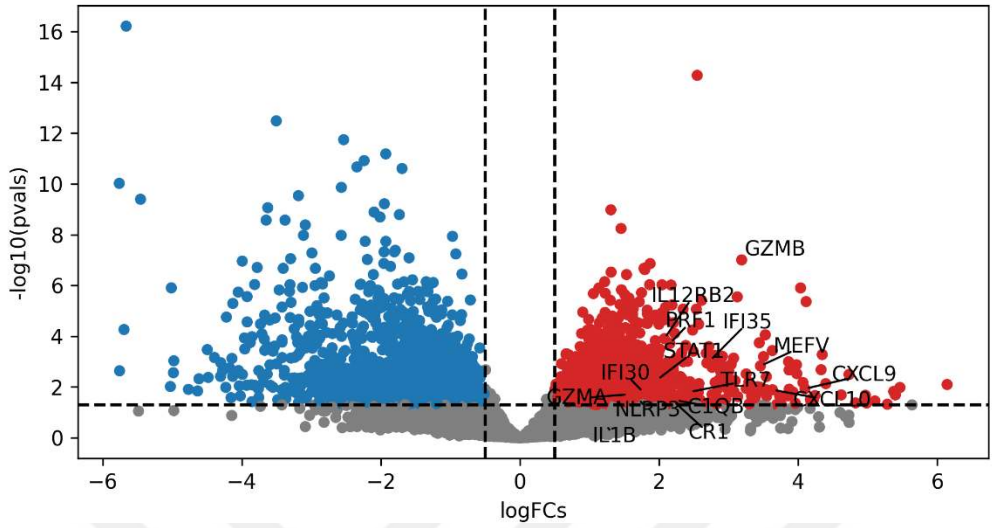

Figure 3.14. Volcano plot showing the differentially expressed genes in BD skin lesions compared to HC skin cells, as identified through pseudobulk analysis.

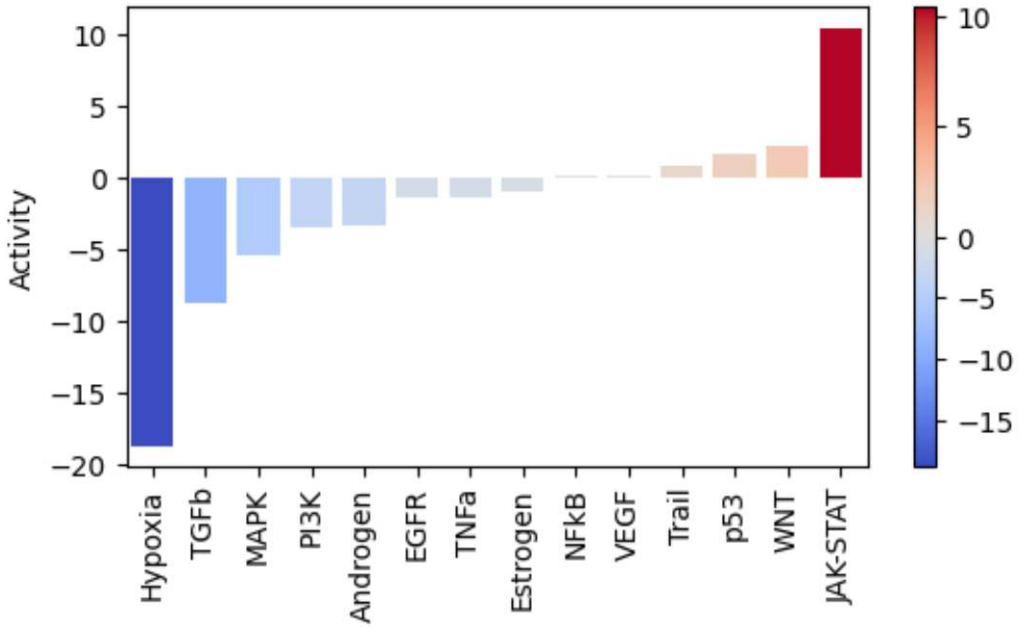

Figure 3.15. Functional enrichment analysis of skin lesions in BD. Enriched biological pathways were identified, revealing significant activation of the JAK-STAT pathway in Behcet's disease skin lesions.

In addition, to demonstrate the cellular distribution of some genes of interest, their expression in BD and HC skin UMAPs are depicted in Figures 3.16–3.23. In Figure 3.16, the expression of IL3RA, a marker confirming the pDC cluster, was evaluated alongside TYROBP, VAMP8, and PLD4 to investigate the functional heterogeneity of pDCs in BD and HC skin cells. The analysis revealed a prominent pDC cluster in BD skin cells, characterized by the expression of these genes. Notably, this cluster displayed two distinct subsets, with one subset showing increased expression of activation-associated genes (TYROBP, VAMP8, and PLD4), suggesting the presence of activated pDCs in BD lesions. In contrast, almost no pDCs were detected in HC skin samples, consistent with the results of the differential abundance analysis, which demonstrated a significant increase in pDCs in BD skin compared to HC.

Figure 3.17 depicts the upregulation of type I interferon response (IFN-α) genes, including IFIT2 and ISG20, in BD skin lesions. This highlights a robust activation of type I interferon pathways, potentially contributing to the pro-inflammatory environment in BD skin. Figure 3.18 illustrates the upregulation of inflammasome-related genes, including NLRP3, MEFV, PYCARD, and IL1B, in macrophages of BD skin lesions. These findings suggest enhanced inflammasome activation, likely driving IL-1β-mediated inflammation in BD pathogenesis. In Figure 3.19, complement-related genes, including CD14, C1QA, C1QB, and C1QC, were found to be upregulated in macrophages of BD skin lesions. This indicates complement pathway activation, which may contribute to immune cell recruitment and tissue damage in BD.

Figure 3.20 demonstrates the upregulation of the IL12A–IL12RB2–STAT4 pathway in BD skin lesions, with increased expression of IL12RB2, STAT4, and JAK2. These findings are consistent with an amplified Th1 immune response and highlight the role of this pathway in promoting inflammation in BD. Figure 3.21 shows the upregulation of type II interferon response (IFN-γ)-related genes, including STAT1, EOMES, IFI6, and CXCL10, in BD skin lesions. This indicates an activated IFN-γ-driven inflammatory response, which likely contributes to the cytotoxic and pro-inflammatory phenotype observed in BD lesions. In Figure 3.22, STAT1 downstream molecules, including MX1, ISG15, IFITM1, and IFI6, were found to be significantly upregulated in BD skin lesions. This further underscores the involvement of STAT1 in mediating interferon-driven immune dysregulation in BD.

Finally, Figure 3.23 illustrates the expression levels of cytotoxic molecules, including granzyme K (GZMK), granzyme A (GZMA), granzyme B (GZMB), and perforin (PRF1). The results indicate that their expression is elevated in BD lesions compared to HC skin, consistent with the enhanced cytotoxic and inflammatory activity of effector cells in BD.

Overall, these findings reveal the complex immune dysregulation in BD skin lesions, involving both innate and adaptive immune responses, and provide further insights into potential therapeutic targets for this chronic inflammatory disorder.

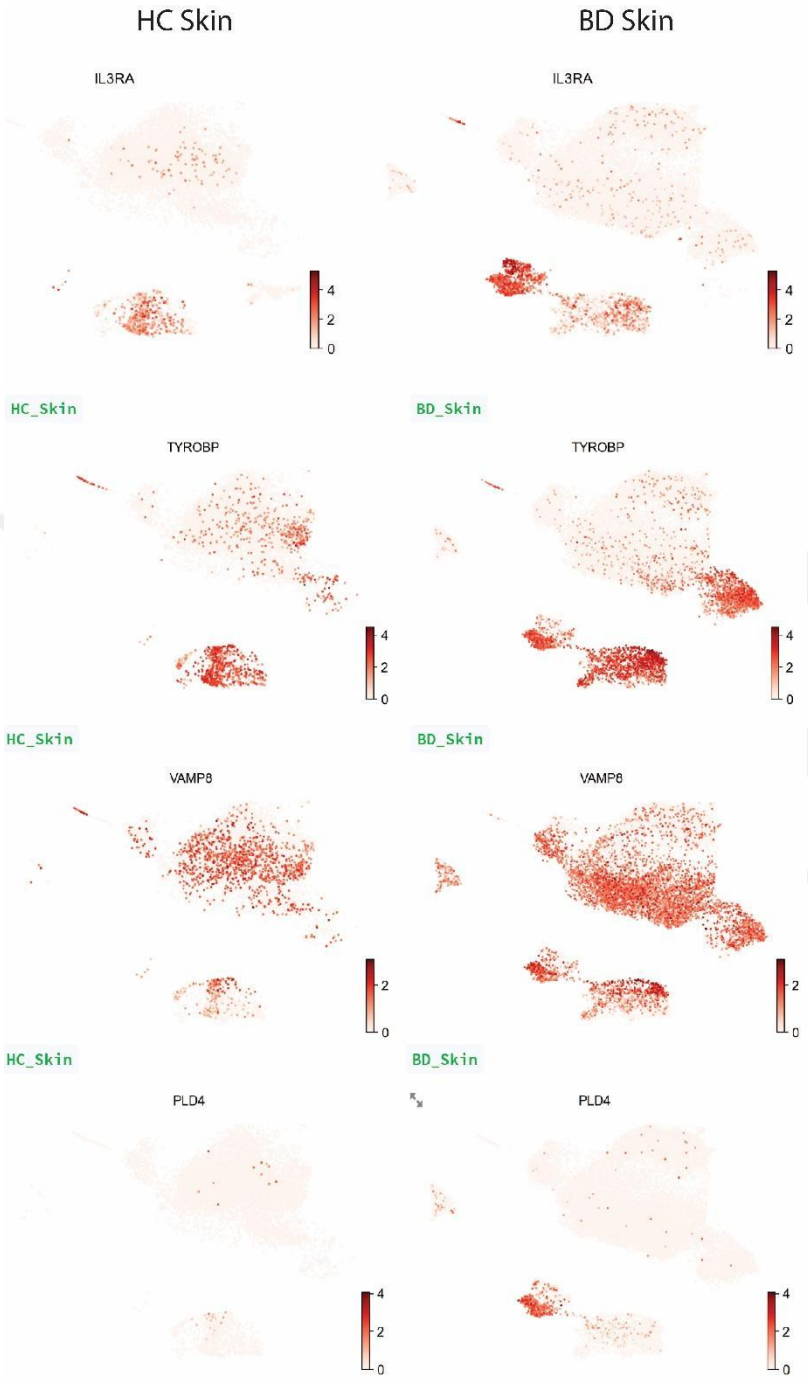

Figure 3.16. UMAP visualization of gene expression highlighting the pDC cluster and its activation state in skin cells from BD and HC. IL3RA expression confirming the presence of the pDC cluster, primarily observed in BD skin. Expression of TYROBP, VAMP8, and PLD4 showing functional heterogeneity within the pDC cluster in BD skin, with one subset demonstrating activation.

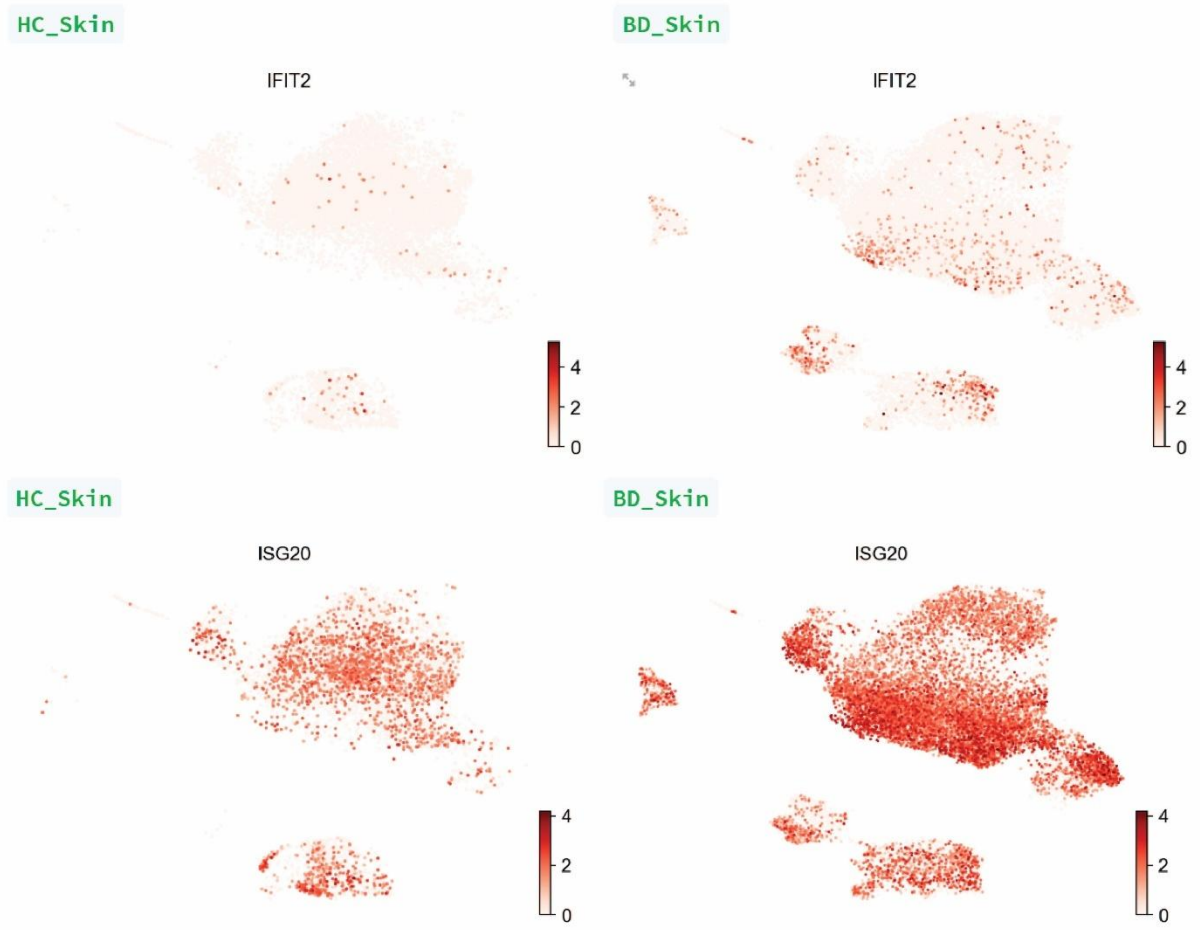

Figure 3.17. Upregulation of type I interferon response (IFN-α) genes in BD skin lesions.

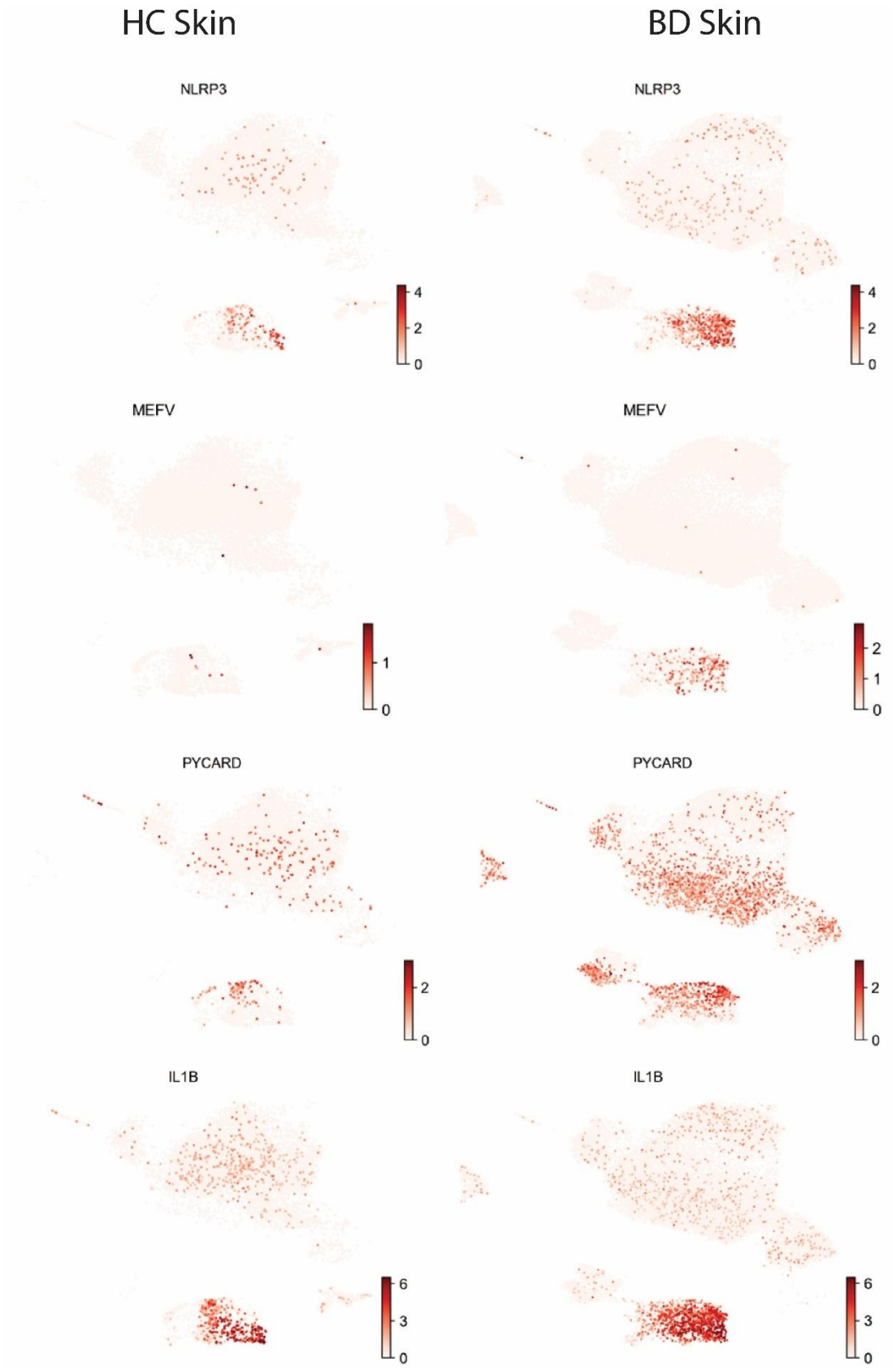

Figure 3.18. Inflammasome Upregulation in Skin Macrophages of BD lesions.

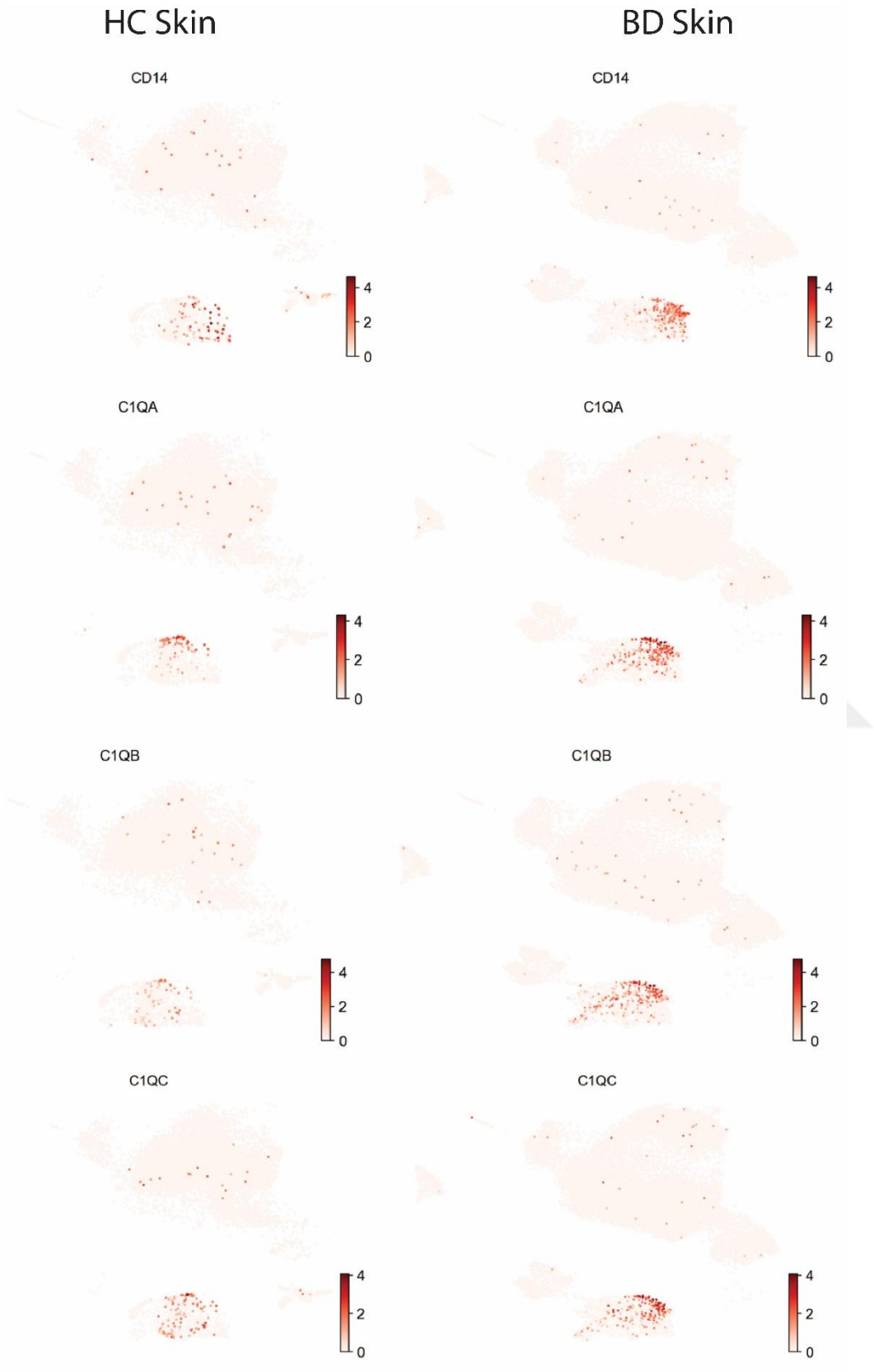

Figure 3.19. Complement Upregulation in Macrophages in BD skin cells.

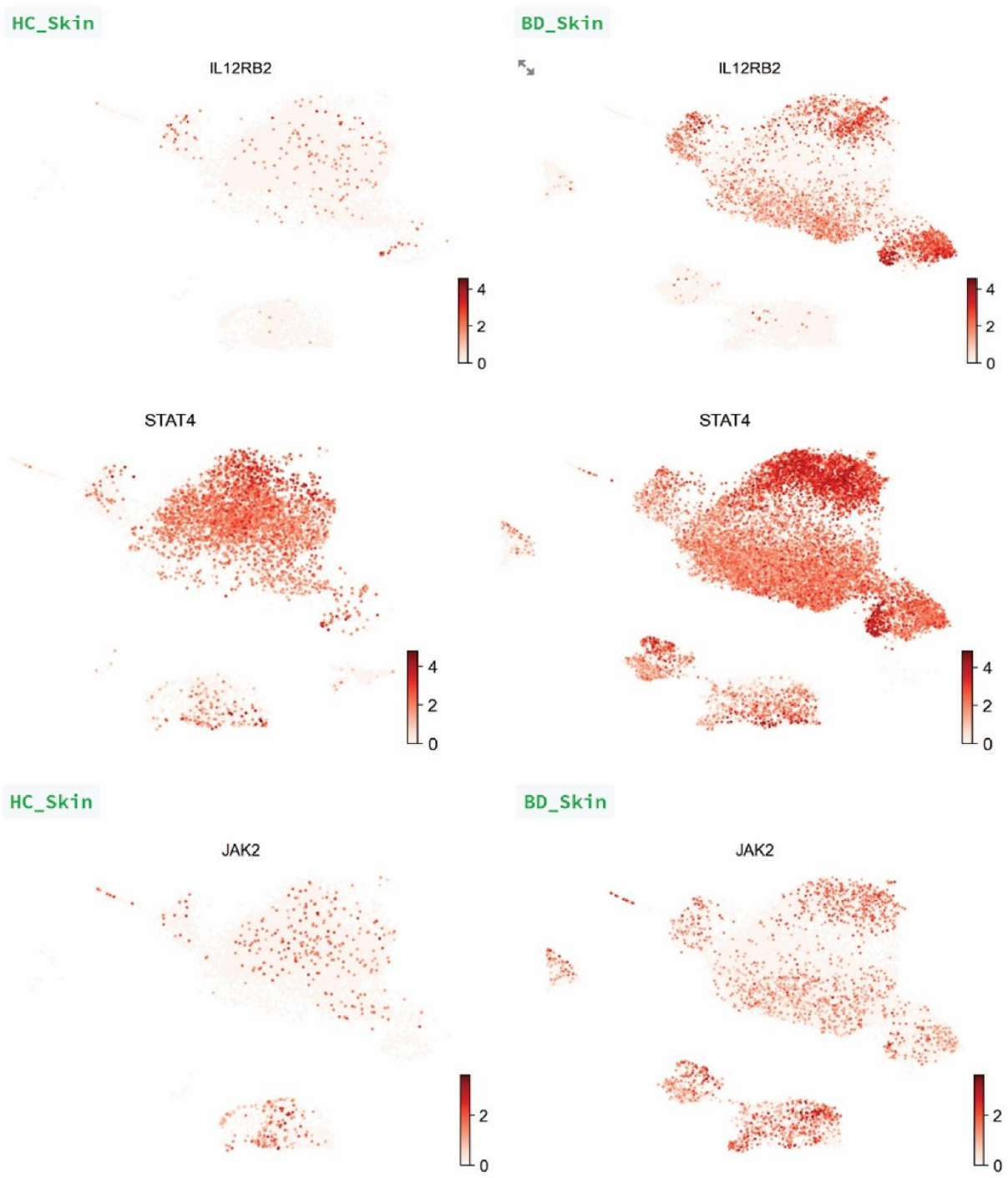

Figure 3.20. Upregulation of IL12A-IL12RB-STAT4 Pathway in BD skin.

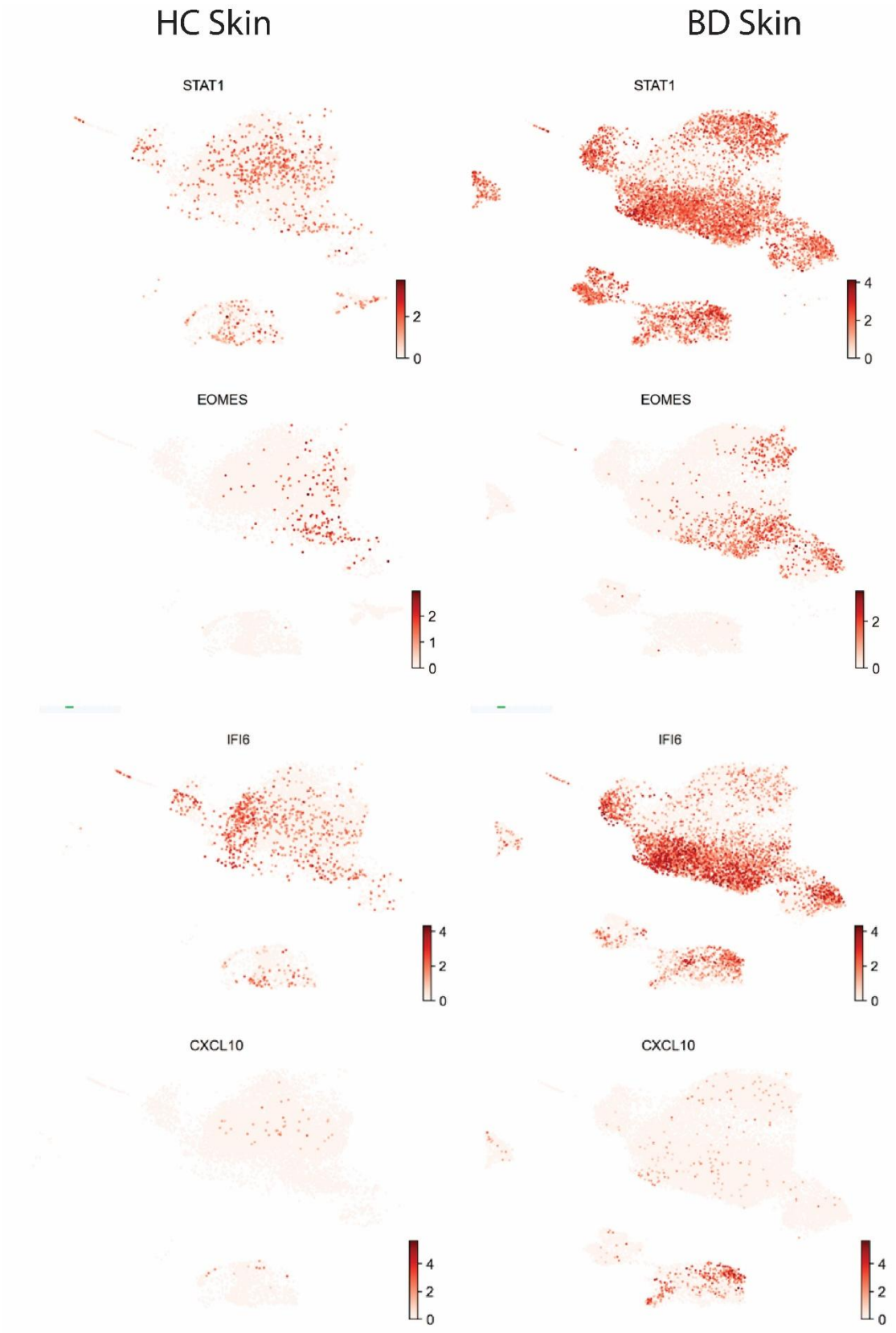

Figure 3.21. Upregulation of type II IFN response (IFN-γ) related genes in BD skin lesions

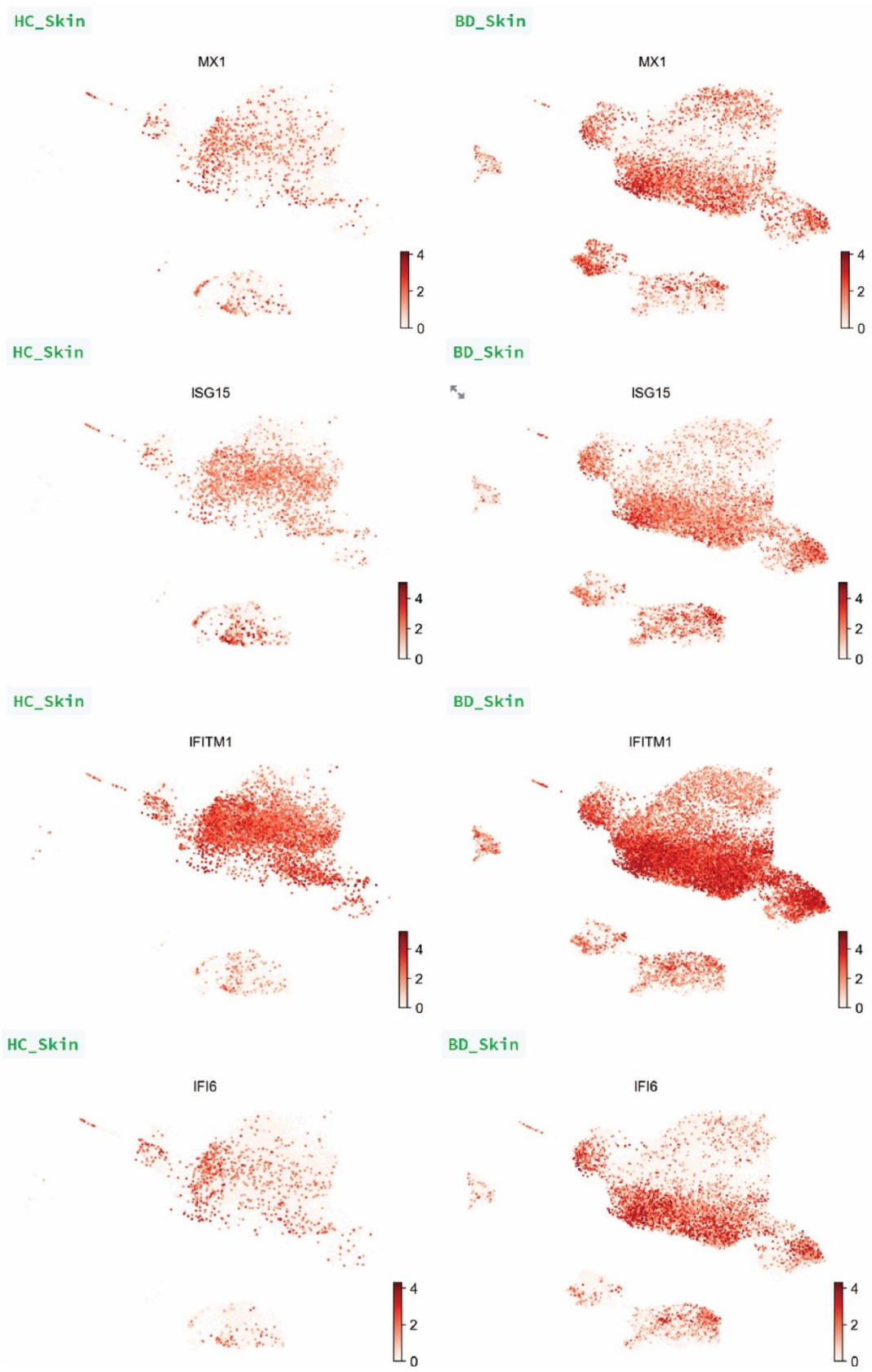

Figure 3.22. STAT1 Downstream molecules are upregulated in BD skin lesions.

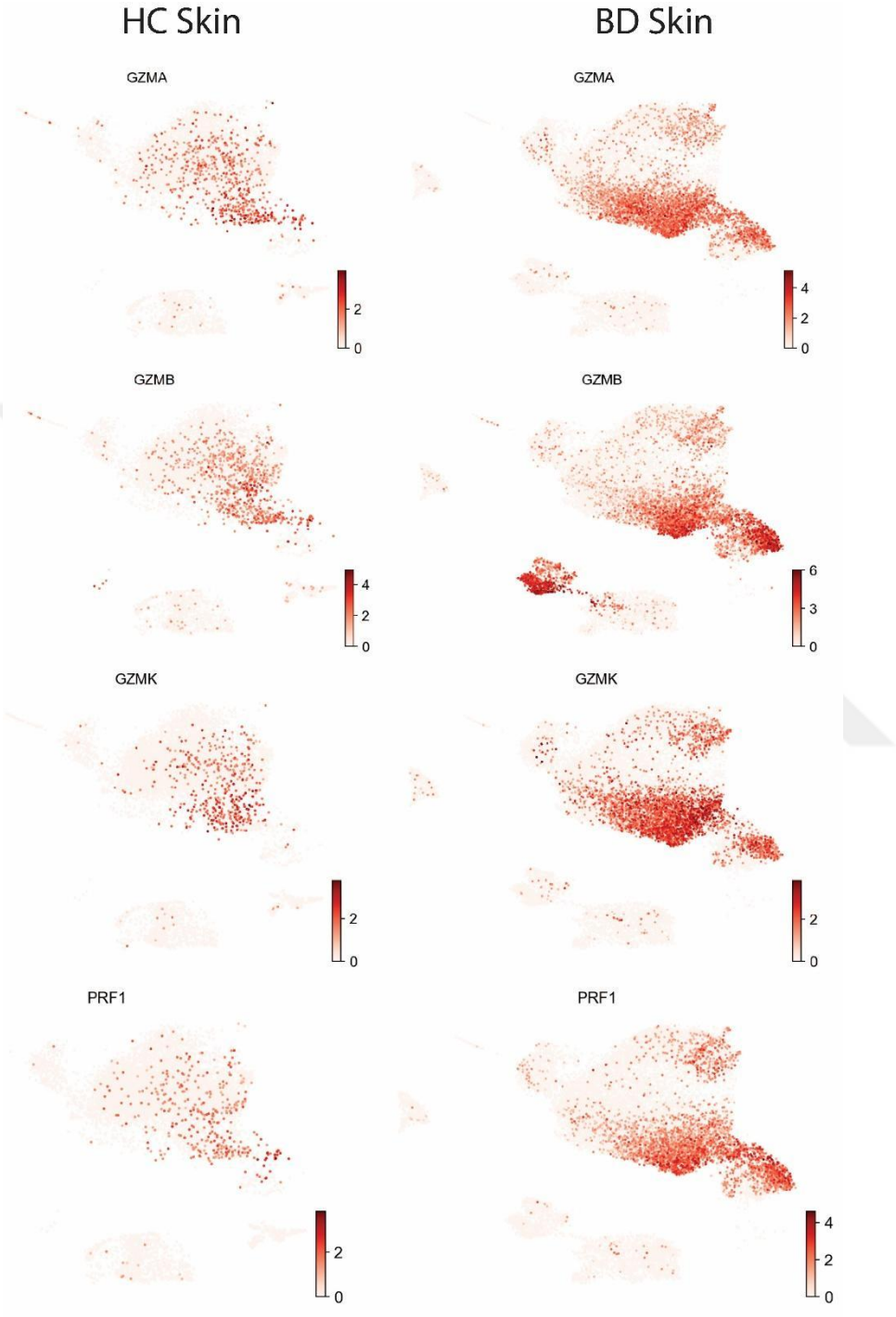

Figure 3.23. Elevated expression of cytotoxic molecules in BD skin lesions. The graphs depict the expression levels of granzyme K (GZMK), granzyme A (GZMA), granzyme B (GZMB), and perforin (PRF1) in skin lesions of BD compared to HC skin, demonstrating significantly higher expression in BD lesions.

3.2.5. TCR Sequencing Analysis of Clonality in BD Skin Lesions

To assess the clonality of T cells in BD lesions and HC skin cells, we analyzed the clonal distribution of T cell populations from TCR sequencing data. In Figure 3.26, the overall clonality of skin cells from both BD patients and HC individuals is depicted. The pie chart reveals that BD skin cells were not clonally expanded compared to HC skin cells. Clonality profiles for individual HC and BD subjects are also depicted, illustrating the distinct patterns of T cell clonal expansion in each case.

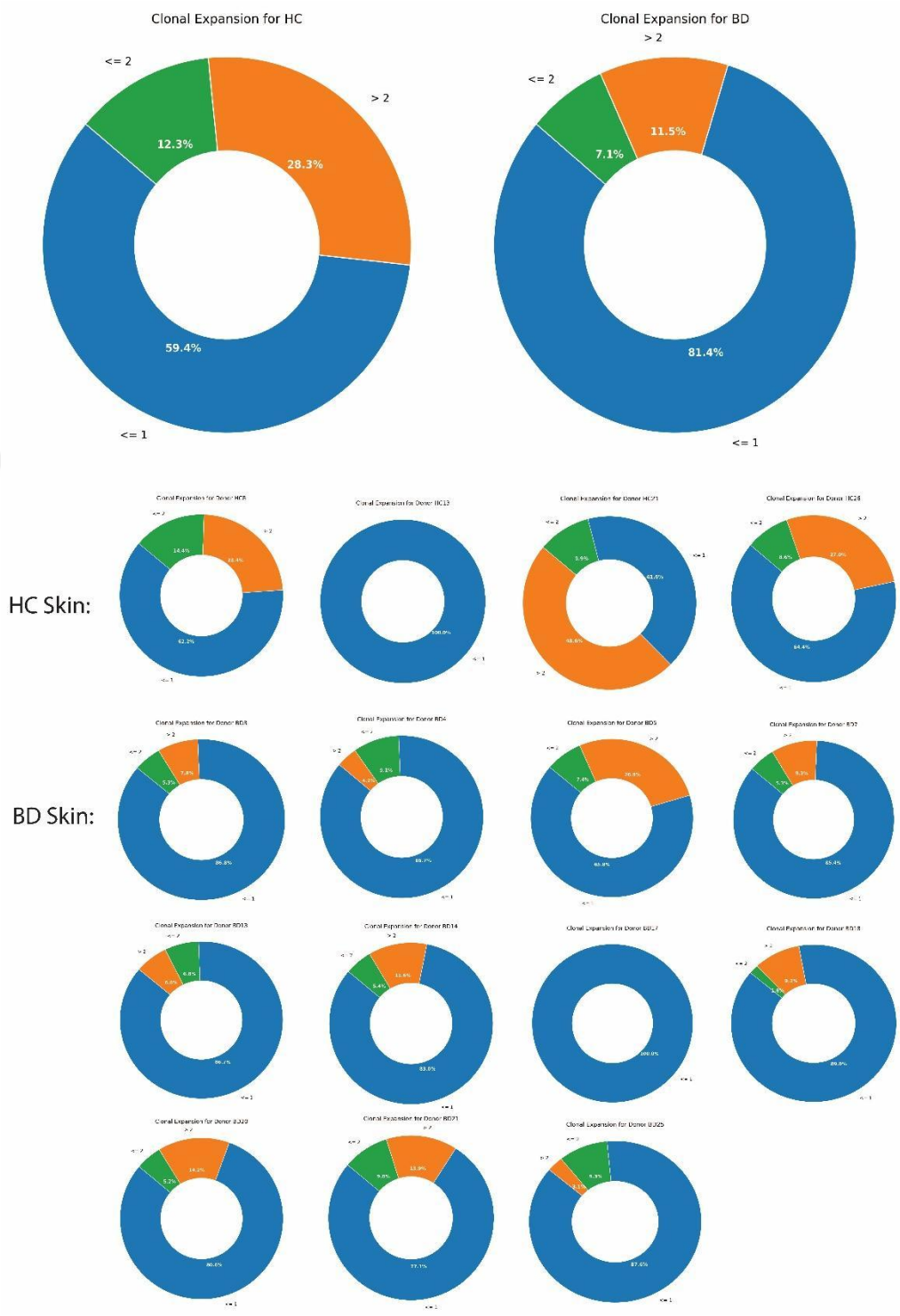

Figure 3.24. Clonality analysis of T cells in BD lesions and HC skin cells. Pie chart showing the overall clonality of skin cells in BD and HC. BD skin cells exhibit a lower level of clonal expansion compared to HC skin cells. Clonality profiles for individual HC individuals and BD patients.

3. 3 Flow Cytometry Analysis of Behçet's Disease Skin Lesions and Healthy Skin Samples

After dissociation of skin samples, flow cytometry analysis was done freshly as described above. For flow cytometry analysis, skin samples from 24 healthy controls and 22 Behcet's disease patients were used. The BD skin lesions used contained 9 Papulopustular Eruptions (PPE), 8 Erythema Nodosum-like lesions (EN), 3 Genital Ulcers (GU), and 2 Positive Pathergy Test (PPT). B cells, T cells, NK cells, T helper and cytotoxic T cells, CD69+ resident memory T cells, granzyme K and granzyme B expressing T cell subsets were analyzed. Our gating strategy for flow cytometry analysis of Panel 1, is demonstrated in Figure 3.7. The cell types in our analysis and their corresponding Flow cytometry markers are demonstrated in Table 10. The results of cell percentages were compared with the Mann-Whitney U test and the results (Figure 3.8) demonstrated a statistically significant elevation in B cells ($p=0.0059$), NK cells ($P<0.001$), THLs ($p=0.0041$) and Granzyme K+ CTLs ($p=0.037$) in BD skin samples. Also, a reduction with statistical significance was observed in T cells ($p=0.0001$), CTLs ($p=0.003$), and CD69+ resident memory T cells ($p<0.0001$) in BD skin compared to healthy controls.

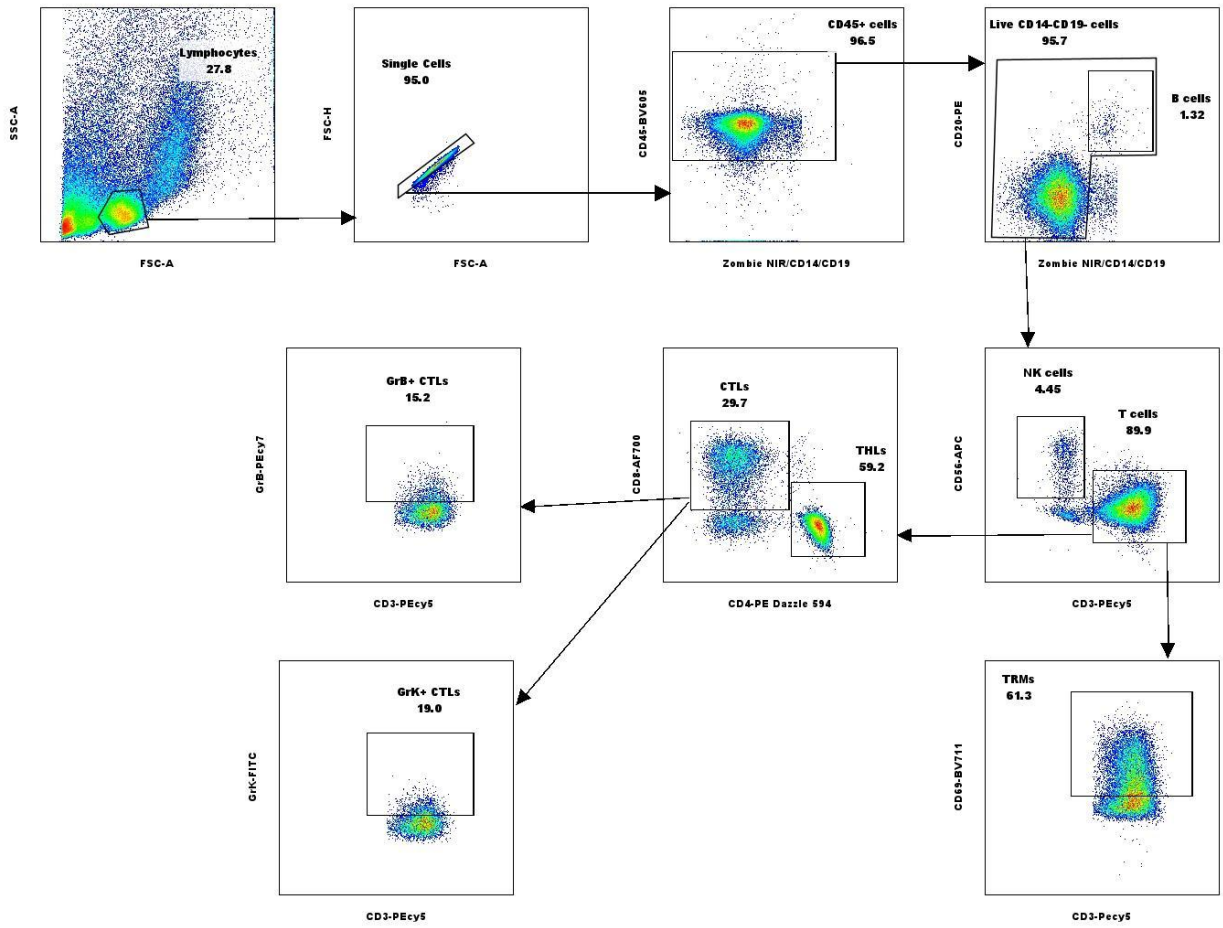

Figure 3.25. Representative gating strategy of the flow cytometry analysis.

Table 10. Cell Types and Their Corresponding Flow Cytometry Markers

Cell Type	Subtypes	Markers
B cells	**Total B cells**	CD14-CD19+
	Memory B cells	CD14-CD19+CD27+
	Naive B cells	CD14-CD19+CD27-
T cells	**Total T cells**	CD14-CD19-CD3+
	CTLs	CD14-CD19-CD3+CD8+
	THLs	CD14-CD19-CD3+CD4+
	Naive	CD14-CD19-CD3+ CD45RO-CCR7+
	Central Memory	CD14-CD19-CD3+CD45RO+CCR7+
	Effector Memory	CD14-CD19-CD3+ CD45RO+CCR7-
	MAIT	CD14-CD19-CD3+ CD161+TCR Vα7.2+
	γδ T cells	CD14-CD19-CD3+ TCR γδ+
NK cells	**Total NK cells**	CD3-CD14-CD19-CD56+
	CD56bright	CD3-CD14-CD19-CD56bright
	CD56dim	CD3-CD14-CD19-CD56dim
Monocytes	**Total Monocytes**	CD14+
	Classical	CD14++CD16-

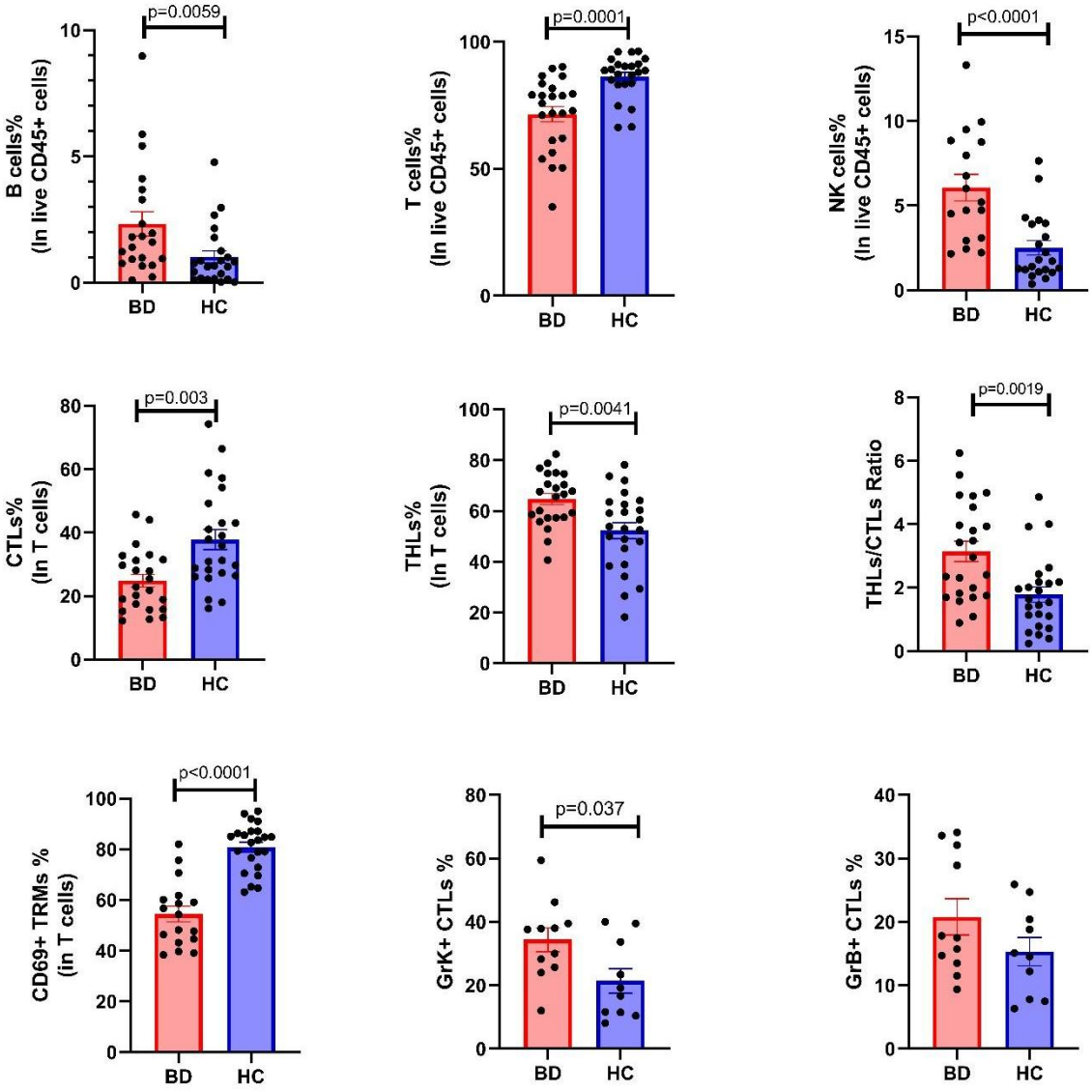

Figure 3.26. Flow cytometry analysis results comparing immune cells in Behcet's disease skin lesions and healthy control skin samples. Statistically significant increase in the percentage of B cells (p=0.0059), NK cells (p<0.0001), helper T cells (p=0.0041), and Granzyme K+ cytotoxic T cells (p=0.037) was found in BD skin versus healthy control skin. Also, a reduction with statistical significance was observed in the percentage of T cells (p=0.0001), cytotoxic T cells (p=0.003), and resident memory T cells (p<0.0001).

For 9 BD skin samples, their paired blood samples were also analyzed and statistically compared with the paired t-test (Figure 3.9), showing a higher ratio of granzyme K+ CTLs (p=0.0197) in skin compared to PBMC.

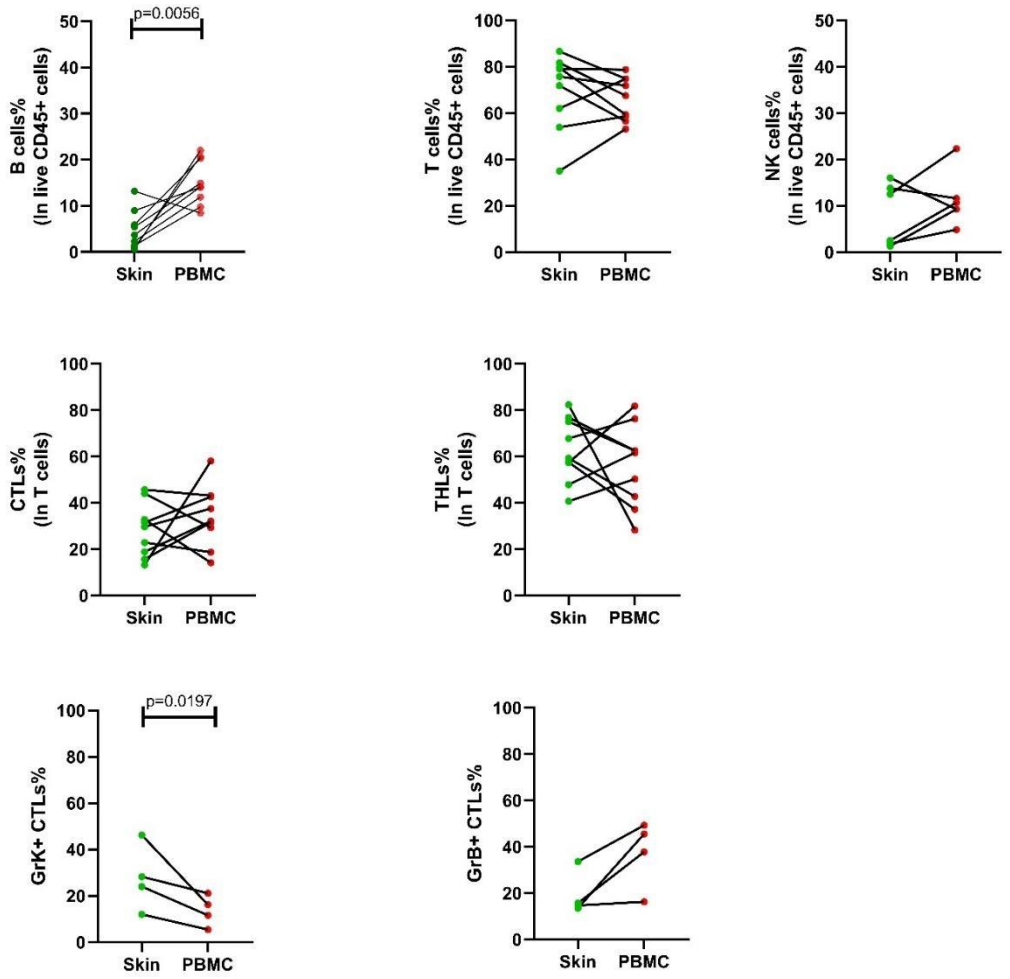

Figure 3.27. Flow cytometry analysis results of paired comparison of immune cells in BD skin lesions and PBMC. The results compared with paired t-test, showed a higher percentage of granzyme K+ cytotoxic T cells in the skin lesions compared to PBMC. In comparison, the B cell percentage was higher in the PBMC.

3. 4 Flow Cytometry Analysis of PBMC from Patients with Behçet's Disease and Healthy Controls

In addition, 15 Behcet's disease patient PBMC samples were compared to 15 age-matched healthy control PBMCs for a more detailed immunphenotyping including MAIT cells, gamma-delta T cells, memory T cell subtypes, memory B cells, monocyte subtypes, plasmacytoid and myeloid dendritic cells. The results demonstrated in Figure 3.10, revealed that BD patient PBMC had a lower percentage of effector memory T cells (p=0.0059) and THLs (p=0.0299), and enhanced percentage of CTLs (p=0.0268) and naïve T cells (0.0191), with other cell type percentages unchanged in comparison to HC. Moreover, comparing granzyme B (GrB) and granzyme K (GrK) expression in different cell types showed that BD PBMC had higher percentages of GrB+ cytotoxic T cells (p=0.046), GrB+ THLs (p=0.0082), GrB+ γδ T cells (p=0.0409), and GrB+ MAIT cells (p=0.003); with lower percentage of GrK+ cytotoxic T cells (p=0.0188) compared to HC. Also, there is a trend of decreased MAIT cells percentage (p=0.062) and GrK+ THLs (p=0.0559) in BD PBMC compared to HC.

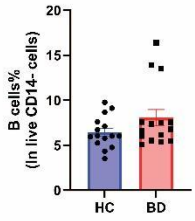
B cells%
(In live CD14- cells)
HC
BD

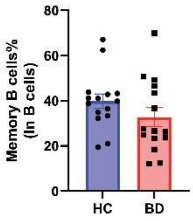
Memory B cells%
(In B cells)
HC
BD

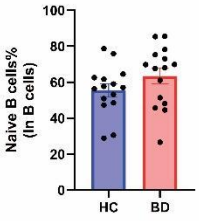
Naive B cells%
(In B cells)
HC
BD

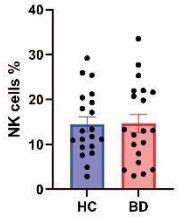
NK cells %
HC
BD

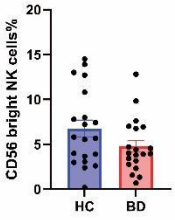
CD56 bright NK cells%
HC
BD

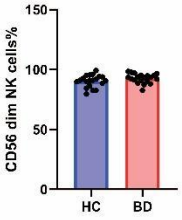
CD56 dim NK cells%
HC
BD

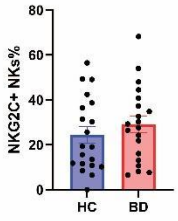
NKG2C+ NKs%
HC
BD

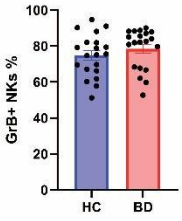
GrB+ NKs %
HC
BD

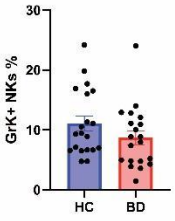
GrK+ NKs %
HC
BD

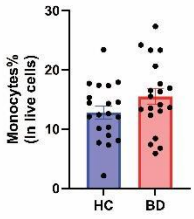
Monocytes%
(In live cells)
HC
BD

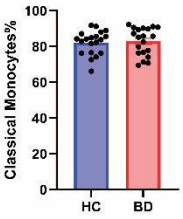
Classical Monocytes%
HC
BD

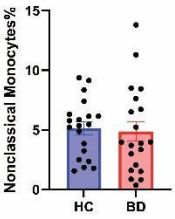
Nonclassical Monocytes%
HC
BD

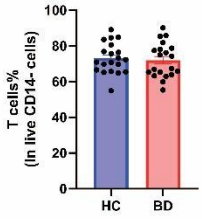
T cells%
(In live CD14- cells)
HC
BD

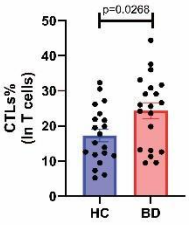
p=0.0268
CTLs%
(In T cells)
HC
BD

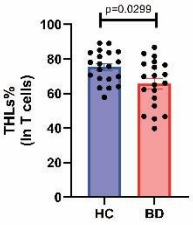
p=0.0299
THLs%
(In T cells)
HC
BD

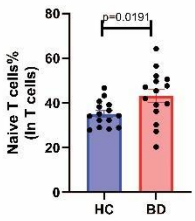
p=0.0191
Naive T cells%
(In T cells)
HC
BD

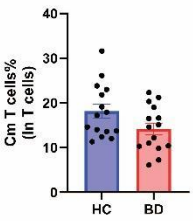
Cm T cells%
(In T cells)
HC
BD

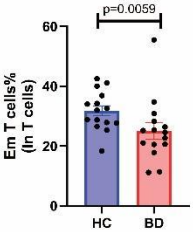
p=0.0059
Em T cells%
(In T cells)
HC
BD

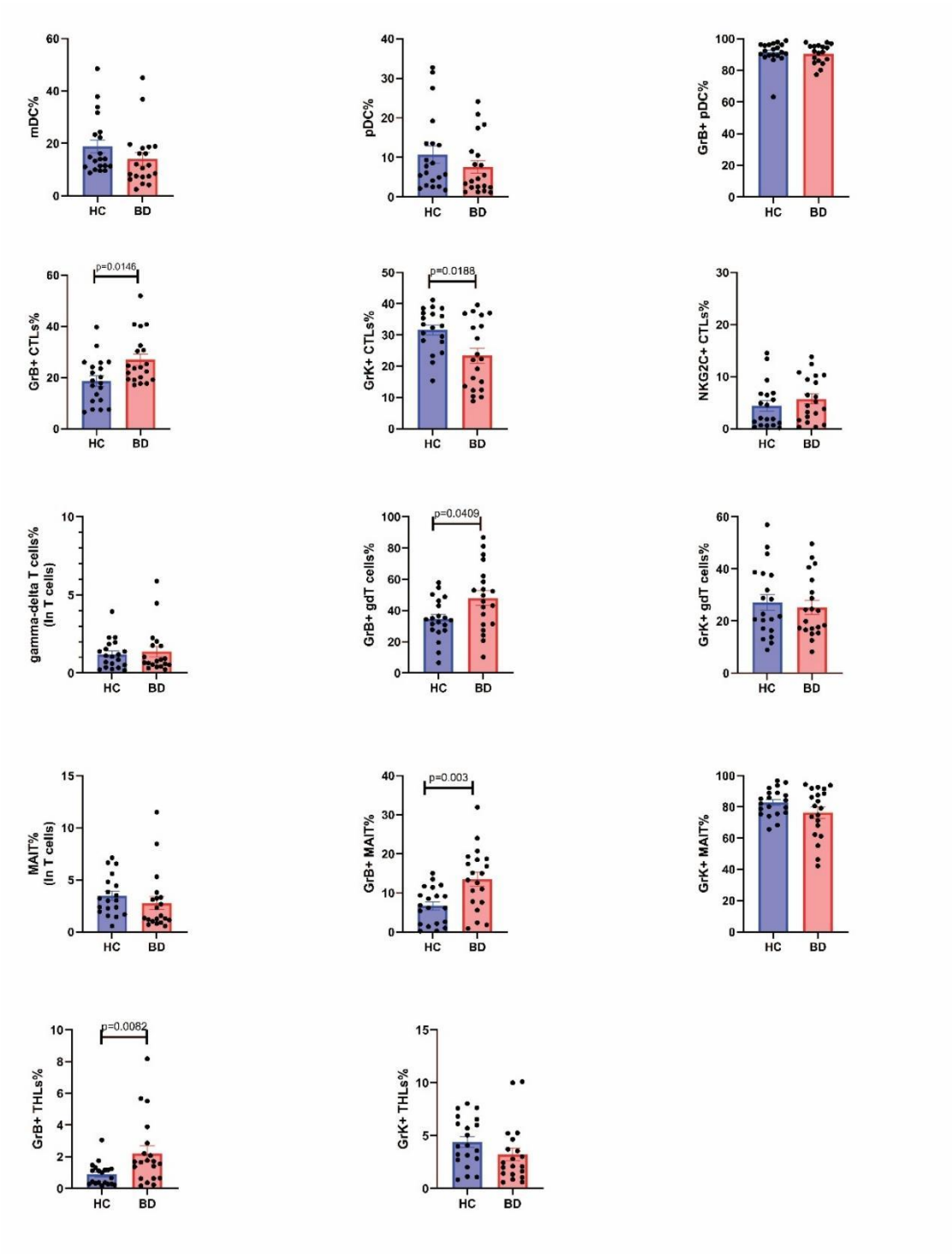

Figure 3.28. Flow cytometry Analysis of Behcet's disease versus healthy control PBMC samples.

3. 5 Functional Analysis of PBMC and Skin Immune Cells with Flow Cytometry

Immune cell stimulation with PMA/Ionomycin was performed on PBMC samples of 16 BD patients and 16 healthy controls, and the results are illustrated in Figure 3.11. The results showed declined percentages of IFNγ+ ($p=0.0012$) and TNFα+ ($p=0.0034$) helper T cells, CD107a+ ($p=0.0041$) and IFNγ+ ($p=0.0009$) NK cells in stimulated BD PBMC in comparison with healthy controls. In addition, there is a trend of decreased percentage of IFNγ+ γδ T cells ($p=0.0659$), IFNγ+ MAIT ($p=0.1$), IFNγ+ CTLs ($p=0.0846$) in BD PBMC compared to HC.

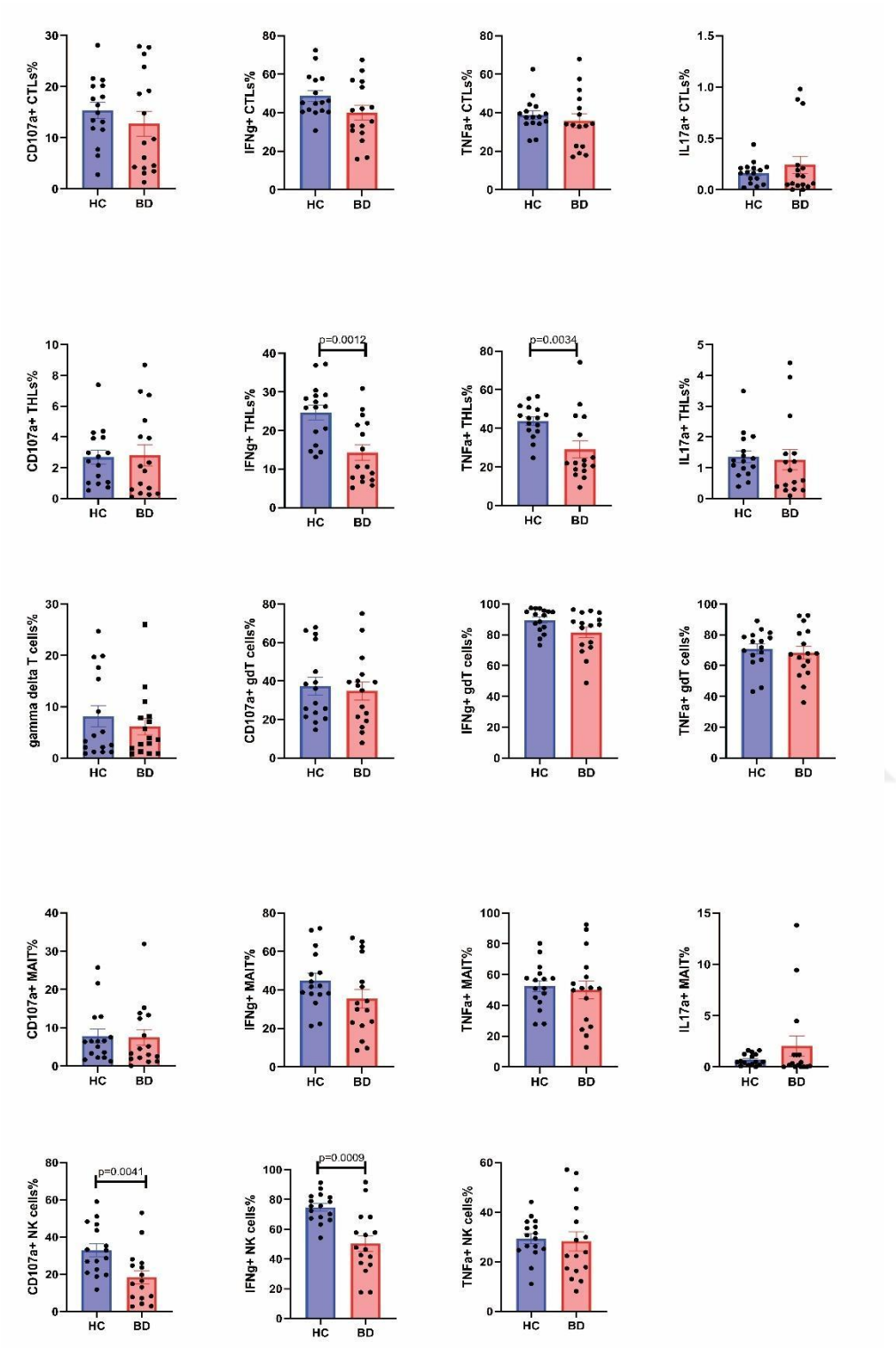

Figure 3.29. Flow cytometry results of functional studies in PBMC of BD patients and HCs.

In addition, we performed functional studies on BD and HC skin samples, and the results are demonstrated in Figure 3.12. The findings demonstrated that there were higher IFNγ+ CTLs (p=0.0071), IFNγ+ THLs (p=0.0071), TNFα+ THLs (p=0.0071), IFNγ+ MAIT (p=0.0002), TNFα+ MAIT (p=0.0311), and CD107a+ NK cells (p=0.0352) in BD skin compared to HC.

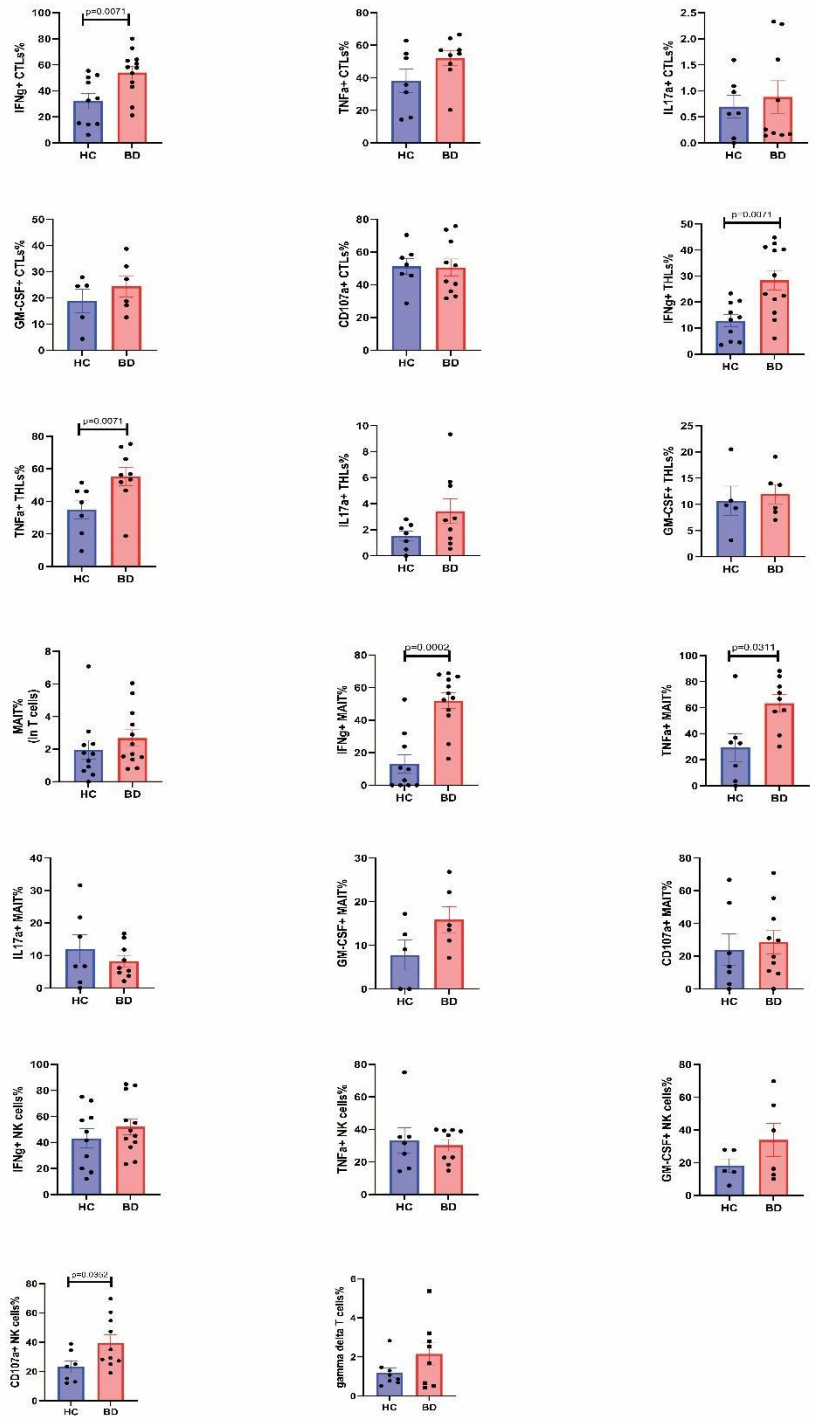

Figure 3.30. Flow cytometry results of functional studies in the skin of BD patients and healthy controls.

Our analysis compared immune cell distribution and functional characteristics across different BD lesion types, including erythema nodosum-like lesions (EN), papulopustular eruptions (PPE), genital ulcers (GU), and positive pathergy tests (PPT). The results showed no statistically significant differences in the immune cell composition or functional characteristics among these lesion types, indicating a shared immunological profile underlying BD skin lesions regardless of clinical presentation (Figure 3.13).

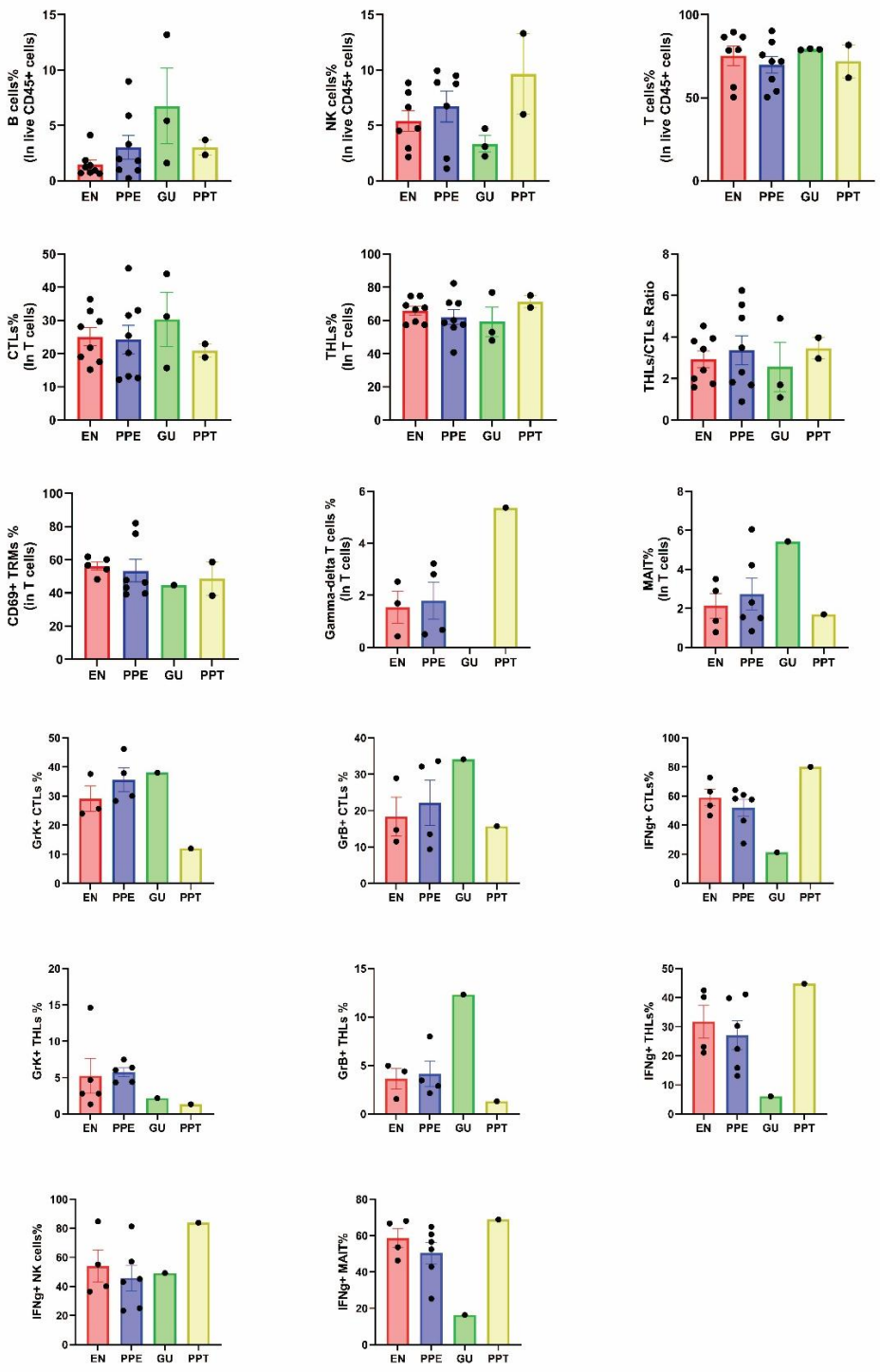

Figure 3.31. Immune cell distribution and functional characteristics across different BD lesion types. The comparison includes erythema nodosum-like lesions (EN), papulopustular eruptions (PPE), genital ulcers (GU), and positive pathergy tests (PPT). No statistically significant differences were observed in immune cell composition or functional characteristics among the lesion types.

CHAPTER 4

DISCUSSION

CHAPTER 4

DISCUSSION

4.1. Protocol Optimization

Single cell analysis of skin immune cells is challenging because of the collagen-rich nature of skin and combined analysis of RNA and protein data is rarely done in the literature. Therefore, we first completed protocol optimization and the result of this improved protocol is now published (195).

The quantity of tissue needed for analysis is a key factor to consider. Our results are consistent with previous studies suggesting that a 6 mm punch biopsy is ideal for collecting enough skin cells from healthy tissue for scRNAseq analysis (197, 198). Saluzzo et al. previously demonstrated that a 6 mm punch biopsy yields 1-2 $\times 10^5$ cells after a 3-hour incubation with enzyme P. In our research, a 3-hour digestion without enzyme P produced an average of 1.125 $\times 10^5$ cells, which aligns with Saluzzo et al. We suggest using two 6 mm biopsies for healthy skin when both flow cytometry and scRNAseq are intended. For BD skin lesions, a 4 mm punch biopsy provided an average of 4.6 $\times 10^5$ cells, notably more than healthy skin, which is adequate for both experiments.

Another key factor for single-cell studies is deciding between the use of fresh or cryopreserved cells. A study carried out in the past few years employed scRNAseq on freshly isolated cells from 4 mm punch biopsies taken from psoriasis and atopic dermatitis patients (187). Although fresh samples might appear to be the optimal choice, coordinating all steps across various patients presents significant challenges. We used frozen cells, which provided benefits like increased experimental flexibility, easier sample multiplexing, and minimized technical batch effects, and as a result a reduction in scRNAseq costs. Importantly, we found no significant difference in CD45+ lymphocyte viability between fresh and cryopreserved cells, consistent with earlier research on pig skin cells preserved in 90% FBS + 10% DMSO, which reported no impact on gene expression, aggregation, or cell viability through scRNAseq analysis (197).

Generating high-quality GEMs is crucial for scRNAseq utilizing the 10X Chromium system and requires cells of good quality and proper concentration. The quality demands for scRNAseq are more stringent than those for flow cytometry and ensuring cell quality after FACS sorting can be difficult. Previous studies noted that mitigating the time between sorting and GEM generation is critical (198). In our approach, we combined 2-3 samples per reaction and used two sorting devices concomitantly to minimize post-sorting time. If the post-sort cell concentration is too low, Saluzzo et al. recommend to use a volume reduction device (198), though not all labs have access to this. We suggest centrifuging cells at 850 g for 5 minutes, and resuspend them in lower volume, and recounting them afterward.

Although enzyme P has been used to boost cell yield in previous protocols, we advise against its use in protein-based methods like flow cytometry or CITE-Seq since it cleaves surface markers such as CD8, CD56, and CD69. Notably, CD45 remains unaffected, allowing successful sorting of CD45+ cells even with enzyme P use.

The length of incubating with enzymes is another key factor for single-cell studies. We investigated different incubation times and observed that 1-hour, 3-hour, and 16-hour digestions demonstrated almost the same results in flow cytometry. While, longer incubations led to decreased granzyme B-expressing cytotoxic T cells and lower CD4 expression on T cells. Given that granzyme B is an effector molecule in cytotoxic lymphocytes, a 3-hour incubation strikes a well-balanced approach between cell yield and preservation of effector cells. Longer incubation times should be avoided when possible.

A method for rapid flow cytometry with 4 mm punch biopsies, using collagenase IV and DNase I, has been described in a published protocol by Polakova et al. (199). Their method yielded 12,000 CD45+ cells per 4 mm biopsy after digestion for 30 minutes. The distribution of primary immune cell types such as B cells, T cells, NK cells, and ILCs was similar across their method and the whole skin dissociation kit (including enzyme P). Moreover, shorter digestion times were shown to better preserve chemokine receptor staining.

Sample multiplexing is a crucial technique for improving experimental efficiency, minimizing technical batch effects, and considerably cutting the expenses of scRNAseq. A

range of demultiplexing methods have been outlined in previous studies, for example utilizing oligonucleotide-labeled hashtag antibodies to assign unique identifiers to cells (200). Saluzzo et al. employed hashtag antibodies for sample demultiplexing in their scRNAseq protocol for human skin (198). However, in comparison with our label-free approach, this method introduces extra steps and additional expenses as a result of the use of antibodies, cDNA library preparation, and sequencing.

Another method, demuxlet, relies on SNPs from a genotype reference acquired from a whole-genome or exome sequencing and has been considered a gold standard for demultiplexing (201). The souporcell algorithm was developed in recent times for sample demultiplexing using scRNAseq data without the necessity of a genotype reference or any external labels (186). Souporcell outperforms demuxlet in comparative analysis studies, making it a promising tool for scRNAseq research. Given these advantages, we chose souporcell as the foundation of our multiplexing strategy.

While souporcell can effectively separate multiplexed samples, the main difficulty is accurately assigning each sample to its proper donor. The initial souporcell publication suggested addressing this issue by including a donor-specific sample in multiple experiments, where donor presence or absence is encoded as a bit (0 or 1), and samples are matched to their respective donors based on this method (186). Here, we refined this strategy By allocating matched PBMC and skin samples from the same donor into separate experimental reactions, creating a straightforward way to determine donor identity. Additionally, we enhanced this approach by adding genetic sex data as an extra step of encoding. This two-layer method allowed us to successfully demultiplex and identify donors, while also lowering the number of reactions and overall expenses of the experiments by two-thirds.

4.2. Immune Profiling of Behcet's disease with scRNAseq

scRNA-seq analysis revealed a significant increase in pDCs, MAIT cells, NK cells, ILC3, in addition to B cells compared to healthy skin. In addition to immune cell infiltration, the expression of cytotoxic molecules such as GZMB, GZMA, GZMK, and perforin was notably elevated in BD lesions. CD4+ and CD8+ Tem cells exhibited a heightened cytotoxic profile, with increased production of IFN-γ, GZMK, and CCL5. These results indicate a immune response mediated by Th1/Tc1 cells and innate lymphocytes (MAIT cells, NK cells and ILC3) in BD skin lesions. This was accompanied by significant activation of the JAK-STAT pathway, further underscoring the strong type I and type II interferons in BD.

Our flow cytometry findings corroborated and expanded the scRNA-seq results. CTL percentage increased in the blood but decreased in the skin, whereas THL percentage were reduced in the blood but enriched in the skin, suggesting preferential infiltration of THLs into BD lesions. While the overall percentage of MAIT cells was not found to be different by flow cytometry between BD and HC in either the skin or blood, functional analyses revealed distinct patterns. IFN-γ+ MAIT cell percentage decreased in BD blood but elevated in BD skin, along with increased TNF-α+ MAIT cells in the skin. Similarly, GrB+ CTL percentage was higher in BD blood, whereas GrK+ and IFN-γ+ CTL percentage were lower in the blood but elevated in BD skin indicating that GrK+ cells preferentially migrate to skin from blood. Among THLs, GrB+ THL percentage was again increased in BD blood, but IFN-γ+ and TNF-α+ THLs were reduced; conversely, these cytokine-producing THLs were enriched in BD skin, indicating that IFN-γ+ and TNF-α+ THLs migrate to BD skin lesions from blood. Our findings also showed that effector memory T cell percentage is decreased in BD blood, along with the increase in naive T cells, reflecting the migration of effector memory T cells to the skin. Lastly, CD107a+ NK cells, indicative of degranulation, were lower in BD blood but significantly higher in BD skin compared to HC. Overall, these results show that activated GzK+ T cells carrying a memory Th1/Tc1 phenotype preferentially locate to BD skin lesions, in addition to activated MAIT cells and NK cells.

Our findings build upon and extend previous reports on the immune dysregulation in BD. For the first time in the literature, we showed an increase in pDCs in BD skin. A similar situation has been highlighted in psoriasis by Nestle et al, demonstrating an enrichment of

pDCs in psoriatic plaque and uninvolved skin from psoriasis patients compared to normal skin, while a decrease was seen in the percentage of these cells in the psoriasis patients' blood (202). Plasmacytoid dendritic cells are normally very low in healthy skin, but their infiltration and increase have been reported in different inflammatory skin diseases like lichen planus (203), psoriasis (202), and acute graft-versus-host disease (GVHD) (204). These cells are known to be the major source of type I interferons, which regulate T cell immune response by memory Th1 polarization, CTLs cytotoxic activity, and IFN-Ɣ production. They also promote NK cells cytotoxicity and IFN-Ɣ production and help in the differentiation of B cells to plasma cells (205). Also, previous studies of BD patients revealed an increase in IFN-α in the serum of BD patients, with a lower number of pDCs in the PBMC (168) or unchanged cell percentage (170). Our data suggests that pDCs contribute to BD pathogenesis in skin lesions by amplifying type I interferon responses and activating the downstream cytotoxic pathways.

Additionally, our scRNAseq analysis showed that CXCL10 was one of the major chemokines that are enhanced in BD skin lesions. This is consistent with findings by Di Domizio et al. (206), who demonstrated that commensal skin microbiota in wounds triggers neutrophil activation to express CXCL10, leading to pDC recruitment and type I interferon production, which in turn accelerates skin inflammation and wound repair. While this study highlights the role of CXCL10 in normal skin healing processes, the heightened CXCL10 expression we observed in BD lesions may suggest a dysregulated inflammatory response that amplifies pDC recruitment and type I interferon production in BD skin. Moreover, Lee et al (207) reported elevated serum CXCL10 levels in BD patients, correlating with disease activity, and an increased presence of CXCR3-positive mononuclear cells in BD lesions. This aligns with our findings and suggests a significant contribution of the CXCL10/CXCR3 axis to BD pathogenesis, potentially driving T cell recruitment to inflamed tissue.

Additionally, Ambrose et al. (208) described dysfunctional post-transcriptional regulation of CXCL10 in BD monocytes, resulting in excessive CXCL10 protein production in response to IFN-γ. This abnormality was more pronounced in patients with high disease activity and certain clinical manifestations, such as ocular and neurological involvement. These findings support the idea that overexpression of CXCL10 in BD could exacerbate

mononuclear cell recruitment and the inflammatory response in skin lesions, potentially contributing to the exaggerated immune activation seen in BD. Together, these studies underscore the importance of CXCL10 in BD pathogenesis and further support our observations of heightened pDC-driven type I interferon responses in BD skin lesions.

Our data suggests a prominent cytotoxic activity of immune response in BD skin lesions, demonstrated by the heightened NK cell percentage and enhanced expression of cytotoxic molecules like granzyme K (GZMK), granzyme A (GZMA), granzyme B (GZMB), and perforin (PRF1). These findings are consistent with previous studies showing an enhanced population of NK cells in BD skin lesions (106), and PBMC compared to healthy controls (142). Accardo-Palumbo et al reported that active BD patients exhibited a significant increase in granzyme A in their serum in comparison with healthy individuals and inactive BD patients (140), also perforin, IFN-Ɣ, and granzyme A release was significantly higher enhanced in active BD patients in contrast to healthy individuals in cultured PBMC with Dimethylallyl pyrophosphate and interleukin-2 (209). In our data, CTLs in lesional skin in addition to having high expression of cytotoxic molecules like GZMA, GZMB, GZMK, perforin, and IFN-Ɣ; expression of chemokines like CCL4 and CCL5 is enhanced, which would potentially increase immune cell recruitment to the site of inflammation. These findings align with genetic studies identifying a gain-of-function polymorphism in IFNGR1 that significantly increases IFNGR1 expression in stimulated monocytes, suggesting a genetic predisposition for heightened IFN-γ-mediated immune responses in BD (210). In a study by Zhan et al, they mentioned CCL4 as a potential diagnostic biomarker for predicting vascular involvement and inflammation status in BD, as their results revealed an elevation in the fraction of CTLs, NK cells, M1 macrophages, and active mast cells in patients with higher expression of CCL4 (211). This cytotoxic and inflammatory activity can establish a feedback loop, perpetuating tissue damage and sustaining the immune response in the lesions. Further supporting this concept, study by Kulaber et al. (212) have shown that BD patients exhibit higher IFN-γ and IL-12 production in response to microbial peptides like BES-1 and antigens such as IPP. These findings highlight a pro-inflammatory cytokine milieu, which could amplify cytotoxic activity and contribute to the chronic inflammation seen in BD lesions. Consistent with these findings, our differential gene expression (DGE) analysis revealed that the expression of IL12B and

IL12RB2 was significantly higher in BD skin lesions compared to HC skin, further supporting the role of the IL-12/IL-12 receptor axis in driving inflammation in BD.

Additionally, genetic studies provide further insights into the inflammatory pathways involved in BD. For instance, a GWAS by Remmers et al. (14) while confirming the well-known association of BD with HLA-B*51, also identified additional independent associations at the IL10 and IL23R-IL12RB2 loci. Similarly, Mizuki et al. (62) conducted a GWAS in a Japanese cohort, identifying two susceptibility loci associated with BD: IL23R-IL12RB2 (rs12119179) and IL10 (rs1554286). Meta-analyses with Turkish and Korean cohorts further confirmed these associations, implicating interleukin and interleukin receptor genes central to immune response pathways. These findings collectively underscore the interplay between genetic predisposition and the pro-inflammatory cytokine environment in BD.

The importance of IL-12 in immune responses is underscored by several studies. Guia et al. (213) demonstrated that human NK cells require in vivo priming with IL-12/23 to achieve their full spectrum of functional reactivity, including IFN-γ production and cytotoxicity. Patients with IL12RB1 or IL12p40 mutations show diminished NK cell functionality, including reduced IFN-γ production and decreased CD56+ effector memory T cells, emphasizing the critical role of the IL-12/23 axis in maintaining immune cell activation and reactivity. Further, IL-12, primarily produced by dendritic cells and macrophages, plays a central role in promoting Th1 polarization and IFN-γ production by CD4+ T cells, as well as enhancing NK cell-mediated cytotoxicity (214, 215). IL-12 has also been implicated in generating memory-like NK cells and augmenting macrophage-NK cell cross-talk, leading to the production of nitric oxide and the upregulation of co-stimulatory molecules like CD86 (216). These mechanisms highlight the cytokine's broad impact on both innate and adaptive immune responses, which may contribute to the chronic inflammation seen in BD.

IL-12 also plays a crucial role in activating MAIT cells, which express semi-invariant Vα7.2-Jα33/12/20 (TRAV1-2-TRAJ33/12/20) T cell receptors specific for microbial riboflavin metabolites presented by MR1. Interestingly, MAIT cells can also be activated independently of their TCR by cytokines such as IL-12 and IL-18, linking IL-12 to the activation of key effector cells involved in inflammation (217). Ussher et al. (218)

demonstrated that CD161(++) CD8(+) T cells, which include MAIT cells, are the primary T cell population responding to IL-12 and IL-18 stimulation, producing IFN-γ. This response is not limited to MAIT cells but also includes other CD161(++) T cells, whether Vα7.2(+) or Vα7.2(-), thus expanding the role of IL-12 beyond microbial riboflavin sensing. Additionally, bacteria and TLR agonists can indirectly trigger IFN-γ production via IL-12 and IL-18, suggesting that these T cells may respond to viral infections and other inflammatory stimuli, further highlighting the broader role of IL-12 in activating inflammatory T cell responses.

Henry et al. (219) demonstrated that IL-12 augments naive CD8+ T cell activation by promoting chemokine production (e.g., CCL1 and CCL17), which facilitates prolonged cognate interactions between CD8+ T cells and dendritic cells. This mechanism enhances IFN-γ production and promotes effective T cell priming. Similarly, Xiao et al. (220) showed that IL-12 programs early memory development in CD8+ T cells during infections, resulting in central memory cells capable of strong expansion upon rechallenge.

Together, these findings underline the pivotal role of the IL-12/IL-12 receptor axis in orchestrating immune responses through the activation of NK cells, Th1 cells, and CD8+ T cells. The increased expression of IL12B and IL12RB2 in BD skin lesions suggests that this cytokine axis may contribute to the amplification of pro-inflammatory signals and sustained tissue damage observed in the disease. Future studies targeting IL-12 signaling pathways could offer valuable insights into potential therapeutic strategies for BD.

This pronounced cytotoxic profile suggesting type I immune response is further supported by the significant activation of the JAK-STAT pathway observed in BD skin lesions in pseudobulk pathway analysis. The implications of the JAK-STAT pathway have been reported in different autoimmune diseases like psoriasis, IBD, and RA; and several JAK inhibitors are in various clinical trial phases for the treatment of these diseases (221). There have been only a few studies in BD, and in accordance with our findings, Tulunay et al, reported enhanced expression of JAK1 and activated JAK/STAT signaling in monocytes and THLs in the PBMC of BD patients in comparison with healthy individuals (222). Also, Puccetti et al found enrichment of JAK/STAT, type I IFN, and TLR signaling pathways of BD patients (223). There has been a pilot study on the efficacy and safety of usage of tofacitinib, a JAK1/3 inhibitor, for the treatment of refractory BD (224). They enrolled 13

patients with active BD despite combination of glucocorticoids, and multiple immunosuppressant and biologic medications. All patients received 5 mg tofacitinib twice a day, plus low or medium dose of glucocorticoid and unchanged or decreased immunosuppressants. They reported improved clinical outcome for 8 patients, which was defined as resolved BD manifestations without new onset BD-related findings. To get a bit more in the details after a median of 8 months follow-up, patients with vascular/cardiac (n=5) and articular (n=2) involvement achieved remission both in clinical and radiological findings and significant decreased C-reactive protein and erythrocyte sedimentation rate; while in patients with gastrointestinal involvement (n=6) only one patient showed resolved intestinal ulcerations but it remained in the other five individuals (224). As the JAK-STAT signaling pathway is involved in cytokine response, its activation in BD may reflect the enhanced IFN-Ɣ and type I interferon response observed in our study. By promoting the transcription of genes involved in immune cell activation and survival, the JAK/STAT pathway contributes to the chronic nature of BD. Given the success of JAK inhibitors in treating other autoimmune diseases, these medications could have the potential to modulate the immune response in BD.

The role of MAIT cells in BD is another intriguing finding in our study. These cells, typically involved in mucosal immunity, are increased in BD skin lesions. Previous studies using flow cytometry no significant variation was noted in MAIT cell population in PBMC of BD patients (225), and a scRNA-seq study revealed no significant enrichment in genes associated with MAITs, namely *Vα2/Vα7/Vβ2/Vβ13,* in the aqueous humour of BD uveitis patients (226). A recent study by Chang et al performed scRNA-seq from 2 skin lesions and 4 PBMC of BD patients and observed a significant number of MAIT cells in their data (227). Recent single-cell transcriptomic and epigenetic study from PBMC of BD patients revealed a significant number of MAIT cells showing activation in NF-kB, TNF, and VEGFA-VEGFR2 signaling pathways (228). In our study, MAIT cells in BD skin lesions exhibit high GrB expression and produce enhanced levels of IFN-γ and TNF-α upon activation compared to healthy skin. These findings suggest that MAIT cells may contribute to the pro-inflammatory environment and tissue damage characteristics of BD skin lesions, potentially playing a key role in the pathogenesis of the disease. Also, based

on this information MAIT-1 cells, rather than MAIT-17 cells, are activated in BD skin lesions.

Our study demonstrates a notable enrichment of memory B cells in BD skin lesions compared to healthy skin, as revealed by scRNAseq data. Additionally, flow cytometry analysis further supports this finding by showing an increased percentage of B cells in BD skin. Previous studies showed an increase in memory and activated B cells in the blood of BD patients (171), enhanced B cells with spontaneous secretion of immunoglobulins and decreased B cell response to T cell-dependent mitogens or T cell-dependent polyclonal activator (172), and increased B cells in active mucosal ulcers shown with immunohistochemistry (173). In addition, a recent single-cell transcriptomic and epigenetic study from PBMC of BD patients and healthy controls identified 4 subsets of B cells including naive B cells, memory B cells, double negative B cells, and plasma B cells. Also, the transcription data revealed high expression of HLA-DQB1 (molecule related to antigen processing and presenting), IRF1 and IFITM2 (genes stimulated by interferon), IL2RG, JUNB (of AP-1 family genes), MAPK signaling, and NF-ƙB signaling in all B cell groups of BD. In addition, by overlapping differentially accessible chromatin regions and differentially expressed genes (DEGs), the results demonstrated high expression of CD69 (an activation marker) in double negative B cells, and high expression of CD83 (antigen presenting and activation marker) in memory and naive B cells. These findings indicate a heightened activation state of B cells in BD patients (228). B cells have been reported as a treatment target with a case report of a BD patient with retinal vasculitis resistant to azathioprine and prednisolone, who was successfully treated with rituximab, a monoclonal anti-CD20 antibody, and the remission was sustained during 24 months of follow-up (229). This study was followed by a pilot study to evaluate the efficacy of rituximab in BD retinal vasculitis resistant to cytotoxic medications. Having 20 patients randomized to two groups of the rituximab group (RG) or cytotoxic combination therapy group (CCTG), the results showed significant improvement of total adjusted disease activity and posterior uveitis in RG group, but not CCTG (174). The involvement of the B cell compartment in BD skin lesions is further supported in our results by the differential expression of immunoglobulin genes, including IGHV3-30, IGHG2, and IGHG1. Importantly, the increased expression of TLR10 (log2FC = 4.42) in B cells suggests an enhanced pathogen-sensing capability,

contributing to active humoral immune responses. These findings underline the augmented pattern recognition capacity of B cells in BD, further supporting their potential as therapeutic targets. The accumulation of B cells in BD skin lesions may contribute to chronic inflammation by antigen presentation, antibody, and cytokine production. These findings collectively indicate that B cells in BD not only contribute to inflammation through antigen presentation and cytokine production but also play a significant role in complement activation, Fc receptor signaling, and enhanced pathogen sensing. These multifaceted functions suggest an active involvement of B cells in linking innate and adaptive immunity, reinforcing their contribution to BD pathogenesis. The precise role of B cells in BD skin lesions needs further investigation, as understanding their function could reveal new therapeutic targets.

Further supporting this heightened immune activation in BD lesions, we observed the upregulation of C1QB (log2FC = 3.67), a key initiator of the classical complement pathway. This finding suggests antibody-mediated complement activation, likely driven by antibodies produced by plasma cells. Additionally, genes related to Fc receptor signaling were differentially expressed, including FCER1G (log2FC = 1.69), the common signaling chain; FCGR1A (log2FC = 2.70), a high-affinity IgG receptor; and FCGR1B (log2FC = 2.90). These findings highlight enhanced antibody-dependent responses, which bridge innate and adaptive immunity, as well as the activation of phagocytic programs in BD skin lesions. This suggests a coordinated interaction between antibodies produced by B cells and macrophages, which are key producers of complement proteins. The classical complement pathway and Fc receptor signaling may play a significant role in propagating inflammation and tissue damage in BD lesions.

TCR sequencing results showed that T cell clonality is not increased in BD skin lesions. This finding provides significant insights into the pathogenesis of BD. It has been widely accepted that BD is an auto-inflammatory disease with a possible autoimmune component, supported by its association with HLA-B51. Our study shows that T cells that are causing BD skin lesions are not clonally expanded. Paired with our findings showing that innate lympohcytes (NK cells), innate T cells (MAIT and ILC3) and Th1/Tc1 and cytotoxic pathways are the major players in the formation of BD skin lesions, it is possible to say that BD is a disease with increased innate lymphocytic activation, without clonal expansion of

T cells. However, it should be kept in mind that pathogenesis of other BD lesions in other sites such as uveitis can have different characteristics and should be investigated in future studies.

Interestingly, our findings differ from studies that demonstrated increased T cell clonality in peripheral blood from BD patients. For example, Zou et al. (230) observed higher T cell clonality and reduced repertoire diversity in the peripheral blood of BD patients compared to healthy controls, with a significant clustering of TCR-β sequences indicative of antigen-driven clonal expansion. The study highlighted distinct TCR clusters potentially recognizing shared antigens, suggesting antigen-driven T cell responses in BD pathology. Similarly, Direskeneli et al. (91) reported oligoclonal T cell expansions in the CD4+ and CD8+ compartments of BD patients' peripheral blood, indicating antigen-driven T cell proliferation.

The discrepancy between our findings and those of Zou et al. and Direskeneli et al. may reflect tissue-specific differences in T cell activity and clonality. While clonal T cell expansion is evident in the peripheral blood of BD patients, it may not translate to the skin, where innate immune cells and non-clonal T cell populations may dominate the inflammatory response. Alternatively, our data suggest that the mechanisms driving inflammation in BD skin lesions may be distinct from those in the systemic circulation, potentially shaped by local tissue-specific factors such as the cytokine milieu, resident immune cell populations, or antigen presentation pathways.

It is also important to consider the differences in methodology. Zou et al. and Direskeneli et al. focused on peripheral blood using bulk TCR sequencing and flow cytometry, respectively, whereas our study utilized single-cell RNA sequencing (scRNA-seq) of skin lesions, providing a localized view of the immune landscape. These differences underscore the need for more comprehensive studies integrating data from multiple tissues and employing advanced spatial and single-cell technologies to better understand the immune dynamics in BD.

In summary, our results show that the immune pathology of BD skin lesions is driven by an interplay of pDC-derived IFN-α production, heightened cytotoxic activity from NK and CTLs, and increased Th1/Tc1 type response including non-conventional T cells like MAIT

cells, all contributing to an inflammatory environment sustained by the JAK-STAT signaling pathway. These findings not only demonstrate the mechanism of BD pathogenesis but also suggest various targets for new therapeutic strategies to control the chronic inflammation and tissue damage in this disease.

While our findings give new insights of immune landscape of BD lesions, several limitations should be noted. First, our study focused on acute inflammatory lesions and a single time point analysis, which may not fully show the immune changes in chronic or resolved lesions over time or in response to treatment. Second, our study did not investigate the functional consequences of the JAK-STAT pathway activation or the production of cytotoxic molecules in BD lesions. Future research can explore the functional role of these molecules in BD pathogenesis and assess if inhibition of their activity could improve clinical outcomes and decrease inflammation. Third, the sample size for each lesion type (EN, PPE, GU, and PPT) was limited, which precluded a comprehensive analysis of differences in the immune response across various skin lesions. Another limitation was the lack of B cell receptor (BCR) sequencing, which could provide a deeper insight into B cell clonal expansion and antigen specificity in BD. Finally, our findings may be limited in their generalizability due to the relatively small sample size. A larger and multi-center study with a more diverse population can validate the results and ensure the representation of a broader BD patient population.

CHAPTER 5

CONCLUSION

CHAPTER 5

Conclusion

In conclusion, our study provides a comprehensive analysis of the immune cell composite and molecular pathways involved in BD skin lesions, highlighting significant differences between healthy and BD skin. The enrichment of pDCs, MAIT cells, NK cells, and B cells, coupled with the activation of the JAK-STAT pathway, shows the complexity of immune dysregulation in BD. In our findings of immune response in BD skin, pDCs appear to play a central role, producing IFN-α, which activates NK cells, CTLs (Tc1), and Th1 cells. This type I interferon response drives these cells to enhanced cytotoxic activity, contributing to tissue damage through increased production of granzyme A, granzyme B, granzyme K, and perforin, particularly in CD8+ effector memory T cells. Simultaneously, the JAK-STAT pathway activation enhances the inflammatory profile by promoting cytokine signaling, amplifying IFN-Ɣ production by T cells. B cells likely contribute to antigen-presenting to T cells and sustain the inflammatory state by producing antibodies. Together this network of pDCs, T cells, MAIT cells, and B cells form an immune map of a robust inflammatory response in BD, with each cell type and pathway potentiating the others to maintain a chronic inflammatory state. These findings highlight potential therapeutic targets, including JAK-STAT pathway, which could be explored to develop novel treatments for BD.

Additionally, our study did not observe increased clonal expansion of T cells in BD skin lesions, suggesting that the immune response is more reliant on innate immune activation rather than adaptive T cell-mediated inflammation. This lack of T cell clonality aligns with our broader finding of heightened innate lymphocytic activation in BD lesions. This finding provides further insights into the pathogenesis of BD, where immune responses seem to be driven by innate immune cells, including MAIT cells and NK cells, rather than clonal T cell expansions.

Based on our findings, several future research directions emerge. First, further research is needed on the role of MAIT cells, that could offer a promising treatment option for BD patients. Second, functional studies focusing on the JAK-STAT pathway and cytotoxic molecules in BD

lesions, exploring the downstream effects of this pathway and their role in inflammation and tissue damage are crucial. Also, exploring the efficacy of JAK inhibitors in modulating the immune responses in BD and clinical trials assessing the safety and efficacy if JAK inhibitors in BD could provide a novel treatment for this disease. Third, using BCR sequencing in future studies could provide more insight into B cell clonal expansion and antigen specificity, and uncover new therapeutic targets and biomarkers related to B cell activity. Finally, longitudinal studies are needed to examine immune cell dynamics throughout the different stages of BD, which would provide valuable information about the role of specific immune cell populations in disease progression.

References

1. Sonmez C, Yucel AA, Yesil TH, Kucuk H, Sezgin B, Mercan R, et al. Correlation between IL-17A/F, IL-23, IL-35 and IL-12/-23 (p40) levels in peripheral blood lymphocyte cultures and disease activity in Behcet's patients. Clinical rheumatology. 2018;37(10):2797-804.
2. Jo YG, Ortiz-Fernández L, Coit P, Yilmaz V, Yentür SP, Alibaz-Oner F, et al. Sex-specific analysis in Behçet's disease reveals higher genetic risk in male patients. J Autoimmun. 2022;132:102882.
3. Alpsoy E. Behçet's disease: A comprehensive review with a focus on epidemiology, etiology and clinical features, and management of mucocutaneous lesions. The Journal of dermatology. 2016;43(6):620-32.
4. Leccese P, Alpsoy E. Behçet's disease: An overview of etiopathogenesis. Frontiers in Immunology. 2019;10(MAY).
5. Vural S, Boyvat A. The skin in Behçet's disease: Mucocutaneous findings and differential diagnosis. JEADV Clinical Practice. 2022;1(1):11-20.
6. Greco A, De Virgilio A, Ralli M, Ciofalo A, Mancini P, Attanasio G, et al. Behçet's disease: New insights into pathophysiology, clinical features and treatment options. Autoimmunity Reviews. 2018;17(6):567-75.
7. Gholijani N, Daryabor G, Yazdani MR, Vazani N, Shabbooei B, Zahed M, et al. Serum interleukin-37 (IL-37) and its gene polymorphism in Iranian Behcet's disease patients: Association with disease manifestations and activity. Meta Gene. 2020;26.
8. Mattioli I, Bettiol A, Saruhan-Direskeneli G, Direskeneli H, Emmi G. Pathogenesis of Behçet's Syndrome: Genetic, Environmental and Immunological Factors. Front Med (Lausanne). 2021;8:713052.
9. Giza M, Koftori D, Chen L, Bowness P. Is Behçet's disease a 'class 1-opathy'? The role of HLA-B*51 in the pathogenesis of Behçet's disease. Clinical and Experimental Immunology. 2018;191(1):11-8.
10. Takeuchi M, Kastner DL, Remmers EF. The immunogenetics of Behçet's disease: A comprehensive review. Journal of Autoimmunity. 2015;64:137-48.
11. Ahn HS, Kim HJ, Kazmi SZ, Kang T, Jun J-B, Kang MJ, et al. Familial risk of Behçet's disease among first-degree relatives: a population-based aggregation study in Korea. Rheumatology. 2020;60(6):2697-705.
12. van der Houwen T, van Laar J. Behçet's disease, and the role of TNF-α and TNF-α blockers. International Journal of Molecular Sciences. 2020;21(9).
13. Mahmoudi M, Aslani S, Meguro A, Akhtari M, Fatahi Y, Mizuki N, et al. A comprehensive overview on the genetics of Behçet's disease. Int Rev Immunol. 2022;41(2):84-106.
14. Remmers EF, Cosan F, Kirino Y, Ombrello MJ, Abaci N, Satorius C, et al. Genome-wide association study identifies variants in the MHC class I, IL10, and IL23R-IL12RB2 regions associated with Behçet's disease. Nature Genetics. 2010;42(8):698-702.
15. Dalvi SR, Yildirim R, Yazici Y. Behcet's Syndrome. Drugs. 2012;72(17):2223-41.
16. Nelson CA, Stephen S, Ashchyan HJ, James WD, Micheletti RG, Rosenbach M. Neutrophilic dermatoses: Pathogenesis, Sweet syndrome, neutrophilic eccrine hidradenitis, and Behçet disease. Journal of the American Academy of Dermatology. 2018;79(6):987-1006.

17. Alpsoy E, Yilmaz E, Coşkun M, Savaş A, Yeğin O. HLA Antigens and Linkage Disequilibrium Patterns in Turkish Behçet's Patients. The Journal of Dermatology. 1998;25(3):158-62.
18. Ideguchi H, Suda A, Takeno M, Ueda A, Ohno S, Ishigatsubo Y. Behçet Disease: Evolution of Clinical Manifestations. Medicine. 2011;90(2):125-32.
19. Rajaei E, Jalali TM, Pezeshki MSS, Rezaeeyan H, Maniati M, Elyasi M, et al. Dose HLA-B5, 7, 8, 27, and 51 Antigens Associated to Behcet's disease? A Study in Southwestern Iran. Current Rheumatology Reviews. 2020;16(2):120-4.
20. de Menthon M, LaValley MP, Maldini C, Guillevin L, Mahr A. HLA–B51/B5 and the risk of Behçet's disease: A systematic review and meta-analysis of case–control genetic association studies. Arthritis Care & Research. 2009;61(10):1287-96.
21. Koumantaki Y, Stavropoulos C, Spyropoulou M, Messini H, Papademetropoulos M, Giziaki E, et al. HLA-B∗5101 in Greek Patients with Behçet's Disease. Human Immunology. 1998;59(4):250-5.
22. Itoh Y, Inoko H, Kulski JK, Sasaki S, Meguro A, Takiyama N, et al. Four-digit allele genotyping of the HLA-A and HLA-B genes in Japanese patients with Behcet's disease by a PCR-SSOP-Luminex method. Tissue Antigens. 2006;67(5):390-4.
23. Pirim I, Atasoy M, Ikbal M, Erdem T, Aliagaoglu C. HLA class I and class II genotyping in patients with Behcet's disease: a regional study of eastern part of Turkey. Tissue Antigens. 2004;64(3):293-7.
24. Horie Y, Meguro A, Ohta T, Lee EB, Namba K, Mizuuchi K, et al. HLA-B51 Carriers are Susceptible to Ocular Symptoms of Behçet Disease and the Association between the Two Becomes Stronger towards the East along the Silk Road: A Literature Survey. Ocul Immunol Inflamm. 2017;25(1):37-40.
25. Maldini C, Lavalley MP, Cheminant M, de Menthon M, Mahr A. Relationships of HLA-B51 or B5 genotype with Behcet's disease clinical characteristics: systematic review and meta-analyses of observational studies. Rheumatology (Oxford). 2012;51(5):887-900.
26. Zouboulis CC, Büttner P, Djawari D, Kirch W, Keitel W, Garbe C, et al. [The HLA pattern in Adamantiades-Behçet's disease in Germany. Association of occurrence, clinical symptoms and follow-up in 39 patients]. Hautarzt. 1993;44(2):81-5.
27. Ryu HJS, M.R.; Choi, H.J.; Baek, H.J. Clinical phenotypes of Korean patients with Behcet disease according to gender, age at onset, and HLA-B51 FAU - Ryu, Hee Jung FAU - Seo, Mi Ryoung FAU - Choi, Hyo Jin FAU - Baek, Han Joo. Korean J Intern Med. 2018;33(5):1025-31.
28. Pamukcu M, Duran TI, Demirag MD. HLA-B51 Impact on Clinical Symptoms in Behcet's Disease. J Coll Physicians Surg Pak. 2022;32(7):904-8.
29. Mizuki Y, Horita N, Horie Y, Takeuchi M, Ishido T, Mizuki R, et al. The influence of HLA-B51 on clinical manifestations among Japanese patients with Behçet's disease: A nationwide survey. Modern Rheumatology. 2020;30(4):708-14.
30. Krause I, Molad Y, Weinberger A. Association of HLA-B5 with Clinical Expression and Severity of Behcet's Disease in Israel. J Clin Rheumatol. 1999;5(3):137-40.
31. Kirino Y, Ideguchi H, Takeno M, Suda A, Higashitani K, Kunishita Y, et al. Continuous evolution of clinical phenotype in 578 Japanese patients with Behçet's disease: a retrospective observational study. Arthritis Research & Therapy. 2016;18(1):217.
32. Al-Obeidi AF, Nowatzky J. Immunopathogenesis of Behçet's disease. Clinical Immunology. 2023;253:109661.
33. Guasp P, Alvarez-Navarro C, Gomez-Molina P, Martín-Esteban A, Marcilla M, Barnea E, et al. The Peptidome of Behçet's Disease–Associated HLA–B*51:01 Includes Two Subpeptidomes Differentially Shaped by Endoplasmic Reticulum Aminopeptidase 1. Arthritis \& Rheumatology. 2016;68(2):505-15.
34. Jonas JWK, Jörg CP, Efstratios S, Piotr K, Akiko A, Sebastian S, et al. EULAR study group on 'MHC-I-opathy': identifying disease-overarching mechanisms across disciplines and borders. Annals of the Rheumatic Diseases. 2023;82(7):887.

35. McGonagle D, Aydin SZ, Gül A, Mahr A, Direskeneli H. 'MHC-I-opathy'-unified concept for spondyloarthritis and Behçet disease. 2015. p. 731-40.
36. Takeno M. The association of Behçet's syndrome with HLA-B51 as understood in 2021. Current Opinion in Rheumatology. 2022;34(1).
37. Rock KL, Reits E, Neefjes J. Present Yourself! By MHC Class I and MHC Class II Molecules. Trends in immunology. 2016;37(11):724-37.
38. Capittini C, Rebuffi C, Lenti MV, Di Sabatino A, Tinelli C, Martinetti M, et al. Global Meta-Analysis on the Association between Behcet Syndrome and Polymorphisms from the HLA Class I (A, B, and C) and Class II (DRB1, DQB1, and DPB1) Genes. Disease Markers. 2021;2021:9348697.
39. Kirino Y, Bertsias G, Ishigatsubo Y, Mizuki N, Tugal-Tutkun I, Seyahi E, et al. Genome-wide association analysis identifies new susceptibility loci for Behçet's disease and epistasis between HLA-B*51 and ERAP1. Nature genetics. 2013;45(2):202-7.
40. Sousa I, Shahram F, Francisco D, Davatchi F, Abdollahi BS, Ghaderibarmi F, et al. Brief report: association of CCR1, KLRC4, IL12A-AS1, STAT4, and ERAP1 With Behçet's disease in Iranians. Arthritis Rheumatol. 2015;67(10):2742-8.
41. Tedeschi V, Paldino G, Paladini F, Mattorre B, Tuosto L, Sorrentino R, et al. The Impact of the 'Mis-Peptidome' on HLA Class I-Mediated Diseases: Contribution of ERAP1 and ERAP2 and Effects on the Immune Response. International journal of molecular sciences. 2020;21(24).
42. López de Castro JA. How ERAP1 and ERAP2 Shape the Peptidomes of Disease-Associated MHC-I Proteins. Front Immunol. 2018;9:2463.
43. Takeuchi M, Ombrello MJ, Kirino Y, Erer B, Tugal-Tutkun I, Seyahi E, et al. A single endoplasmic reticulum aminopeptidase-1 protein allotype is a strong risk factor for Behçet's disease in HLA-B*51 carriers. Ann Rheum Dis. 2016;75(12):2208-11.
44. Cavers A, Kugler MC, Ozguler Y, Al-Obeidi AF, Hatemi G, Ueberheide BM, et al. Behçet's disease risk-variant HLA-B51/ERAP1-Hap10 alters human CD8 T cell immunity. Ann Rheum Dis. 2022;81(11):1603-11.
45. Guasp P, Barnea E, González-Escribano MF, Jiménez-Reinoso A, Regueiro JR, Admon A, et al. The Behcet's disease-associated variant of the aminopeptidase ERAP1 shapes a low-affinity HLA-B*51 peptidome by differential subpeptidome processing. Journal of Biological Chemistry. 2017;292(23):9680-9.
46. Cifaldi L, Romania P, Falco M, Lorenzi S, Meazza R, Petrini S, et al. ERAP1 regulates natural killer cell function by controlling the engagement of inhibitory receptors. Cancer Res. 2015;75(5):824-34.
47. Ryu H-M, Islam SMS, Sayeed HM, Babita R, Seong JK, Lee H, et al. Characterization of immune responses associated with ERAP-1 expression in HSV-induced Behçet's disease mouse model. Clinical Immunology. 2023;250:109305.
48. Pepelyayeva Y, Rastall DPW, Aldhamen YA, O'Connell P, Raehtz S, Alyaqoub FS, et al. ERAP1 deficient mice have reduced Type 1 regulatory T cells and develop skeletal and intestinal features of Ankylosing Spondylitis. Scientific Reports. 2018;8(1):12464.
49. Gebreselassie D, Spiegel H, Vukmanovic S. Sampling of major histocompatibility complex class I-associated peptidome suggests relatively looser global association of HLA-B*5101 with peptides. Human immunology. 2006;67(11):894-906.
50. Falk K, Rötzschke O, Takiguchi M, Gnau V, Stevanović S, Jung G, et al. Peptide motifs of HLA-B51,-B52 and-B78 molecules, and implications for Behcet's disease. International immunology. 1995;7(2):223-8.
51. Gur M, Golcuk M, Gul A, Erman B. Molecular dynamics simulations provide molecular insights into the role of HLA-B51 in Behçet's disease pathogenesis. Chemical Biology & Drug Design. 2020;96(1):644-58.
52. Ombrello MJ, Kirino Y, de Bakker PIW, Gül A, Kastner DL, Remmers EF. Behçet disease-associated MHC class I residues implicate antigen binding and regulation of cell-mediated

cytotoxicity. Proceedings of the National Academy of Sciences of the United States of America. 2014;111(24):8867-72.
53. Huyton T, Ladas N, Schumacher H, Blasczyk R, Bade-Doeding C. Pocketcheck: updating the HLA class I peptide specificity roadmap. Tissue Antigens. 2012;80(3):239-48.
54. Sanjanwala B, Draghi M, Norman PJ, Guethlein LA, Parham P. Polymorphic Sites Away from the Bw4 Epitope That Affect Interaction of Bw4+ HLA-B with KIR3DL11. The Journal of Immunology. 2008;181(9):6293-300.
55. Al-Okaily F, Al-Rashidi S, Al-Balawi M, Mustafa M, Arfin M, Al-Asmari A. Genetic Association of HLA-A*26, -A*31, and -B*51 with Behcet's Disease in Saudi Patients. Clin Med Insights Arthritis Musculoskelet Disord. 2016;9:167-73.
56. Kang EH, Kim JY, Takeuchi F, Kim JW, Shin K, Lee EY, et al. Associations between the HLA-Apolymorphism and the clinical manifestations of Behcet's disease. Arthritis Research & Therapy. 2011;13(2):R49.
57. Kuranov AB, Kötter I, Henes JC, Abisheva ST, Steiert I, Riewerts F, et al. Behçet's disease in HLA-B*51 negative Germans and Turks shows association with HLA-Bw4-80I. Arthritis Research & Therapy. 2014;16(3):R116.
58. Petrushkin H, Norman PJ, Lougee E, Parham P, Wallace GR, Stanford MR, et al. KIR3DL1/S1 Allotypes Contribute Differentially to the Development of Behçet Disease. The Journal of Immunology. 2019;203(6):1629-35.
59. Single RM, Martin MP, Gao X, Meyer D, Yeager M, Kidd JR, et al. Global diversity and evidence for coevolution of KIR and HLA. Nature Genetics. 2007;39(9):1114-9.
60. Erer B, Takeuchi M, Ustek D, Tugal-Tutkun I, Seyahi E, Özyazgan Y, et al. Evaluation of KIR3DL1/KIR3DS1 polymorphism in Behçet's disease. Genes & Immunity. 2016;17(7):396-9.
61. Saruhan-Direskeneli G, Uyar FA, Çefle A, Onder SC, Ekşioğlu-Demiralp E, Kamalı S, et al. Expression of KIR and C-type lectin receptors in Behçet's disease. Rheumatology. 2003;43(4):423-7.
62. Mizuki N, Meguro A, Ota M, Ohno S, Shiota T, Kawagoe T, et al. Genome-wide association studies identify IL23R-IL12RB2 and IL10 as Behçet's disease susceptibility loci. Nat Genet. 2010;42(8):703-6.
63. Touitou I, Magne X, Molinari N, Navarro A, Quellec AL, Picco P, et al. MEFV mutations in Behçet's disease. Human Mutation. 2000;16(3):271-2.
64. Atagunduz P, Ergun T, Direskeneli H. MEFV mutations are increased in Behçet's disease (BD) and are associated with vascular involvement. Clin Exp Rheumatol. 2003;21(4 Suppl 30):S35-7.
65. Kirino Y, Zhou Q, Ishigatsubo Y, Mizuki N, Tugal-Tutkun I, Seyahi E, et al. Targeted resequencing implicates the familial Mediterranean fever gene MEFV and the toll-like receptor 4 gene TLR4 in Behçet disease. Proc Natl Acad Sci U S A. 2013;110(20):8134-9.
66. Vural S, Gündoğdu M, Gökpınar İli E, Durmaz CD, Vural A, Steinmüller-Magin L, et al. Association of pyrin mutations and autoinflammation with complex phenotype hidradenitis suppurativa: a case-control study. Br J Dermatol. 2019;180(6):1459-67.
67. Ishikawa H, Shindo A, Ii Y, Kishida D, Niwa A, Nishiguchi Y, et al. MEFV gene mutations in neuro-Behçet's disease and neuro-Sweet disease. Ann Clin Transl Neurol. 2019;6(12):2595-600.
68. Chae JJ, Cho YH, Lee GS, Cheng J, Liu PP, Feigenbaum L, et al. Gain-of-function Pyrin mutations induce NLRP3 protein-independent interleukin-1β activation and severe autoinflammation in mice. Immunity. 2011;34(5):755-68.
69. Zhang J, Liao D, Yang L, Hou S. Association between Functional MICA-TM and Behcet's Disease: A Systematic Review and Meta-analysis. Scientific Reports. 2016;6(1):21033-.
70. Xavier JMS, F.; Sousa, I.; Davatchi, F.; Matos, M.; Abdollahi, B.S.; Sobral, J.; Nadji, A.; Oliveira, M.; Ghaderibarim, F.; Mojarad Shafiee,N., Oliveira SA. FUT2: filling the gap between genes and environment in Behçet's disease? Annals of the Rheumatic Diseases. 2015;74(3):618.
71. Mehmood N, Low L, Wallace GR. Behçet's Disease—Do Microbiomes and Genetics Collaborate in Pathogenesis? Frontiers in Immunology. 2021;12.

72. Ferrer-Admetlla A, Sikora M, Laayouni H, Esteve A, Roubinet F, Blancher A, et al. A natural history of FUT2 polymorphism in humans. Mol Biol Evol. 2009;26(9):1993-2003.
73. Kolde R, Franzosa EA, Rahnavard G, Hall AB, Vlamakis H, Stevens C, et al. Host genetic variation and its microbiome interactions within the Human Microbiome Project. Genome Med. 2018;10(1):6.
74. Horie Y, Meguro A, Ota M, Kitaichi N, Katsuyama Y, Takemoto Y, et al. Association of TLR4 polymorphisms with Behcet's disease in a Korean population. Rheumatology (Oxford). 2009;48(6):638-42.
75. Meguro A, Ota M, Katsuyama Y, Oka A, Ohno S, Inoko H, et al. Association of the toll-like receptor 4 gene polymorphisms with Behcet's disease. Ann Rheum Dis. 2008;67(5):725-7.
76. Fang J, Hu R, Hou S, Ye Z, Xiang Q, Qi J, et al. Association of TLR2 gene polymorphisms with ocular Behcet's disease in a Chinese Han population. Invest Ophthalmol Vis Sci. 2013;54(13):8384-92.
77. Tsuchida N, Kirino Y, Soejima Y, Onodera M, Arai K, Tamura E, et al. Haploinsufficiency of A20 caused by a novel nonsense variant or entire deletion of TNFAIP3 is clinically distinct from Behçet's disease. Arthritis Research & Therapy. 2019;21(1):137.
78. Li H, Liu Q, Hou S, Du L, Zhou Q, Zhou Y, et al. TNFAIP3 gene polymorphisms confer risk for Behcet's disease in a Chinese Han population. Human Genetics. 2013;132(3):293-300.
79. Deng Y, Zhu W, Zhou X. Immune Regulatory Genes Are Major Genetic Factors to Behcet Disease: Systematic Review. Open Rheumatol J. 2018;12:70-85.
80. Boone DL, Turer EE, Lee EG, Ahmad R-C, Wheeler MT, Tsui C, et al. The ubiquitin-modifying enzyme A20 is required for termination of Toll-like receptor responses. Nature Immunology. 2004;5(10):1052-60.
81. Hitotsumatsu O, Ahmad R-C, Tavares R, Wang M, Philpott D, Turer EE, et al. The Ubiquitin-Editing Enzyme A20 Restricts Nucleotide-Binding Oligomerization Domain Containing 2-Triggered Signals. Immunity. 2008;28(3):381-90.
82. Plenge RM, Cotsapas C, Davies L, Price AL, de Bakker PI, Maller J, et al. Two independent alleles at 6q23 associated with risk of rheumatoid arthritis. Nat Genet. 2007;39(12):1477-82.
83. Graham RR, Cotsapas C, Davies L, Hackett R, Lessard CJ, Leon JM, et al. Genetic variants near TNFAIP3 on 6q23 are associated with systemic lupus erythematosus. Nat Genet. 2008;40(9):1059-61.
84. Nair RP, Duffin KC, Helms C, Ding J, Stuart PE, Goldgar D, et al. Genome-wide scan reveals association of psoriasis with IL-23 and NF-kappaB pathways. Nat Genet. 2009;41(2):199-204.
85. Beecham AH, Patsopoulos NA, Xifara DK, Davis MF, Kemppinen A, Cotsapas C, et al. Analysis of immune-related loci identifies 48 new susceptibility variants for multiple sclerosis. Nat Genet. 2013;45(11):1353-60.
86. Berteau F, Rouviere B, Delluc A, Nau A, Le Berre R, Sarrabay G, et al. Autosomic dominant familial Behçet disease and haploinsufficiency A20: A review of the literature. Autoimmunity Reviews. 2018;17(8):809-15.
87. Korman BD, Kastner DL, Gregersen PK, Remmers EF. STAT4: Genetics, mechanisms, and implications for autoimmunity. Current Allergy and Asthma Reports. 2008;8(5):398-403.
88. Hou S, Yang Z, Du L, Jiang Z, Shu Q, Chen Y, et al. Identification of a susceptibility locus in STAT4 for Behçet's disease in Han Chinese in a genome-wide association study. Arthritis & Rheumatism. 2012;64(12):4104-13.
89. Ortiz-Fernández L, Carmona FD, Montes-Cano MA, García-Lozano JR, Conde-Jaldón M, Ortego-Centeno N, et al. Genetic Analysis with the Immunochip Platform in Behçet Disease. Identification of Residues Associated in the HLA Class I Region and New Susceptibility Loci. PLoS One. 2016;11(8):e0161305.
90. Esin S, Gül A, Hodara V, Jeddi-Tehrani M, Dilsen N, Koniçe M, et al. Peripheral blood T cell expansions in patients with Behcet's disease. Clin Exp Immunol. 1997;107(3):520-7.
91. Direskeneli H, Eksioglu-Demiralp E, Kibaroglu A, Yavuz S, Ergun T, Akoglu T. Oligoclonal T cell expansions in patients with Behçet's disease. Clin Exp Immunol. 1999;117(1):166-70.

92. Lehner T, Lavery E, Smith R, van der Zee R, Mizushima Y, Shinnick T. Association between the 65-kilodalton heat shock protein, Streptococcus sanguis, and the corresponding antibodies in Behçet's syndrome. Infect Immun. 1991;59(4):1434-41.
93. Nomura Y, Kitteringham N, Shiba K, Goseki M, Kimura A, Mineshita S. Use of the highly sensitive PCR method to detect the Herpes simplex virus type 1 genome and its expression in samples from Behçet disease patients. J Med Dent Sci. 1998;45(1):51-8.
94. Kaneko F, Oyama N, Yanagihori H, Isogai E, Yokota K, Oguma K. The role of streptococcal hypersensitivity in the pathogenesis of Behçet's Disease. European journal of dermatology : EJD. 2008;18(5):489-98.
95. Cheng L, Zhan H, Liu Y, Chen H, Zhang F, Zheng W, et al. Infectious agents and pathogenesis of Behçet's disease: An extensive review. Clin Immunol. 2023;251:109631.
96. Direskeneli H, Ekşioglu-Demiralp E, Yavuz S, Ergun T, Shinnick T, Lehner T, et al. T cell responses to 60/65 kDa heat shock protein derived peptides in Turkish patients with Behçet's disease. J Rheumatol. 2000;27(3):708-13.
97. de Chambrun MP, Wechsler B, Geri G, Cacoub P, Saadoun D. New insights into the pathogenesis of Behcet's disease. Autoimmunity reviews. 2012;11(10):687-98.
98. Yazici H, Seyahi E, Hatemi G, Yazici Y. Behçet syndrome: a contemporary view. Nature Reviews Rheumatology. 2018;14(2):107-19.
99. Lule S, Colpak AI, Balci-Peynircioglu B, Gursoy-Ozdemir Y, Peker S, Kalyoncu U, et al. Behçet disease serum is immunoreactive to neurofilament medium which share common epitopes to bacterial HSP-65, a putative trigger. Journal of autoimmunity. 2017;84:87-96.
100. Kibaroglu A, Eksioglu-Demiralp E, Akoglu T, Direskeneli H. T and NK cell subset changes with microbial extracts and human HSP60-derived peptides in Behçet's disease. Clinical and experimental rheumatology. 2004;22(4 Suppl 34):S59-63.
101. Pervin K, Childerstone A, Shinnick T, Mizushima Y, van der Zee R, Hasan A, et al. T cell epitope expression of mycobacterial and homologous human 65-kilodalton heat shock protein peptides in short term cell lines from patients with Behçet's disease. The Journal of Immunology. 1993;151(4):2273-82.
102. Hasan A, Fortune F, Wilson A, Warr K, Shinnick T, Mizushima Y, et al. Role of gamma delta T cells in pathogenesis and diagnosis of Behcet's disease. Lancet. 1996;347(9004):789-94.
103. Yasuoka H, Okazaki Y, Kawakami Y, Hirakata M, Inoko H, Ikeda Y, et al. Autoreactive CD8+ cytotoxic T lymphocytes to major histocompatibility complex class I chain-related gene A in patients with Behçet's disease. Arthritis Rheum. 2004;50(11):3658-62.
104. Bettiol A, Emmi G, Low L, Sofi F, Wallace GR. Microbiome in Behcet's syndrome. Clin Immunol. 2023;250:109304.
105. Ogunkolade W, Senusi AA, Desai P, Sacoor S, Bibi A, Gokani B, et al. Profiling the microbiome of oral and genital mucosal surfaces in Behçet's disease. Clin Immunol. 2023;253:109654.
106. Vural S, Kerl K, Ertop Doğan P, Vollmer S, Puchta U, He M, et al. Lesional activation of T(c) 17 cells in Behçet disease and psoriasis supports HLA class I-mediated autoimmune responses. Br J Dermatol. 2021;185(6):1209-20.
107. Geri G, Terrier B, Rosenzwajg M, Wechsler B, Touzot M, Seilhean D, et al. Critical role of IL-21 in modulating TH17 and regulatory T cells in Behçet disease. Journal of Allergy and Clinical Immunology. 2011;128(3):655-64.
108. Yamaguchi Y, Takahashi H, Satoh T, Okazaki Y, Mizuki N, Takahashi K, et al. Natural killer cells control a T-helper 1 response in patients with Behçet's disease. Arthritis Research & Therapy. 2010;12(3):R80-R.
109. Yu HG, Lee DS, Seo JM, Ahn JK, Yu YS, Lee WJ, et al. The number of CD8+ T cells and NKT cells increases in the aqueous humor of patients with Behçet's uveitis. Clinical and experimental immunology. 2004;137(2):437-43.

110. Yasuoka H, Yamaguchi Y, Mizuki N, Nishida T, Kawakami Y, Kuwana M. Preferential activation of circulating CD8+ and gammadelta T cells in patients with active Behçet's disease and HLA-B51. Clinical and experimental rheumatology. 2008;26(4 Suppl 50):S59-63.
111. Okubo M, Sumitomo S, Tsuchida Y, Nagafuchi Y, Takeshima Y, Yanaoka H, et al. Transcriptome analysis of immune cells from Behçet's syndrome patients: the importance of IL-17-producing cells and antigen-presenting cells in the pathogenesis of Behçet's syndrome. Arthritis Res Ther. 2022;24(1):186.
112. Yang JY, Park MJ, Park S, Lee E-S. Increased senescent CD8+ T cells in the peripheral blood mononuclear cells of Behçet's disease patients. Archives of Dermatological Research. 2018;310(2):127-38.
113. Takase H, Sugita S, Taguchi C, Imai Y, Mochizuki M. Capacity of ocular infiltrating T helper type 1 cells of patients with non-infectious uveitis to produce chemokines. The British journal of ophthalmology. 2006;90(6):765-8.
114. Ye Z, Deng B, Wang C, Zhang D, Kijlstra A, Yang P. Decreased B and T lymphocyte attenuator in Behcet's disease may trigger abnormal Th17 and Th1 immune responses. Scientific Reports. 2016;6(1):20401-.
115. Tong B, Liu X, Xiao J, Su G. Immunopathogenesis of Behcet's Disease. Front Immunol. 2019;10:665-.
116. Tesmer LA, Lundy SK, Sarkar S, Fox DA. Th17 cells in human disease. Immunological Reviews. 2008;223(1):87-113.
117. Bettelli E, Carrier Y, Gao W, Korn T, Strom TB, Oukka M, et al. Reciprocal developmental pathways for the generation of pathogenic effector TH17 and regulatory T cells. Nature. 2006;441(7090):235-8.
118. Xu L, Kitani A, Fuss I, Strober W. Cutting edge: regulatory T cells induce CD4+CD25-Foxp3- T cells or are self-induced to become Th17 cells in the absence of exogenous TGF-beta. Journal of immunology (Baltimore, Md : 1950). 2007;178(11):6725-9.
119. Wilson NJ, Boniface K, Chan JR, McKenzie BS, Blumenschein WM, Mattson JD, et al. Development, cytokine profile and function of human interleukin 17–producing helper T cells. Nature Immunology. 2007;8(9):950-7.
120. Acosta-Rodriguez EV, Napolitani G, Lanzavecchia A, Sallusto F. Interleukins 1beta and 6 but not transforming growth factor-beta are essential for the differentiation of interleukin 17-producing human T helper cells. Nature immunology. 2007;8(9):942-9.
121. Manel N, Unutmaz D, Littman DR. The differentiation of human T(H)-17 cells requires transforming growth factor-beta and induction of the nuclear receptor RORgammat. Nature immunology. 2008;9(6):641-9.
122. Volpe E, Servant N, Zollinger R, Bogiatzi SI, Hupé P, Barillot E, et al. A critical function for transforming growth factor-beta, interleukin 23 and proinflammatory cytokines in driving and modulating human T(H)-17 responses. Nature immunology. 2008;9(6):650-7.
123. Lucherini OM, Lopalco G, Cantarini L, Emmi G, Lopalco A, Venerito V, et al. Critical regulation of Th17 cell differentiation by serum amyloid-A signalling in Behcet's disease. Immunology Letters. 2018;201:38-44.
124. Shimizu J, Takai K, Takada E, Fujiwara N, Arimitsu N, Ueda Y, et al. Possible association of proinflammatory cytokines including IL1β and TNFα with enhanced Th17 cell differentiation in patients with Behcet's disease. Clinical Rheumatology. 2016;35(7):1857-63.
125. Aktas Cetin E, Cosan F, Cefle A, Deniz G. IL-22-secreting Th22 and IFN-γ-secreting Th17 cells in Behçet's disease. Modern rheumatology. 2014;24(5):802-7.
126. Ahmadi M, Yousefi M, Abbaspour-Aghdam S, Dolati S, Aghebati-Maleki L, Eghbal-Fard S, et al. Disturbed Th17/Treg balance, cytokines, and miRNAs in peripheral blood of patients with Behcet's disease. Journal of Cellular Physiology. 2019;234(4):3985-94.
127. Berzins SP, Ritchie DS. Natural killer T cells: drivers or passengers in preventing human disease? Nature Reviews Immunology. 2014;14(9):640-6.

128. Bendelac A, Savage PB, Teyton L. The Biology of NKT Cells. Annual Review of Immunology. 2007;25(1):297-336.
129. Godfrey DI, Stankovic S, Baxter AG. Raising the NKT cell family. Nature immunology. 2010;11(3):197-206.
130. Cameron G, Pellicci DG, Uldrich AP, Besra GS, Illarionov P, Williams SJ, et al. Antigen Specificity of Type I NKT Cells Is Governed by TCR β-Chain Diversity. Journal of immunology (Baltimore, Md : 1950). 2015;195(10):4604-14.
131. Bonacini M, Soriano A, Zerbini A, Calò E, Cimino L, Muratore F, et al. Higher Frequencies of Lymphocytes Expressing the Natural Killer Group 2D Receptor in Patients With Behçet Disease. Frontiers in Immunology. 2018;9:2157-.
132. Hamzaoui K, Kamoun M, Houman H, Hentati F, Hamza MH, Ayed K, et al. Discrepancies of NKT cells expression in peripheral blood and in cerebrospinal fluid from Behçet's disease. Journal of neuroimmunology. 2006;175(1-2):160-8.
133. Kalyan S, Kabelitz D. Defining the nature of human γδ T cells: a biographical sketch of the highly empathetic. Cellular & Molecular Immunology. 2013;10(1):21-9.
134. Chien Y-h, Meyer C, Bonneville M. γδ T Cells: First Line of Defense and Beyond. Annual Review of Immunology. 2014;32(1):121-55.
135. Parlakgul G, Guney E, Erer B, Kılıcaslan Z, Direskeneli H, Gul A, et al. Expression of regulatory receptors on γδ T cells and their cytokine production in Behcet's disease. Arthritis Res Ther. 2013;15(1):R15.
136. Brandes M, Willimann K, Moser B. Professional antigen-presentation function by human gammadelta T Cells. Science (New York, NY). 2005;309(5732):264-8.
137. Brandes M, Willimann K, Bioley G, Lévy N, Eberl M, Luo M, et al. Cross-presenting human γδ T cells induce robust CD8+ αβ T cell responses. Proceedings of the National Academy of Sciences. 2009;106(7):2307 LP-12.
138. Clemente A, Cambra A, Munoz-Saá I, Crespí C, Pallarés L, Juan A, et al. Phenotype markers and cytokine intracellular production by CD8+ gammadelta T lymphocytes do not support a regulatory T profile in Behçet's disease patients and healthy controls. Immunology letters. 2010;129(2):57-63.
139. Dieli F, Caccamo N. Immunomodulatory role of statins in autoimmune disease: is there a role for human γδT cells? Nature Reviews Immunology. 2006;6(7):564-.
140. Accardo-Palumbo A, Ferrante A, Cadelo M, Ciccia F, Parrinello G, Lipari L, et al. The level of soluble Granzyme A is elevated in the plasma and in the Vgamma9/Vdelta2 T cell culture supernatants of patients with active Behçet's disease. Clinical and experimental rheumatology. 2004;22(4 Suppl 34):S45-9.
141. Fortune F, Walker J, Lehner T. The expression of gamma delta T cell receptor and the prevalence of primed, activated and IgA-bound T cells in Behçet's syndrome. Clin Exp Immunol. 1990;82(2):326-32.
142. Suzuki Y, Hoshi K, Matsuda T, Mizushima Y. Increased peripheral blood gamma delta+ T cells and natural killer cells in Behçet's disease. J Rheumatol. 1992;19(4):588-92.
143. Freysdottir J, Lau S, Fortune F. Gammadelta T cells in Behçet's disease (BD) and recurrent aphthous stomatitis (RAS). Clin Exp Immunol. 1999;118(3):451-7.
144. Abbasova V, Gül A, Saruhan-Direskeneli G. IL-17A and IFN-γ are Up-regulated in CD4 and γδ T Cells in Active Behcet's Disease Patients. Immunology Letters. 2022;242:37-45.
145. Bank I, Duvdevani M, Livneh A. Expansion of gammadelta T-cells in Behçet's disease: role of disease activity and microbial flora in oral ulcers. J Lab Clin Med. 2003;141(1):33-40.
146. Ergun T, İnce Ü, Ekşioğlu-Demiralp E, Direskeneli H, Gürbüz O, Gürses L, et al. HSP 60 expression in mucocutaneous lesions of Behçet's disease. Journal of the American Academy of Dermatology. 2001;45(6):904-9.
147. Triolo G, Accardo-Palumbo A, Dieli F, Ciccia F, Ferrante A, Giardina E, et al. Vgamma9/Vdelta2 T lymphocytes in Italian patients with Behçet's disease: evidence for expansion,

and tumour necrosis factor receptor II and interleukin-12 receptor beta1 expression in active disease. Arthritis Res Ther. 2003;5(5):R262-8.
148. Dominguez-Villar M, Hafler DA. Regulatory T cells in autoimmune disease. Nature Immunology. 2018;19(7):665-73.
149. Vignali DAA, Collison LW, Workman CJ. How regulatory T cells work. Nature Reviews Immunology. 2008;8(7):523-32.
150. Feuerer M, Hill JA, Mathis D, Benoist C. Foxp3+ regulatory T cells: differentiation, specification, subphenotypes. Nature Immunology. 2009;10(7):689-95.
151. Li Z, Li D, Tsun A, Li B. FOXP3+ regulatory T cells and their functional regulation. Cellular & Molecular Immunology. 2015;12(5):558-65.
152. Hamzaoui K, Borhani Haghighi A, Ghorbel IB, Houman H. RORC and Foxp3 axis in cerebrospinal fluid of patients with Neuro-Behçet's Disease. Journal of Neuroimmunology. 2011;233(1):249-53.
153. Moretta A, Marcenaro E, Parolini S, Ferlazzo G, Moretta L. NK cells at the interface between innate and adaptive immunity. Cell Death & Differentiation. 2008;15(2):226-33.
154. Tian Z, Gershwin ME, Zhang C. Regulatory NK cells in autoimmune disease. Journal of Autoimmunity. 2012;39(3):206-15.
155. French AR, Yokoyama WM. Natural killer cells and autoimmunity. Arthritis Res Ther. 2003;6(1):8-.
156. Hasan MS, Ryan PL, Bergmeier LA, Fortune F. Circulating NK cells and their subsets in Behçet's disease. Clinical & Experimental Immunology. 2017;188(2):311-22.
157. Cosan F, Aktas Cetin E, Akdeniz N, Emrence Z, Cefle A, Deniz G. Natural Killer Cell Subsets and Their Functional Activity in Behçet's Disease. Immunological Investigations. 2017;46(4):419-32.
158. Kucuksezer UC, Aktas-Cetin E, Bilgic-Gazioglu S, Tugal-Tutkun I, Gul A, Deniz G. Natural killer cells dominate a Th-1 polarized response in Behçet's disease patients with uveitis. Clin Exp Rheumatol. 2015;33(6 Suppl 94):S24-9.
159. Kawakami T, Ohashi S, Kawa Y, Takahama H, Ito M, Soma Y, et al. Elevated Serum Granulocyte Colony-Stimulating Factor Levels in Patients With Active Phase of Sweet Syndrome and Patients With Active Behçet Disease: Implication in Neutrophil Apoptosis Dysfunction. Archives of Dermatology. 2004;140(5):570-4.
160. Balta S, Ozturk C, Balta I, Demirkol S, Demir M, Celik T, et al. The neutrophil–lymphocyte ratio and inflammation. Angiology. 2016;67(3):298-9.
161. Djaballah-Ider F, Touil-Boukoffa C. Effect of combined colchicine-corticosteroid treatment on neutrophil/lymphocyte ratio: a predictive marker in Behçet disease activity. Inflammopharmacology. 2020;28(4):819-29.
162. Le Joncour A, Martos R, Loyau S, Lelay N, Dossier A, Cazes A, et al. Critical role of neutrophil extracellular traps (NETs) in patients with Behcet's disease. Annals of the Rheumatic Diseases. 2019;78(9):1274 LP-82.
163. Mendoza-Pinto C, García-Carrasco M, Jiménez-Hernández M, Jiménez Hernández C, Riebeling-Navarro C, Nava Zavala A, et al. Etiopathogenesis of Behcet's disease. Autoimmunity Reviews. 2010;9(4):241-5.
164. Patente TA, Pinho MP, Oliveira AA, Evangelista GC, Bergami-Santos PC, Barbuto JA. Human dendritic cells: their heterogeneity and clinical application potential in cancer immunotherapy. Frontiers in immunology. 2019;9:3176.
165. Zengin HB, Pukhalskaya T, Smoller BR. Role of CD123 (+) Plasmacytoid Dendritic Cells in Etiologically Different Variants of Erythema Multiforme: A Monocentric Retrospective Study. Dermatopathology (Basel). 2021;8(2):89-96.
166. Dias de Oliveira NF, Santi CG, Maruta CW, Aoki V. Plasmacytoid dendritic cells in dermatology. An Bras Dermatol. 2021;96(1):76-81.

167. Pay S, Pekel A, Simsek I, Musabak U, Erdem H, Dinc A, et al. Pronounced interferon-alpha production from plasmacytoid dendritic cells in patients with Behçet's disease following CpG D ODN stimulation. Clin Exp Rheumatol. 2009;27(2 Suppl 53):S37-42.
168. Pay S, Simsek I, Erdem H, Pekel A, Musabak U, Sengul A, et al. Dendritic cell subsets and type I interferon system in Behçet's disease: does functional abnormality in plasmacytoid dendritic cells contribute to Th1 polarization? Clin Exp Rheumatol. 2007;25(4 Suppl 45):S34-40.
169. Qiu Y, Zhu Y, Yu H, Yi S, Su W, Cao Q, et al. Ocular Behcet's disease is associated with aberrant methylation of interferon regulatory factor 8 (IRF8) in monocyte-derived dendritic cells. Oncotarget. 2017;8(31):51277-87.
170. Yilmaz S, Cinar M, Pekel A, Simsek I, Musabak U, Erdem H, et al. The expression of transmembrane and soluble CXCL16 and the relation with interferon-alpha secretion in patients with Behçet's disease. Clin Exp Rheumatol. 2013;31(3 Suppl 77):84-7.
171. Ekşioglu-Demiralp E, Kibaroglu A, Direskeneli H, Yavuz S, Karsli F, Yurdakul S, et al. Phenotypic characteristics of B cells in Behçet's disease: increased activity in B cell subsets. The Journal of rheumatology. 1999;26(4):826-32.
172. Suzuki N, Sakane T, Ueda Y, Tsunematsu T. Abnormal B cell function in patients with Behçet's disease. Arthritis & Rheumatism. 1986;29(2):212-9.
173. van der Houwen TB, van Hagen PM, Timmermans WM, Bartol SJ, Lam KH, Kappen JH, et al. Chronic signs of memory B cell activation in patients with Behçet's disease are partially restored by anti-tumour necrosis factor treatment. Rheumatology (Oxford). 2017;56(1):134-44.
174. Davatchi F, Shams H, Rezaipoor M, Sadeghi-Abdollahi B, Shahram F, Nadji A, et al. Rituximab in intractable ocular lesions of Behcet's disease; randomized single-blind control study (pilot study). Int J Rheum Dis. 2010;13(3):246-52.
175. Hetta HF, Mohamed AAA, Zahran AM, S AM, My Sayed M, Ga Saleh M, et al. Possible Role of Regulatory B Cells in Different Behçet's Disease Phenotypes and Therapies: First Report from Egypt. J Inflamm Res. 2021;14:737-44.
176. Debes GF, McGettigan SE. Skin-Associated B Cells in Health and Inflammation. J Immunol. 2019;202(6):1659-66.
177. Schor SL, Schor AM. Phenotypic and genetic alterations in mammary stroma: implications for tumour progression. Breast Cancer Res. 2001;3(6):373-9.
178. Blainey PC, Quake SR. Dissecting genomic diversity, one cell at a time. Nat Methods. 2014;11(1):19-21.
179. Taniguchi K, Kajiyama T, Kambara H. Quantitative analysis of gene expression in a single cell by qPCR. Nat Methods. 2009;6(7):503-6.
180. Citri A, Pang ZP, Südhof TC, Wernig M, Malenka RC. Comprehensive qPCR profiling of gene expression in single neuronal cells. Nat Protoc. 2011;7(1):118-27.
181. Grada A, Weinbrecht K. Next-generation sequencing: methodology and application. J Invest Dermatol. 2013;133(8):e11.
182. Whitley SK, Horne WT, Kolls JK. Research Techniques Made Simple: Methodology and Clinical Applications of RNA Sequencing. J Invest Dermatol. 2016;136(8):e77-e82.
183. Engel I, Seumois G, Chavez L, Samaniego-Castruita D, White B, Chawla A, et al. Innate-like functions of natural killer T cell subsets result from highly divergent gene programs. Nat Immunol. 2016;17(6):728-39.
184. Islam S, Kjällquist U, Moliner A, Zajac P, Fan JB, Lönnerberg P, et al. Characterization of the single-cell transcriptional landscape by highly multiplex RNA-seq. Genome Res. 2011;21(7):1160-7.
185. Patel AP, Tirosh I, Trombetta JJ, Shalek AK, Gillespie SM, Wakimoto H, et al. Single-cell RNA-seq highlights intratumoral heterogeneity in primary glioblastoma. Science. 2014;344(6190):1396-401.
186. Heaton H, Talman AM, Knights A, Imaz M, Gaffney DJ, Durbin R, et al. Souporcell: robust clustering of single-cell RNA-seq data by genotype without reference genotypes. Nat Methods. 2020;17(6):615-20.

187. Zhang B, Roesner LM, Traidl S, Koeken V, Xu CJ, Werfel T, et al. Single-cell profiles reveal distinctive immune response in atopic dermatitis in contrast to psoriasis. Allergy. 2023;78(2):439-53.
188. Polański K, Young MD, Miao Z, Meyer KB, Teichmann SA, Park JE. BBKNN: fast batch alignment of single cell transcriptomes. Bioinformatics. 2020;36(3):964-5.
189. Park JE, Botting RA, Domínguez Conde C, Popescu DM, Lavaert M, Kunz DJ, et al. A cell atlas of human thymic development defines T cell repertoire formation. Science. 2020;367(6480).
190. Korsunsky I, Millard N, Fan J, Slowikowski K, Zhang F, Wei K, et al. Fast, sensitive and accurate integration of single-cell data with Harmony. Nat Methods. 2019;16(12):1289-96.
191. Wolf FA, Angerer P, Theis FJ. SCANPY: large-scale single-cell gene expression data analysis. Genome Biology. 2018;19(1):15.
192. Badia-i-Mompel P, Vélez Santiago J, Braunger J, Geiss C, Dimitrov D, Müller-Dott S, et al. decoupleR: ensemble of computational methods to infer biological activities from omics data. Bioinformatics Advances. 2022;2(1):vbac016.
193. Büttner M, Ostner J, Müller CL, Theis FJ, Schubert B. scCODA is a Bayesian model for compositional single-cell data analysis. Nature Communications. 2021;12(1):6876.
194. Sturm G, Szabo T, Fotakis G, Haider M, Rieder D, Trajanoski Z, et al. Scirpy: a Scanpy extension for analyzing single-cell T-cell receptor-sequencing data. Bioinformatics. 2020;36(18):4817-8.
195. Khoshbakht S, Albayrak Ö, Tiryaki E, Ağcaoğlu O, Öktem A, Pınar Sun G, et al. A cost-effective protocol for single-cell RNA sequencing of human skin. Frontiers in Immunology. 2024;15.
196. Domínguez Conde C, Xu C, Jarvis LB, Rainbow DB, Wells SB, Gomes T, et al. Cross-tissue immune cell analysis reveals tissue-specific features in humans. Science. 2022;376(6594):eabl5197.
197. Han L, Jara CP, Wang O, Shi Y, Wu X, Thibivilliers S, et al. Isolating and cryopreserving pig skin cells for single-cell RNA sequencing study. PLoS One. 2022;17(2):e0263869.
198. Saluzzo S, Gail LM, Neuwirth T, Pandey RV, Farlik M, Stary G. Processing human skin samples for single-cell assays. STAR Protoc. 2022;3(3):101470.
199. Polakova A, Hudemann C, Wiemers F, Kadys A, Gremke N, Lang M, et al. Isolation of Lymphocytes from Human Skin and Murine Tissues: A Rapid and Epitope-Preserving Approach. JID Innovations. 2023;3(1):100155.
200. Stoeckius M, Zheng S, Houck-Loomis B, Hao S, Yeung BZ, Mauck WM, et al. Cell Hashing with barcoded antibodies enables multiplexing and doublet detection for single cell genomics. Genome Biology. 2018;19(1):224.
201. Kang HM, Subramaniam M, Targ S, Nguyen M, Maliskova L, McCarthy E, et al. Multiplexed droplet single-cell RNA-sequencing using natural genetic variation. Nat Biotechnol. 2018;36(1):89-94.
202. Nestle FO, Conrad C, Tun-Kyi A, Homey B, Gombert M, Boyman O, et al. Plasmacytoid predendritic cells initiate psoriasis through interferon-α production. Journal of Experimental Medicine. 2005;202(1):135-43.
203. De Vries HJC, Van Marle J, Teunissen MBM, Picavet D, Zorgdrager F, Bos JD, et al. Lichen planus is associated with human herpesvirus type 7 replication and infiltration of plasmacytoid dendritic cells. British Journal of Dermatology. 2006;154(2):361-4.
204. Malard F, Bossard C, Brissot E, Chevallier P, Guillaume T, Delaunay J, et al. Increased plasmacytoid dendritic cells and RORγt-expressing immune effectors in cutaneous acute graft-versus-host disease. Journal of Leukocyte Biology. 2013;94(6):1337-43.
205. Vermi W, Vescovi R, Facchetti F. Plasmacytoid Dendritic Cells in Cutaneous Disorders. Current Dermatology Reports. 2013;2(1):1-10.
206. Di Domizio J, Belkhodja C, Chenuet P, Fries A, Murray T, Mondéjar PM, et al. The commensal skin microbiota triggers type I IFN–dependent innate repair responses in injured skin. Nature Immunology. 2020;21(9):1034-45.
207. Lee SJ, Kang SE, Kang EH, Choi BY, Masek-Hammerman K, Syed J, et al. CXCL10/CXCR3 axis is associated with disease activity and the development of mucocutaneous lesions in patients with Behçet's disease. Sci Rep. 2017;7(1):14720.

208. Ambrose N, Khan E, Ravindran R, Lightstone L, Abraham S, Botto M, et al. The exaggerated inflammatory response in Behçet's syndrome: identification of dysfunctional post-transcriptional regulation of the IFN-γ/CXCL10 IP-10 pathway. Clinical and Experimental Immunology. 2015;181(3):427-33.
209. Accardo-Palumbo A, Giardina AR, Ciccia F, Ferrante A, Principato A, Impastato R, et al. Phenotype and functional changes of Vgamma9/Vdelta2 T lymphocytes in Behçet's disease and the effect of infliximab on Vgamma9/Vdelta2 T cell expansion, activation and cytotoxicity. Arthritis Res Ther. 2010;12(3):R109.
210. Ortiz Fernández L, Coit P, Yilmaz V, Yentür SP, Alibaz-Oner F, Aksu K, et al. Genetic Association of a Gain-of-Function IFNGR1 Polymorphism and the Intergenic Region LNCAROD/DKK1 With Behçet's Disease. Arthritis & Rheumatology. 2021;73(7):1244-52.
211. Zhan H, Li H, Cheng L, Yan S, Zheng W, Li Y. Novel Insights Into Gene Signatures and Their Correlation With Immune Infiltration of Peripheral Blood Mononuclear Cells in Behcet's Disease. Front Immunol. 2021;12:794800.
212. Kulaber A, Tugal-Tutkun I, Yentür SP, Akman-Demir G, Kaneko F, Gül A, et al. Pro-inflammatory cellular immune response in Behçet's disease. Rheumatol Int. 2007;27(12):1113-8.
213. Guia S, Cognet C, de Beaucoudrey L, Tessmer MS, Jouanguy E, Berger C, et al. A role for interleukin-12/23 in the maturation of human natural killer and CD56+ T cells in vivo. Blood. 2008;111(10):5008-16.
214. Vignali DA, Kuchroo VK. IL-12 family cytokines: immunological playmakers. Nat Immunol. 2012;13(8):722-8.
215. Seder RA, Gazzinelli R, Sher A, Paul WE. Interleukin 12 acts directly on CD4+ T cells to enhance priming for interferon gamma production and diminishes interleukin 4 inhibition of such priming. Proc Natl Acad Sci U S A. 1993;90(21):10188-92.
216. Zwirner NW, Ziblat A. Regulation of NK Cell Activation and Effector Functions by the IL-12 Family of Cytokines: The Case of IL-27. Front Immunol. 2017;8:25.
217. Garner LC, Amini A, FitzPatrick MEB, Lett MJ, Hess GF, Filipowicz Sinnreich M, et al. Single-cell analysis of human MAIT cell transcriptional, functional and clonal diversity. Nature Immunology. 2023;24(9):1565-78.
218. Ussher JE, Bilton M, Attwod E, Shadwell J, Richardson R, de Lara C, et al. CD161++ CD8+ T cells, including the MAIT cell subset, are specifically activated by IL-12+IL-18 in a TCR-independent manner. Eur J Immunol. 2014;44(1):195-203.
219. Henry CJ, Ornelles DA, Mitchell LM, Brzoza-Lewis KL, Hiltbold EM. IL-12 Produced by Dendritic Cells Augments CD8+ T Cell Activation through the Production of the Chemokines CCL1 and CCL171. The Journal of Immunology. 2008;181(12):8576-84.
220. Xiao Z, Casey KA, Jameson SC, Curtsinger JM, Mescher MF. Programming for CD8 T cell memory development requires IL-12 or type I IFN. J Immunol. 2009;182(5):2786-94.
221. Banerjee S, Biehl A, Gadina M, Hasni S, Schwartz DM. JAK-STAT Signaling as a Target for Inflammatory and Autoimmune Diseases: Current and Future Prospects. Drugs. 2017;77(5):521-46.
222. Tulunay A, Dozmorov MG, Ture-Ozdemir F, Yilmaz V, Eksioglu-Demiralp E, Alibaz-Oner F, et al. Activation of the JAK/STAT pathway in Behcet's disease. Genes Immun. 2015;16(2):170-5.
223. Puccetti A, Fiore PF, Pelosi A, Tinazzi E, Patuzzo G, Argentino G, et al. Gene Expression Profiling in Behcet's Disease Indicates an Autoimmune Component in the Pathogenesis of the Disease and Opens New Avenues for Targeted Therapy. J Immunol Res. 2018;2018:4246965.
224. Liu J, Hou Y, Sun L, Li C, Li L, Zhao Y, et al. A pilot study of tofacitinib for refractory Behçet's syndrome. Ann Rheum Dis. 2020;79(11):1517-20.
225. Cho Y-N, Kee S-J, Kim T-J, Jin HM, Kim M-J, Jung H-J, et al. Mucosal-Associated Invariant T Cell Deficiency in Systemic Lupus Erythematosus. The Journal of Immunology. 2014;193(8):3891-901.
226. Kang H, Sun H, Yang Y, Tuong ZK, Shu M, Wei Y, et al. Autoimmune uveitis in Behçet's disease and Vogt-Koyanagi-Harada disease differ in tissue immune infiltration and T cell clonality. Clin Transl Immunology. 2023;12(9):e1461.

227. Chang L, Zheng Z, Zou Q, Zhong B, Chen C, Cheng X, et al. Single cell Transcriptome and T cell Repertoire Mapping of the Mechanistic Signatures and T cell Trajectories Contributing to Vascular and Dermal Manifestations of Behcet's Disease. bioRxiv. 2022:2022.03.22.485251.
228. Shi W, Ye J, Shi Z, Pan C, Zhang Q, Lin Y, et al. Single-cell chromatin accessibility and transcriptomic characterization of Behcet's disease. Communications Biology. 2023;6(1):1048.
229. Sadreddini S, Noshad H, Molaeefard M, Noshad R. Treatment of retinal vasculitis in Behçet's disease with rituximab. Mod Rheumatol. 2008;18(3):306-8.
230. Zou J, Li B, Li D, Bao H-f, She C-h, Ye J-f, et al. Comprehensive analysis of T-cell receptor repertoires reveals antigen-driven T-cell clusters in patients with Behçet's syndrome. European Journal of Immunology. 2023;53(4):2250181.